

ASD 8
P5

A STUDY
OF LIQUID CLATHRATES

A thesis submitted to the
UNIVERSITY OF CAPE TOWN
in fulfilment of the requirements for the degree of
MASTER OF SCIENCE

BY

HEIDI CAROLINE JOAO
B.Sc. (Hons) (Cape Town)

Department of Physical Chemistry
University of Cape Town
Rondebosch
7700
Republic of South Africa

November 1987

The University of Cape Town has been given
the right to reproduce this thesis in whole
or in part. Copyright is held by the author.

The copyright of this thesis vests in the author. No quotation from it or information derived from it is to be published without full acknowledgement of the source. The thesis is to be used for private study or non-commercial research purposes only.

Published by the University of Cape Town (UCT) in terms of the non-exclusive license granted to UCT by the author.

ACKNOWLEDGEMENTS

I wish to extend sincere thanks to

Professor L.R. Nassimbeni and Dr D. Bond for their
enthusiastic supervision,

Dr G.E. Jackson, for his patience, advice and assistance
with the N.M.R. work,

Dr M.L. Niven for her expertise and assistance with the
data collections,

Dr Torrington and Mike Taylor for assistance with computer
programming and Ian Fisher for use of his computer,

my mother, for her encouragement in the past,

Mark Graham, for and his support and encouragement.

Financial assistance from the Coal Research Institute is
gratefully acknowledged.

ABSTRACT

Use was made of Nuclear Overhauser effects (nOe) and crystallography to determine the structure and packing in novel liquid clathrate systems.

The stoichiometry of the clathrates was investigated by various chemical methods including: thermogravimetric analysis, differential thermal analysis and proton nuclear magnetic resonance spectroscopy.

The structure of a new Liquid Clathrate host compound $[(C_6H_{13})_4N]^+ [(C_4H_9)_4B]^-$ was partially solved. The structure of $[(C_6H_5)_4N]^+ [(C_4H_9)_4B]^-$ was also solved.

Host-guest non-bonded energy relationships were examined and the minimum stability constant determined for certain liquid clathrate systems. The properties of various liquid clathrate systems were investigated with the aid of nuclear magnetic resonance spectroscopy.

A model of the liquid clathrate was proposed on the basis of the noe and crystallographic results.

CONTENTS

1.	CHAPTER 1: INTRODUCTION	5
2.	CHAPTER 2: EXPERIMENTAL	16
3.	CHAPTER 3: PREPARATION AND CHARACTERIZATION OF NOVEL AIR-STABLE PARENT COMPOUNDS	45
4.	CHAPTER 4: ANALYSIS OF LIQUID CLATHRATE COMPOSITION BY ^1H -NMR SPECTROSCOPY	64
5.	CHAPTER 5: DETERMINATION OF PHYSICAL PROPERTIES	82
6.	CHAPTER 6: DETERMINATION OF STABILITY CONSTANTS	99
7.	CHAPTER 7: LIQUID CLATHRATE STRUCTURE DETERMINATION NUCLEAR OVERHAUSER ENHANCEMENT EXPERIMENTS	107
8.	CHAPTER 8: CRYSTALLOGRAPHIC ANALYSIS OF CLATHRATES	121
9.	CHAPTER 9: CONCLUSION	148
10.	APPENDIX: I Parameter settings for obtaining nOe spectra.	155
	II Modelling the Borate Anion for the calculation of its scattering factor,	157

using MULTAN.

III	Determination of the scattering factor for the borate anion.	160
IV	Calibration curve for DTA/TGA samples.	164
V	Observed and calculated structure factors for: a) Host (1a) b) Host (1b)	166
11.	REFERENCES	188

the appearance of an inspired crystallographer who was prepared to set aside the prevailing notion that all compounds should be stoichiometric, and who would propose a structure for these novel compounds. That crystallographer was H.M. Powell who not only proposed a structure for these compounds but also coined a new word 'clathrate', which has become an accepted part of chemical nomenclature². The term "clathrate" was introduced to describe a particular form of molecular compounds in which one component (the host) forms a cage structure imprisoning another (the guest). It was borrowed from the Latin word "clathratus", meaning enclosed or protected by cross bars or trellis⁴. Consequently, H.M. Powell is considered to be the 'Father' of these compounds.

The forces operating in the formation of these inclusion compounds are dependent on the type of compound formed.

Inclusion compounds may therefore be sub-classified as:

- (i) the intercalate or layer type, where the guest component is situated between layers of host structure;
- (ii) the channel type, in which the guest species are accommodated in continuous canals running through the crystal and
- (iii) the true clathrate type, in which the guest molecules are imprisoned in discrete closed cavities or cages.

The simplest compound to have a layered structure is graphite. Due to the large interlayer separation of 3.35 Å

and the weak Van der Waals interlayer forces, a variety of species such as K, CrO_3 , SbF_5 and AlCl_3 may penetrate between the layers to form graphite intercalates⁵.

Urea and thiourea adducts are examples of inclusion compounds which have channel-like void spaces. Urea molecules undergo hydrogen bonding to form open hexagonal channels large enough to accommodate numerous straight-chain hydrocarbon guest molecules. In addition, Van der Waals forces between the hydrocarbon guest molecule and the urea host molecules which surround it, contribute to the stability of this polynuclear inclusion compound. The thiourea adducts are similar to those of the urea, but have the ability to accommodate larger, branched-chain guest molecules such as trimethylpentane, cyclohexane and triptane due to the channels being approximately 2 Å greater in diameter⁶.

The choleic acids are the oldest of the recorded polynuclear inclusion compounds. The more commonly known choleic acid complexes are those of deoxycholic acid. X-ray studies of these inclusion complexes have shown them to have open structures³⁶, leaving free channels for inclusion of hydrocarbons, esters, alcohols, carboxylic acids, phenols, ethers and alkaloids. Deoxycholic acid molecules are hydrogen bonded to each other and thus produce a series of connected channels.

The zeolites, which are clay minerals, are macromolecular inclusion compounds whose inclusion properties have found wide industrial applications. Zeolites are used to upgrade gasoline, to dry gases on a commercial scale, to separate hydrocarbon mixtures, to act as "carriers" for catalysts to prevent loss of valuable catalytic material during reactions and more commonly as ion exchange media⁸. The zeolites are crystalline structures in which a framework of silicon-oxygen or aluminum-oxygen tetrahedra form the basic structure. They crystallize to provide a three-dimensional network which is permeated with relatively large cavities and channels. These large interstitial spaces normally enclose water molecules. The "holes" which arise on evacuation of the water molecules may be filled by a variety of gas, vapor and straight-chain hydrocarbon molecules. Furthermore the zeolites have stable self-supporting frameworks even in the absence of guest molecules. Besides naturally-occurring zeolites, innumerable types have been synthesised on a tailor-made basis with specified dimensions for selective inclusions.

Two other scientists, C.J. Pedersen and J.M. Lehn, must also be introduced into the inclusion compound story as persons who not only have made substantial contributions to the development of inclusion chemistry but who also introduced two new words of chemical nomenclature.

C.J. Pedersen synthesised the first crown ethers⁹ and J.M. Lehn and his co-workers introduced the cryptates¹⁰. The outstanding property of these ligands is their ability to complex with metal ions, where the metal ion occupies the void in the centre of the molecule. Since the dimension of the void is governed by the number of atoms forming the cyclic system in the ligand, it has been further found that each ligand generally shows a selectivity for a particular metal ion, the highest selectivity being shown towards the metal ion whose diameter best matches the diameter of the void.

Subsequent work on crown and cryptate compounds¹¹ has given rise to an enormous number of compounds which in turn has led to the introduction of new nomenclature so that the literature now abounds with references to coronands, cryptands, podands, spherands, ionophores, tweezer molecules, hexapus molecules, octapus molecules, tentacle molecules, and even 'Mobius Strip' molecules³.

The most important event in the history of inclusion compounds resulted from the pioneering X-ray structural work of H.M. Powell. Powell and his co-workers undertook a comprehensive study of the crystalline nature of the β -hydroquinone clathrate (a hydroquinone-sulphur dioxide molecular compound). They observed the firmness with which the two components were held together even though there appeared to be no strong attractive forces acting between

them and that the components were held simply by enclosure of one by the other. The hydroquinone molecules are linked together through hydrogen bonds between their hydroxyl groups. Six oxygen atoms of six different hydroquinone molecules form a hexagon. Alternating hydroquinone molecules incline upwards and downwards from the hexagon and are further linked in a similar manner through their other hydroxyl groups to form a giant molecular structure¹². The basic framework therefore consists of extended arrays of non-bonded interpenetrating hydroquinone networks. The formation of these networks create cavities. The structure allows for roughly spherical cavities of 4 Å in diameter which enclose various guest molecules such as Ar, Kr, Xe, SO₂, SH₃OH, CO₂, HCl, and H₂S. Guest molecules which are too large do not yield clathrates and those too small form unstable clathrates. However the cage may distort in order to accommodate various guest species: for example, the elliptical CH₃CN molecules. It has been suggested¹³ that a molecule of optimum size which is trapped in the cavity is removed with difficulty due to the appreciable Van der Waals interaction between the guest and host framework.

Clathrate compounds are emerging on the chemical scene and are becoming increasingly important. Their formation is novel, their properties unique and their potential uses extremely wide.

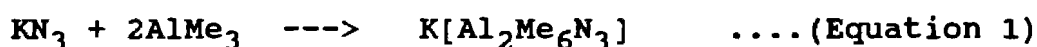
An important field of application is directed towards chemical analysis and molecular separation processes. Corresponding to the size, the shape, and the chemical nature of the holes generated in an inclusion lattice, guest molecules may be included selectively. Out of a mixture of compounds, the one which best matches the conditions of the lattice holes is preferentially accommodated. Chemically different species are separated (e.g. hydrocarbons and ketones), as are constitutional isomers, positional isomers, regioisomers, stereoisomers and even isotopic isomers. Size selectivity, which has been recognized as a characteristic feature of host lattices has definite industrial applications.⁴

An ingenious use to which clathrate compounds have been put is to enclathrate radioactive or highly toxic material. An example of the former is the inclusion of ^{85}Kr in a hydroquinone cage¹⁴ so that it can be powdered into small crystal dimensions for safe and easy handling. Highly toxic organo-mercurials such as dimethylmercury¹⁵ may be handled with comparative safety in the form of its clathrate with thiachroman. Clathrates may also serve as polymerising agents¹⁶ and as catalysts¹⁷.

With regard to the many applications, general guide lines for the easy construction of new clathrate compounds are desirable. Most of the classical clathrate hosts^{12,18-21}

have been discovered by accident and not by directed synthesis. The only starting point for a general study of clathrates and their molecular construction principles until quite recently, came from Powell's fundamental crystallographic work.

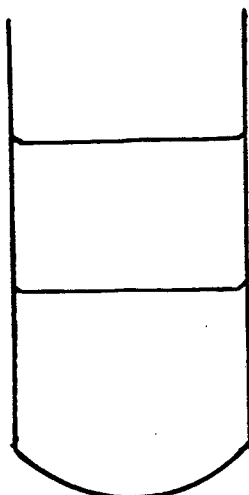
Much attention has recently been focused on the novel solution behavior: liquid clathrate formation. The first liquid clathrate was prepared accidentally by J.L. Atwood and co-workers in late 1969. The reaction of KN_3 with AlMe_3 , as in Equation (i), was under investigation. The product, a white crystalline solid



(mp 105°C), was known to be soluble in polar media (ethers, amines), but was thought to be insoluble in hydrocarbons. In the hope of obtaining an NMR signal, some of the compound was placed with toluene in an NMR tube. The plan was to heat the mixture in the NMR probe, but before the tube was sealed, the solid disappeared, and two immiscible liquid layers resulted. The composition of the lower layer was easily shown to be $\text{K}(\text{Al}_2\text{Me}_6\text{N}_3) \cdot 3.8\text{C}_6\text{H}_5\text{Me}$. The upper layer was pure toluene. This observation led to the study of the liquid clathrate behavior with host compounds of type $\text{M}^+[\text{Al}_2\text{R}_6\text{X}]^-$ (M = alkali metal or tetra-alkylammonium cation, R = Me or Et and X = various anions¹).

The term "liquid clathrate" presents an obvious paradox. Clathrates are by definition solid substances, but it should be possible to apply the same basic concepts to liquids as well. A liquid clathrate can therefore be defined as follows:

"A liquid clathrate is a liquid association compound which has a fixed (host : guest) ratio at a given temperature."



(Lower phase) : liquid clathrate

(Upper phase) : excess hydrocarbon

Figure 1: Representation of a liquid clathrate (lower phase) with an excess of hydrocarbons (upper phase)¹.

The substance thus formed contains a certain maximum number of guest molecules and is immiscible with excess guest.

Figure 1 presents the situation graphically. The guest molecules in the liquid clathrate are trapped as they would be in a solid clathrate, and can be freed by a change in temperature and reclaimed unaltered.

The major disadvantage of conduction studies of organoaluminium compounds are the extremely dangerous and difficult working conditions involved. The components of these liquid clathrates include aluminium alkyls (e.g. trimethylaluminium) which ignite instantly upon exposure to air, and explode if placed in contact with water. Attempts were therefore, made to synthesise parent compounds related geometrically to $[R_4N]^+ [BR_4]^-$ (R = various aliphatic hydrocarbons). The reasons for choosing these compounds was that they are ionic and are known to form low melting point solids, thus implying poor packing. These novel compounds, the tetraalkylammonium tetraalkylborates, were successfully prepared in high yields and found to be air stable. On addition of hydrocarbon, at room temperature, liquid clathrates resulted.

In an attempt to get a general understanding of liquid clathrate behavior and the properties of liquid clathrates, an in depth study was made on these compounds using various techniques, including NMR spectroscopy, Crystallography and Thermal Analysis.

In the course of experiments, it was found that a wide range of substances can serve as guests in the liquid clathrate medium. Thus, a specific liquid clathrate will incorporate benzene, toluene, p-xylene, anthracene, hexane, dioxane, etc., to varying degrees. These observations led to the

idea of using liquid clathrates for coal extraction as was first expounded by J.L. Atwood¹.

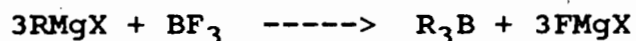
CHAPTER 2

EXPERIMENTAL

1.1 Synthesis of Parent Compounds

1.1.1 Tri-secondary butylboron - Preparation and Purification

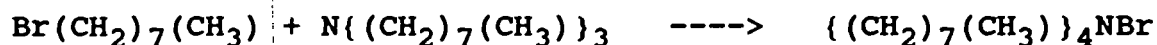
The tri-secondary-butylboron was prepared from Mg turnings (1 mol), secondary-butyl bromide or chloride (1.33 mol) and borontrifluoride etherate (.33 mol) using anhydrous diethyl ether (500 ml). The reaction product was hydrolysed by 250 ml water and the ethereal solution is separated, dried and distilled under nitrogen to remove the ether. The product was distilled under nitrogen atmosphere using a simple fractionating column. The head, tail and middle fractions were collected²².



1.1.2 Bromo-Tetraoctylamine - Preparation and Purification

Tetraoctylamine Bromide was prepared from bromo-octane (1 mol) and trioctylamine (1 mol) using n-Hexane as a diluent (40 ml). The bromo-octane was distilled under reduced pressure ranging between 10 and 13 mm Hg in a dry nitrogen

atmosphere using a simple fractionating column. The trioctylamine (in 30 ml n-Hexane) was placed in a 250 ml two-necked flask equipped with a stirrer, addition funnel, condenser, thermometer, and nitrogen gas inlet. The bromooctane (0.09 mol, 17.379 g, 15.625 ml in 10 ml n-Hexane) was added at room temperature, while stirring. After addition, the mixture was heated to 50 °C and stirred for 10 hrs. After cooling, the resultant solid was washed with excess n-hexane and dried at 60 °C (on a Buchner evaporator) for 3 hours.



1.1.3 Tetraalkylammonium Tetraalkylborates (Parent Compounds 1a,b,c,d) - Preparation and Purification

The preparation of these salts involves the preparation of lithium tetraalkylboron compounds by direct reaction of an organolithium reagent (in hexane diluent) and a trialkylborane in tetrahydrofuran diluent. (A diagram of the apparatus is shown in Figure (2).) The following example illustrates the general procedure. Butyllithium (Aldrich Chemical Co., 0.05 mole, 31.3 ml) was placed in a 500 ml three-necked flask equipped with a stirrer, addition funnel, condenser, thermometer, and nitrogen inlet. Tri-sec-butylborane (0.05 mole, 50 ml) was added at room temperature while stirring. Formation of a white solid was

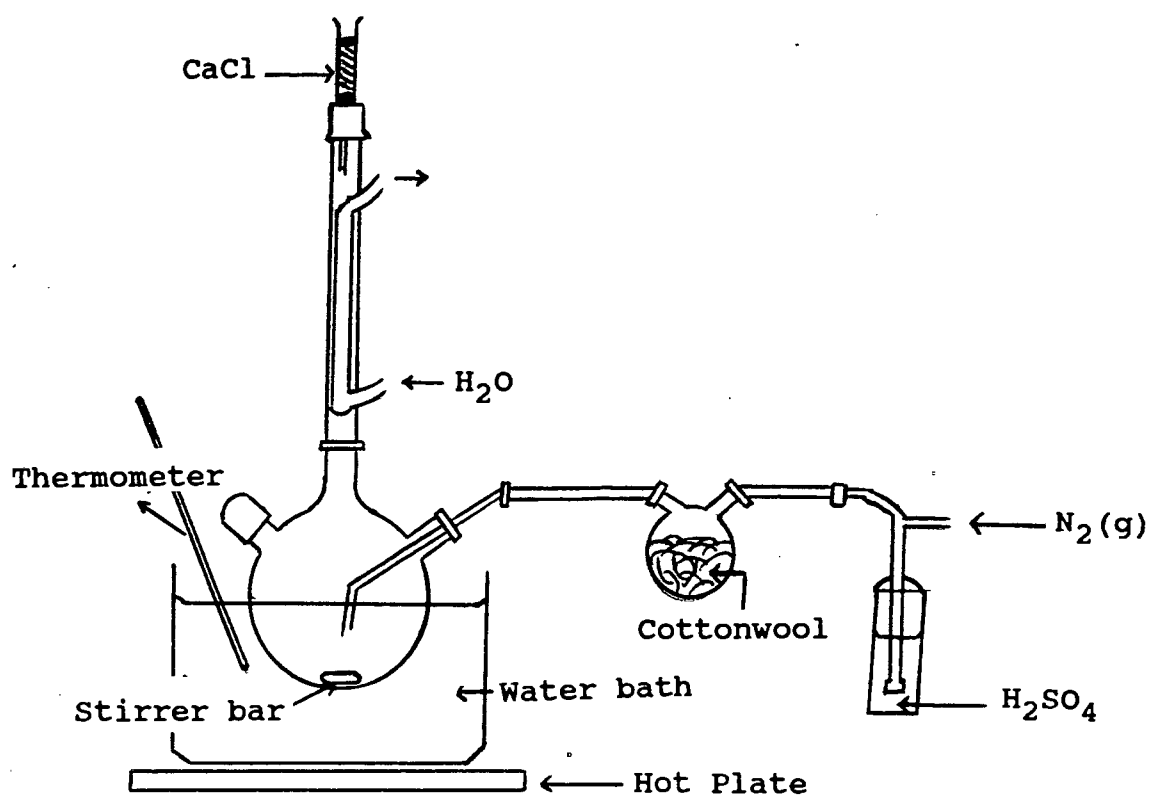
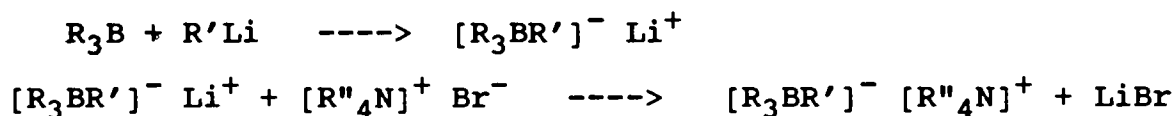


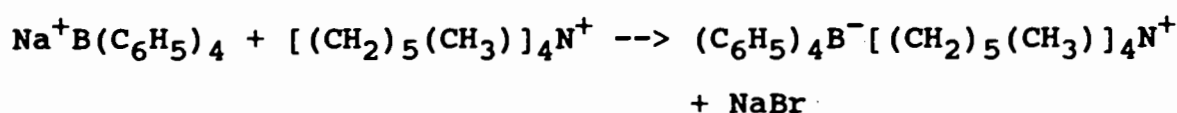
FIGURE 2: A Diagram of the Apparatus used for the Synthesis of Host Compounds 1a,b,c and d.

immediately visible as the temperature rose to 30-40°C. After addition, the heterogeneous mixture was heated to 45°C and stirred for 2 hrs. Tetrahexylammoniumbromide (synthesised or Aldrich Chemical Co., 0.475 moles, 20.6 g) dissolved in a minimum volume of methanol (c.a. 40 ml) was then added to the reaction mixture with stirring and allowed to stir for a further 10 hrs. After cooling, the excess solvent was evaporated off on a Buchner evaporator and the resultant 'oily yellow' product dissolved in a minimum volume of ether. The ethereal layer was washed with fifteen 200-ml portions of water after which NaSO₄ was added to the ethereal layer to remove remaining water. The ethereal layer was then dried at 45°C for 2 hrs. on a Buchner evaporator to yield 21.82 g (81.63% yield, assuming that the first step of the synthesis goes to 90% completion) of tetrahexylammonium (n-butyl)tri-sec-butylboron, m.p. 53-55°C. The texture of the product was noted to be "waxy" and of a light yellow colour. Table 2 summarizes the results from the preparation of stable derivatives.



1.1.4 Tetrahexylammonium Tetrphenylborate (Parent Compound 1e) - Preparation and Purification

This salt was prepared from sodium tetrphenylborate (2.5×10^{-3} moles, 0.856 g) and tetrahexylammoniumbromide (2.5×10^{-3} moles, 1.087 g) in methanol, refluxing the reaction mixture under nitrogen for 2hrs. Formation of a white solid was immediately visible.



The NaBr, being soluble in methanol, remained in solution. The product was washed with five portions of 200-ml methanol/water (50:50) until the washings showed no trace of bromide ion. The resulting solid was dried at 30°C (in an oven) for 3 hrs. to yield 1.582 g (93.9% yield). The tetrahexylammonium tetrphenylboron, m.p. (27-30)°C, was recrystallized from tetrahydrofuran. Table 2 summarizes the results from the preparation of this synthesis.

2.1 Formation and Analysis of Liquid Clathrates

2.1.1 Temperature Dependence Study

A study of the following equilibrium reaction:



was made in order to determine whether a temperature change shifts the equilibrium to the left and whether in so doing decreases the amount of guest material clathrated.

The method involved the preparation of liquid clathrates (from both parent compound 1a and 1b) with different aromatic guests. Each clathrate system was allowed to equilibriate at various temperatures. Aliquots were then sampled and analysed at each temperature by ^1H NMR spectroscopy. A deuterium capillary was used to provide a solvent on to which one could lock without obtaining any interference from the solvent with the liquid clathrate, when the Bruker spectrometer was used. Spectra were also obtained, without using a lock, on the Varian VXR-200. Analysis of a liquid clathrate sample yielded the same result whether analysed on the Bruker (with a deuterium lock) or the Varian (without a lock). This was checked in order to ensure that comparisons could be made between spectra regardless of which spectrometer was used.

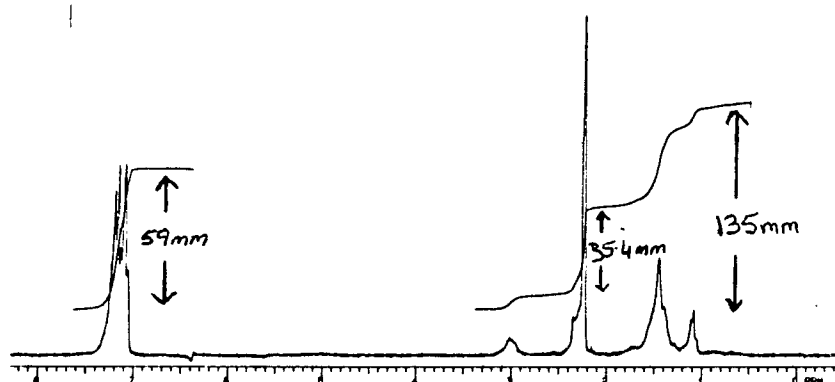
2.1.2 Stoichiometry and Selectivity Studies

For the study of the composition of liquid clathrates of the type H.nG, the clathrates were prepared by adding excess

hydrocarbon guest (G) to the parent compounds. After gentle agitation of the host and guest mixture, the sample was allowed to equilibrate at room temperature. Two immiscible layers separated. Aliquots of both layers were sampled and analyzed by ^1H NMR, using the Varian VXR-200 (no lock being used). The bottom layer revealed parent and guest material whereas the top layer consisted of hydrocarbon (guest) only. The amount of guest material enclathrated was quantified (from the ^1H NMR integration) and hence the G/H ratio could be determined.

The study was extended to include liquid clathrates of type $\text{H}\cdot n_1\text{G}_1\cdot n_2\text{G}_2$. These clathrates were prepared by adding excess G_1 and G_2 (in equal volumes) to the parent compounds at room temperature. The resultant two immiscible layers formed were analyzed by ^1H NMR, as described above. A typical example of an analysis of the liquid clathrate layer is described:

FIGURE 3: ^1H -NMR Spectrum of the Liquid Clathrate $\text{H}\cdot n(\text{Toluene})$



All the host and guest signal in the ^1H -nmr spectrum are integrated. Considering the $\text{H}\cdot n(\text{toluene})$ clathrate (for the

purpose of illustration, see fig. 3), the aromatic protons of the toluene are observed to be well separated from the host protons in the ^1H -spectrum. Since the integration of this signal (59 mm) is due to the presence of the five aromatic protons on n.guest molecules, the integration due to the presence of one proton of n.guest molecules can be calculated ($59 \div 5 \text{ mm} = 11.8 \text{ mm}$). Hence the total integration resulting from the n guest molecules can be subtracted from the total integration measured for the liquid clathrate (158.6 mm). This difference (D, $158.6 - 94.4 \text{ mm}$) gives the integration of the protons for m moles of host molecules. There are 88 protons per molecule of host (for host 1a). Division of D by the number of host protons per molecule therefore yields the integration resulting from m host protons ($64.2 \div 88 = 0.73 \text{ mm}$).

Assuming that m is equal to one, the ratio of moles of guest to host molecules can be determined by dividing the measured integration for one proton of n.guest (11.8 mm) by the measured integration for one proton of host (0.73 mm). This gives a guest to host molar ratio of approximately 16.2 : 1.

The preference of the parent compounds (1a and 1b) for an aromatic guest, as compared to an aliphatic one, namely n-hexane was also studied. The method involves making various mixtures of aromatic and n-hexane in known stoichiometric amounts and adding an excess amount of this mixture of $n_1\text{G}_1$ and $n_2\text{G}_2$ to the parent compound (see

Table 1). The G/H values were then determined from ^1H NMR, as described above. The mass of the Host added in the preparation of the liquid clathrates ($\text{Host} \cdot n_1\text{G}_1 \cdot n_2\text{G}_2$) was noted in each case. The number of moles of host was small in comparison with the number of moles of G_1 and the number of moles of G_2 . Thus the formation of the liquid clathrate did not greatly deplete the total of the combined guest species. However, the initial ratio of $\text{G}_1:\text{G}_2$ was slightly changed in the excess solvent layer after the formation of the liquid clathrate. This was duly calculated in each case. The following example describes one such procedure in full:

Consider the example of the liquid clathrate prepared such that the molar ratio of G_1 (toluene) to G_2 (n-hexane) is (0.5 moles : 0.5 moles). A mass of 1.155 g (0.01253 mol) of toluene was added to 1.004 g (0.01253 mol) of n-hexane. The mole fraction of toluene in this mixture is therefore 0.5. On addition of host material (0.438 g, 7.374×10^{-4} moles), an analysis of the liquid clathrate layer yields the result that the ratio H: G_1 : G_2 is 1 : 3.6 : 2.1. The number of moles of guest remaining in the upper layer (which contains only G_1 and G_2) is then: 0.00987 moles ($0.01253 - 2.655 \times 10^{-4}$ mol) toluene and 0.01010 moles ($0.01253 - 1.534 \times 10^{-3}$ mol) n-hexane. The mole fraction of toluene in this upper layer is therefore 0.494, which is approximately equal to the value (0.5) obtained in the absence of host.

TABLE 1: PREPARATION OF H.AROMATIC.n-HEXANE, FOR THE COMPETITION EXP'S

BENZENE (g)	n-HEXANE (g)	HOST(1a) (g)
0.147	1.36	0.367
0.441	1.055	0.354
0.979	1.004	0.435
1.175	0.245	0.526
TOLUENE (g)	n-HEXANE (g)	HOST(1a) (g)
0.346	2.712	0.387
0.52	1.054	0.392
1.155	1.004	0.438
1.386	0.301	0.537
p-XYLENE (g)	n-HEXANE (g)	HOST(1a) (g)
0.199	1.356	0.411
0.564	1.057	0.475
1.327	1.006	0.387
1.597	0.301	0.406

3.1 Thermal Analysis

3.1.1 Differential Thermal Analysis and Thermogravimetric Analysis of Liquid Clathrates

The energy of clathration (ΔH_c) was calculated using the two methods described below.

A) Equation (2) describes the relationship between the change in enthalpy of vaporization (ΔH_v) and change in temperature.

$$\Delta H_v = m \cdot C_p \cdot (\Delta T) \quad \dots\dots(\text{Equation 2})$$

where m is the mass of the sample for which ΔH is being calculated, and C_p the heat capacity at constant temperature.

Thus, for one mole of substance, Equ.(2) can be written as:

$$\Delta H_v = (K \cdot \Delta T) / n \quad \dots\dots(\text{Equation 3}),$$

where K is a constant, $K = m \cdot C_p$, and n is the number of moles of substance being analyzed. The ratio (R') for the enthalpy of vaporization of Free Guest to Guest trapped in the liquid Clathrate can be calculated from

$$R' = \Delta H_v(\text{fg}) / \Delta H_v(\text{cg}) \quad \dots\dots(\text{Equation 4})$$

$$= (\Delta T_{\text{fg}} \times m_{\text{cg}}) / (\Delta T_{\text{cg}} \times m_{\text{fg}}) \quad \dots(\text{Equation 5})$$

where the subscripts fg and cg refer to free guest and clathrated guest respectively. The change in temperature which occurs when the guest is vaporized, is obtained from the relevant DTA curve. The mass change which accompanies the change in temperature is obtained, over the same furnace temperature range (ΔT_f) over which ΔT was measured, from the relevant TGA curve. The vapor pressure (P) was measured at various temperatures (T) for each of the guests. Using the slope of the plot of $\ln(P)$ versus $1/T$, $\Delta H_v(fg)$ was calculated from

$$\ln(P) = -\Delta H/(RT) + \text{constant} \quad \dots\dots(\text{Equation 6})$$

where R is the Gas constant. (ΔH_v for most of the guests can also be looked up in Tables²³.) Hence, $\Delta H_v(cg)$ (which is the sum of the energy of clathration and the enthalpy of vaporization of the guest) can be obtained by rearrangement of equation (4).

B) The enthalpy of clathration could also be estimated from the measurement of area under the DTA curve. The area was determined by using the cutting and weighing method²⁴.

3.1.2 Isosteniscope Experiments

Liquid clathrate samples were prepared from parent compound (1a) and aromatic guest. The vapor pressures of the clathrate were measured at various temperatures using the Isosteniscope Apparatus. Plotting $\ln P$ versus $1/T$, the enthalpy ($\Delta H_{V(CG)}$) could be obtained as before by using equation (6). The enthalpy of vaporization of the pure guest was obtained as described above. Since $\Delta H_{V(CG)}$ is the sum of the Energy of Clathration and $\Delta H_{V(FG)}$, the value of the clathration energy could be determined.

4.1 Determination of Stability Constants

The parent compound (1a) was weighed into an nmr tube and titrated with aromatic guest. Due to the rapid equilibrium of complexation, $^1\text{H-NMR}$ titrations provided quantitative determination of the binding between the host and guest. Spectra for each titration point were obtained using the Varian VXR-200, with no lock ($T=303\text{ K}$). The TMS peak was taken as the reference. The concentrations of the host and guest were chosen to vary the percentage of complexation from about 10%-100% (see Table 17). The observed chemical shift ($\Delta\delta_{\text{obs.}}$) of the host proton, whose signal could be best observed over the entire titration, was plotted against

the total guest concentration (see fig's. 36 and 37, chapter 6).

These plots were observed to level off at a total guest concentration, which corresponded to the maximum value of n (in H.nG) obtained in earlier experiments. These plots resembled those plots obtained by other researchers in the biochemical field of antibody-antigen reaction studies²⁵. In the latter studies, the association constants were determined from Scatchard plots. It was, therefore, decided to apply the same theory to the liquid clathrate systems, in the hope of determining their association constants.

4.1.1 The use of Scatchard Plots

Equilibria involving the binding of ligands to macromolecules are of great importance in biochemistry. Some macromolecules have more than one binding site and it is often necessary to determine the number of sites involved. Consider first the case of a protein P which binds, per mole, one mole of ligand L. Then



and the association constant K for the binding is given by

$$K = [PL]/([P][L])$$

and the dissociation constant K_d by the reciprocal of K

$$K_d = [P][L]/[PL] \quad \dots\dots(\text{equation 7})$$

Depending on conditions, the binding site may or may not be saturated with L and so we introduce the term saturation fraction, denoted by \bar{y} , where

$$\bar{y} = (\text{conc. of L bound to P})/(\text{total conc. of all forms of P})$$

i.e.

$$\bar{y} = [PL]/([P] + [PL])$$

substituting for [PL] from equ.(7) one has

$$\bar{y} = [L]/(K_d + [L]) \quad \dots\dots(\text{Equation (8)})$$

Now when P is half-saturated with L, $\bar{y}=0.5$ and $[L]=K_d$. Equation 8 can be made to be the basis for a graphical determination of the dissociation constant by rearrangement to the reciprocal form

$$1/\bar{y} = 1 + K_d/[L] \quad \dots\dots(\text{Equation 9})$$

so that a plot of $1/\bar{y}$ versus $1/[L]$ is linear with a slope of K_d .

Consequently if for given initial concentrations of P and L the amount of L bound to P can be ascertained, then K_d can be evaluated. When more than one mole of ligand binds per mole of macromolecules a series of equilibria are set up. Thus, for n binding sites per molecule, it can then be shown that equation 8 now takes the form

$$\bar{Y} = n[L]/(K_d + [L]) \quad \dots\dots\dots(\text{Equation 10})$$

It is assumed that the n sites are equal and independent, i.e. they each display the same standard free energy of binding. K_d is an average dissociation constant and \bar{Y} is the fraction of the total binding sites occupied. Equ.10 can be treated as was equ. 8 to yield the so-called Hughes-Klotz equation

$$1/\bar{Y} = 1/n + K_d/(n[L]) \quad \dots\dots\dots(\text{Equation 11})$$

This can be rearranged to give

$$\bar{Y}/[L] = n/K_d - \bar{Y}/K_d \quad \dots\dots\dots(\text{Equation 12})$$

and the plot of $\bar{Y}/[L]$ against \bar{Y} is linear with a slope of $(-1/K_d)$ and an intercept on the x axis of n/K_d . This form of the equation is called the Scatchard equation²⁶⁻²⁷.

Applying the Scatchard theory to liquid clathrates, consider the parent compound (host) to behave as a macromolecule and the guest to behave as a ligand. By these treatments of

experimental data the value of K_d and the number of binding sites could theoretically be determined.

The change in chemical shift of the host proton being monitored during the titration was noted and used to calculate the value of \bar{y} . The chemical shift (δ) is given by:

$$\delta = (\delta_{ch} \times f_c) + (\delta_{fh} \times f_f) \quad \dots(\text{Equation 13})$$

where δ_{ch} and δ_{fh} represent the chemical shift of the host when clathrated and when free respectively, and the fraction of free and clathrated sites on the host is given by f_f and f_c respectively. Thus, the change in chemical shift of the host, assuming that $\delta_{fh} = 0$, is given by

$$\Delta\delta = \Delta\delta_{ch} \times f_c \quad (\Delta\delta_{ch} = \text{maximum complexation shift when } n \text{ is a maximum for } H.nG)$$

So, the fraction of total binding sites occupied, \bar{y} , can be calculated from equation 14.

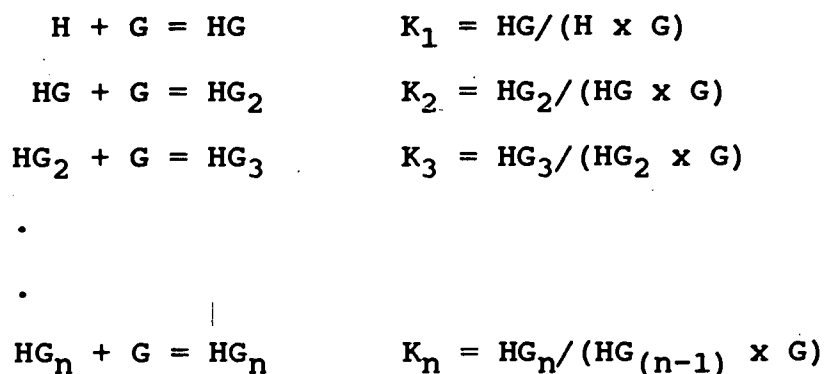
$$\bar{y} = \Delta\delta / \Delta\delta_{ch} \quad \dots(\text{Equation 14})$$

When this theory was applied to the data obtained for the liquid clathrate system, it was observed that the change in chemical shift from one titration point to the next was not significantly large enough for a reasonable calculation of \bar{y} . Thus, the method of using Scatchard plots for the calculation of K_d was not feasible.

The approach of solving two simultaneous equations containing the stability constant (K) proved to be more successful.

4.1.2 Determination of Stability Constants by solving Simultaneous Equations

Consider a system in which n guest molecules are clathrated to the host. Assume that the n sites are equal and independent and the stability constant $K = K_1 = K_2 \dots = K_n$.



Now the total host concentration (TH) and total guest concentration (TG) can be expressed in terms of H, G and K (see equations 15 and 16).

$$\begin{aligned}
 TH &= H + HG + HG_2 + HG_3 + \dots \dots HG_n \\
 &= H(1 + K.G + K^2G^2 + \dots \dots K^nG^n) \quad \dots \dots (\text{Equation 15})
 \end{aligned}$$

$$\begin{aligned}
 TG &= G + HG + 2HG_2 + 3HG_3 + \dots nHG_n \\
 &= G + H(KG + 2(KG)^2 + 3(KG)^3 + \dots n(KG)^n) \dots (\text{Equ.16})
 \end{aligned}$$

For a chosen value of K, equations 15 and 16 are solved for the free guest and host concentrations (G and H respectively). Using this value of K, and the calculated values of G and H, a theoretical value of TG can be calculated (using equ.16).

5 Application of Nuclear Overhauser Effects

5.1 Sample Preparation

Sample preparation involved shaking the parent compound (1a) with an excess of guest at room temperature and then allowing the mixture to equilibrate for approx. 2 hrs. The liquid clathrate layer was transferred to an inner capillary (a 60 μ l insert tube) and placed in a normal NMR tube containing deuterium. Samples were run, using a D₂O lock, on the Varian VXR-200 spectrometer (see Appendix I for experimental parameters used).

The main precaution that needed to be taken was the rigorous exclusion of paramagnetic materials, principally oxygen. An effective means for degassing a sample is the freeze-thaw technique, preferably carried out directly in the NMR tube.

Since the sample was contained in an insert tube, degassing of the sample was carried out directly in this tube. This required the following sequence of events:

- 1) Cool the sample under an anhydrous atmosphere in liquid nitrogen or dry ice/acetone.
- 2) Evacuate the space above the solution by connecting it to a good vacuum line.
- 3) Isolate from the line, and warm back to room temperature.
- 4) Admit nitrogen and repeat from (1).

This sequence was repeated at least six times. It is preferable to perform the degassing immediately before the nOe experiments, because even in a tube with a cap, oxygen diffuses back in easily in a short time period.

5.2 The Difference Method

In measuring an nOe one is required to saturate a resonance signal and then compare the intensities of other resonance signals with their equilibrium values. The scheme known as nOe difference spectroscopy was employed for this purpose (Figure (4)).

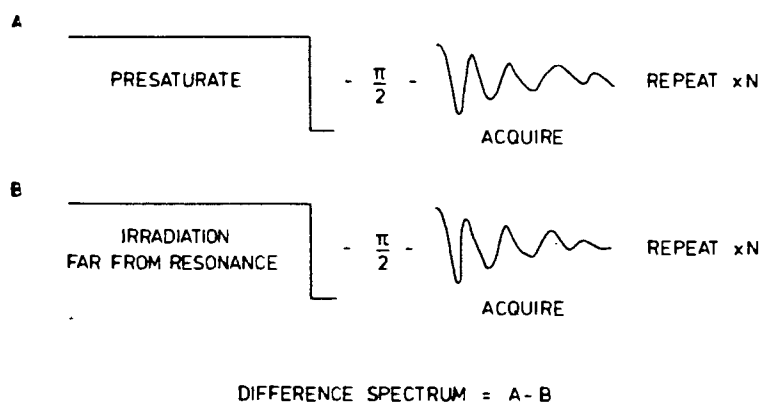


Figure (4): The Experimental Scheme for nOe Difference Spectroscopy.

5.3 Quantitative Measurements

Once a satisfactory nOe difference spectrum had been obtained, it was still necessary to integrate the resonances and determine their various percentage nOe's (η). The method used to determine η , which follows from the definition of η (see chapter 7), was to integrate a multiplet in the off-resonance component of the difference experiment and assign its area as 100%. This corresponded to I_0 . Intergration of the corresponding multiplet in the difference spectrum then yielded η directly, provided that the transform was carried out with the same scaling factor.

6.1 Crystallographic Analysis of Parent Compounds

Crystals of parent compound (1a) were obtained when the liquid clathrate solution (obtained from 1a (host) and cyclo-hexene (guest)) was left standing in a vial for approximately 7 months. Crystals of tetrahexylammonium tetraphenylborate were obtained from a saturated solution of the white solid (synthesis described above) in tetrahydrofuran.

The parent compound 1a was expected to be disordered. This was found to be the case on trying to solve the structure and an attempt was made to model the anion (borate ion) as a disordered sphere by replacing it with a calculated group scattering factor.

6.1.1 Calculation of Spherically Averaged Molecular Scattering Factors.

The disorder problem in a given structure may be approached by the calculation and use of a molecular scattering factor for the disordered group²⁸.

These calculations were carried out for the anion (isobutyl)(tri-sec-butyl)borate in a randomly chosen tetrahedral conformation. The procedure involves two

stages: (1) obtaining a calculated group scattering factor for a range of $\sin\theta/\lambda$ from the program MULTAN, and (2) subsequently obtaining a curve-fit to express the scattering factor in a form suitable for the refinement program used.

1) The MULTAN 78 program NORMAL²⁹ calculates spherically averaged scattering factors for randomly distributed groups or orientationally disordered groups of atoms in a unit cell from the Debye scattering formula:

$$G = \sum_{\text{all } J}^N \sum_{\text{all } K}^N F(J) \cdot F(K) \times (\sin(A) \times r_{jk}) / (A \times r_{jk})$$

where $A = (4\pi \times (\sin\theta)/\lambda)$; N is the number of atoms, r_{jk} the distance between atoms j and k , and $F(J)$ and $F(K)$, the atomic scattering factors of atoms j and k respectively. Spatial co-ordinates for all atoms of the anion in the imaginary cubic unit cell ($a = 30.0 \text{ \AA}$) were calculated (see Appendix II) from a model of the anion.

2) The refinement program SHELX-76 required the scattering factor to be expressed in the form:

$$g = a_1 e^{-b_1 x^2} + a_2 e^{-b_2 x^2} + a_3 e^{-b_3 x^2} + a_4 e^{-b_4 x^2} + c$$

The scattering factors obtained from MULTAN were plotted as a function of $\sin\theta/\lambda$. A simple calculation from statistical

methods was used to fit the approximating function to the calculated curves²⁸ (see fig. 5).

$$g = f(x)$$

$$= a_1 e^{-b_1 x^2} + c$$

$$a = m - c$$

$$b = 1/(2n^2)$$

for $n = x$ such that

$$f(x) = 0.6(m-c) + c$$

$$= k$$

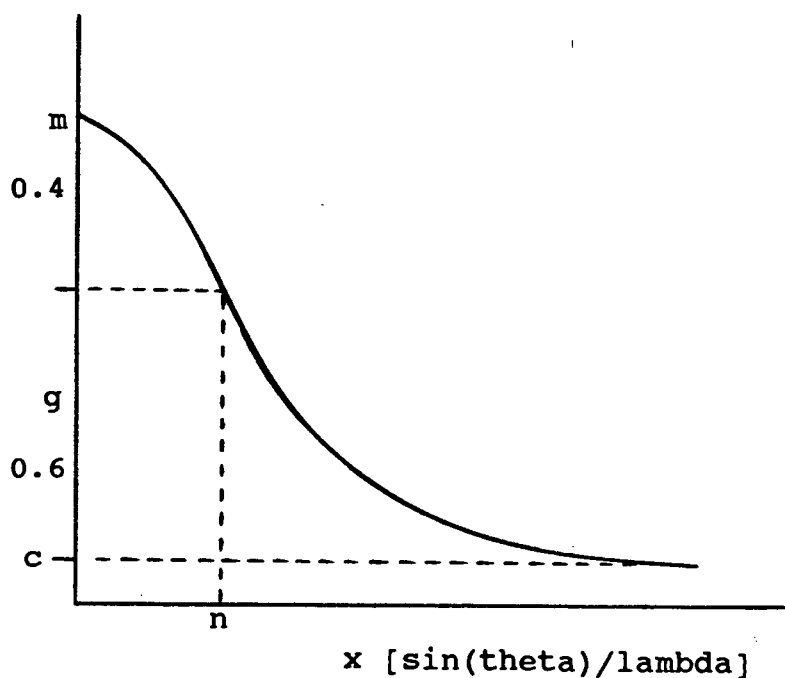


Figure (5): Derivation of curve-fit expression from experimental data.

As the shape of the approximating curve (see figure 6) is derived from the addition of normal distribution functions, it cannot take into account any maxima or minima other than at $\sin\theta/\lambda=0$.

The curve fit needs to be best in the range $0 < \sin\theta/\lambda < 0.5$, because most x-ray crystal data are collected in that range. Curves and values of the scattering factors from MULTAN and

those obtained by the curve-fit expressions are tabulated and depicted in Appendix III.

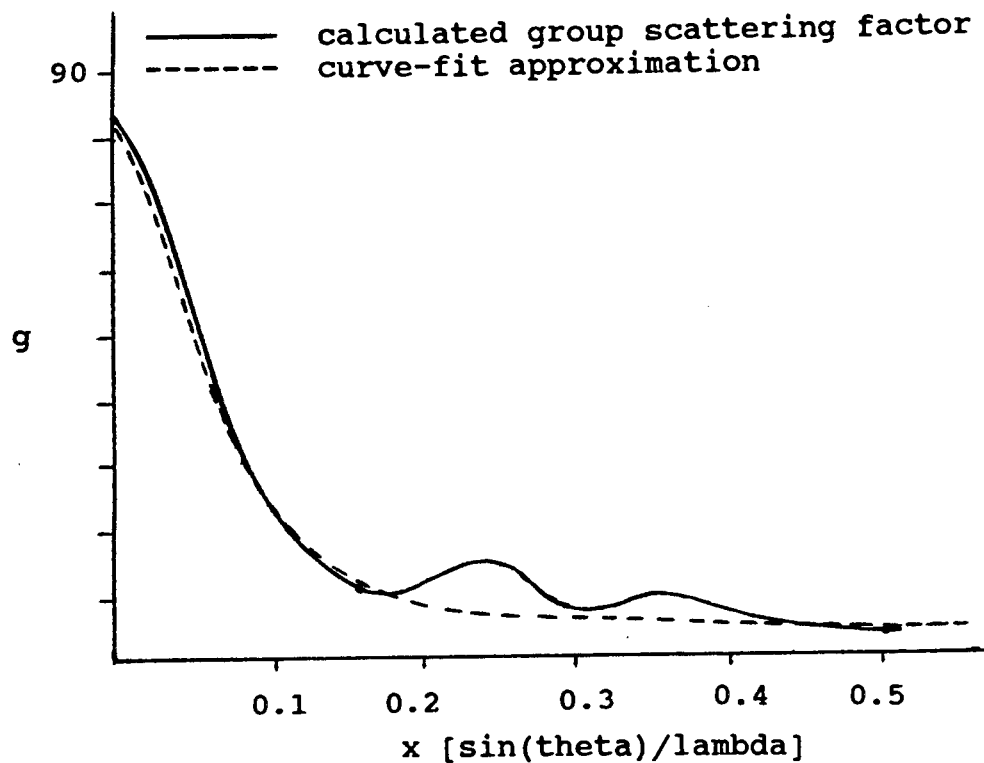


Figure 6: Approximate representation of molecular scattering factors for a spherically disordered molecule generated by MULTAN, and a curve-fit used to express the average spherical molecular scattering factor for use in SHELX76⁴⁶.

6.1.2 Preliminary X-Ray Analysis

Single crystals were selected, checked for reflection quality and then mounted for data collection on the diffractometer. A two-circle optical goniometer was used for the initial alignment. Oscillation photography provided the final precise crystal alignment.

Oscillation and Weissenberg (zero layer and upper layer) photographs were taken using a non-intergrating Stoe (Heidelberg) goniometer attached to a camera of radius 28.65mm. Ni-filtered $\text{CuK}\alpha$ radiation ($\lambda = 1.5418 \text{ \AA}$) was used. The x-ray generators, models Philips PW 1120 and PW 1008, were operated at 0.8 kW (20 mA and 40 kV). X-ray films (3M) were processed in the usual manner with x-ray developer and fixer solutions.

Unit cell dimensions and space group symmetries were determined from the photographs.

6.1.3 Diffractometer Data Collection

Suitable crystals were mounted and given to Dr M. Niven for a diffractometer data collection.

For each structure, the relative intensities of the reflections were measured on an Enraf-Nonius CAD4 diffractometer, with a Philips generator, operating at 1.5 kW (30 mA and 50 kV) and graphite monochromated MoK radiation ($\lambda = 0.7107 \text{ \AA}$) was used.

In each case, accurate cell parameters were obtained (at room temperature) by a least squares analysis on the setting angles of 24 reflections (in the range $16^\circ < \theta < 17^\circ$) on the diffractometer. The three-dimensional intensity data sets were then collected employing the ω - 2θ scan technique.³⁰

To ensure instrumental stability and to monitor any crystal decomposition, the intensities of three reference reflections were measured at approximately hourly intervals throughout the duration of the data collections, and the centering was checked every 200 measured reflections.

An empirical absorption correction³¹ and a Lorentz-polarization correction were applied to both sets of reflection data.

6.1.4 Computation

All computations were performed on a Univac 1106 computer system at the computer centre of the University of Cape Town.

The program SHELX76 was used for crystallographic data reduction, structure solution and refinement. Features of the program which were utilized included data reduction, full-matrix least-squares refinements, geometric positioning and constrained refinement of the hydrogen atoms and structure factor listings.

The agreement between observed (F_o) and calculated (F_c) structure factors is expressed by the conventional residual index R ³² defined as

$$R = \frac{\sum ||F_o| - |F_c||}{\sum |F_o|}$$
$$= \frac{\sum |\Delta|}{\sum |F_o|}$$

or expressed as

$$R_w = \frac{\sum w^{1/2} |\Delta|}{\sum w^{1/2} |F_o|}$$

where $w = k / \{\delta^2(F) + gF^2\}$ upon introduction of a weighting scheme. k was redetermined after each structure factor calculation. The value of g was chosen to give the smallest variation of $w\Delta^2$ with the magnitude of F_c .

Atomic radii used were those of Pauling³³. Scattering factors for all non-hydrogen atoms were from Cromer and Mann³⁴ and those for the hydrogen atoms were from Stewart et al³⁵.

The program PLUTO³⁶ was used for the plotting of individual molecules and molecules in crystalline arrangement.

CHAPTER 3

3.1: Preparation and Characterization of novel air-stable parent compounds

Lithium and sodium tetraalkylboron compounds have been prepared by the reaction of alkyllithium and alkylsodium reagents with trialkylboranes. Over 30 years ago, Thompson and Stephen³⁷ reported an unsuccessful attempt to prepare these compounds. Soon after this report Johnson and his co-workers³⁸ observed a positive reaction when they combined tributylborane and n-butyllithium. In 1940 Schlesinger and Brown³⁹ obtained a white solid from the reaction of equimolar amounts of ethyllithium and trimethylborane, to which they assigned the formula $\text{LiC}_2\text{H}_5\cdot\text{B}(\text{CH}_3)_3$. In the ensuing years Hurd⁴⁰ prepared lithium tetramethyl-boron, and Parsons and co-workers prepared lithium trimethyl-propenylboron by this method. However, the direct reaction of an organometallic with trialkylborane in hydrocarbon diluent, as described by Damico⁴¹, proceeds smoothly to give the desired MBR_4 compounds, which are easily purified. This method was used in the synthesis of the parent compounds. Preparation of the tetraalkylammonium tetraalkylborate parent compounds $[\text{R}_3\text{BR}']^- [\text{R}''_4\text{N}]^+$ (1) involve reacting an organolithium reagent and a trialkylborane to produce a lithium tetraalkylboron intermediate (equation 18) which is highly reactive to air. Thereafter the air-stable parent

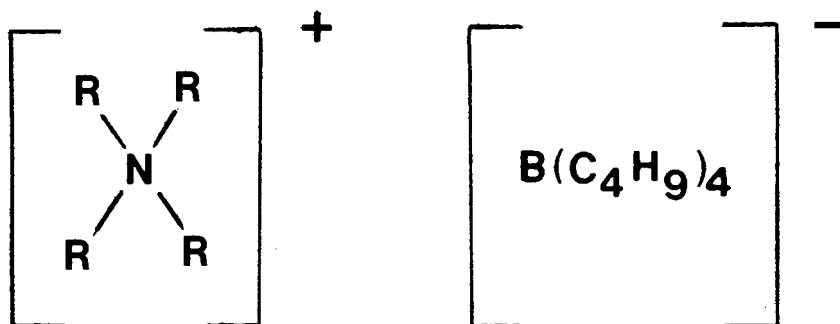
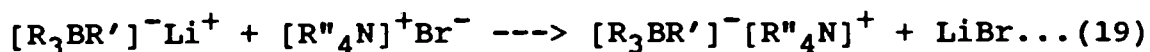


FIGURE 7: Host compounds that were synthesised:

- 1 a : R = hexyl
- b : R = butyl
- c : R = octyl
- d : R = methyl
- e : R = phenyl

compound (1) (see figure 7) is formed by reaction of the lithium tetraalkylboron salt with tetraalkylammonium bromide (equation 19).



The trialkylborane compound is prepared through the Grignard reaction, as described by El-Fayoumy and co-workers⁴².

The reactions described by equation 18 and 19 (above) were carried out, under nitrogen, in methanol.

Since lithium tetraalkylboron compounds are quite reactive to air, direct analysis of these materials is difficult. It was found, however, that the products $[R_3BR']^- [R''_4N]^+$ which are analyzable derivatives of these compounds are easily prepared in high yields. The results of the above reactions are summarized in Table 2.

Since high yields of pure derivatives are obtained in all cases, there can be little doubt that the original organoboron compounds (equation 18) are pure.

The purity and assignment of structures of compounds (1) were obtained from microanalysis (see Table 2) and nuclear magnetic resonance (n.m.r.) studies (discussed below).

3.2: Characterization of Host compounds using NMR Spectroscopy

In order to simplify the interpretation of the tetrahexylammonium tetraalkylborate (host) nmr spectra, the spectra of tetrahexylammonium bromide were first analysed. In the carbon-13 spectrum of tetrahexylammonium bromide (fig. 8), all the carbon assignments could be made by taking shielding effects into account and noting that, generally, CH₂-carbon resonances occur at higher field than CH₃-proton resonances. The CH₃-carbon resonances were confirmed using the APT (Attached Proton Test) experiment⁴³ (fig.9) in which the carbon atoms attached to even numbers of protons are separated from those having an odd number of protons. The remaining CH₂-carbon resonances were assigned on the basis of shielding effects.

Having assigned all the carbon atoms, use was made of the HETCOR (heteronuclear correlation) pulse sequence⁴³ (fig.10) to assign the proton resonance peaks (fig.11).

A cross-peak in the HETCOR plot at 'A' corresponds to 59.125 ppm on the ¹³C-axis and 3.13 ppm on the ¹H-axis. The carbon

TABLE 2: RESULTS OF SYNTHESSES OF HOST COMPOUNDS

HOST	%YIELD	MPnt (C)	% CARBON		% HYDROGEN			% NITROGEN	
			THEOR	OBS	THEOR	OBS	THEOR	OBS	
1a	81	53-55	80.89	80.95	14.93	14.7	2.34	2.4	
1b	84	33-37	79.78	77.65	15.06	15	2.91	3	
1c	87	27-30	76.64	76.5	15.44	15.38	4.47	4.5	
1d	74		83.3	81.2	13.11	12.54	2.02	2.56	
1e	93		85.5	84.6	10.77	10.9	2.08	2.18	

TABLE 3: 1H- AND 13C- ASSIGNMENTS FOR TETRAHEXYLAMMONIUM BROMIDE

A. Proton Assignments

Peak no.	Position (ppm)	Multiplicity	Integration	Assignment
1	3.38	triplet	8 H	a
2	1.6-1.8	broad multiplet	8 H	e
3	1.38	sharp multiplet	24 H	b, c, d
4	0.9	multiplet	12 H	f

B. Carbon Assignments

Peak no.	Position (ppm)	Assignment
1	59.28	a
2	31.21	b
3	26.04	c
4	22.37	d
5	22.30	e
6	13.85	f

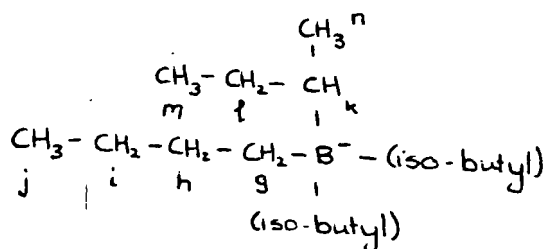


FIGURE 8: ^{13}C -Spectrum of Tetrahexylammonium Bromide

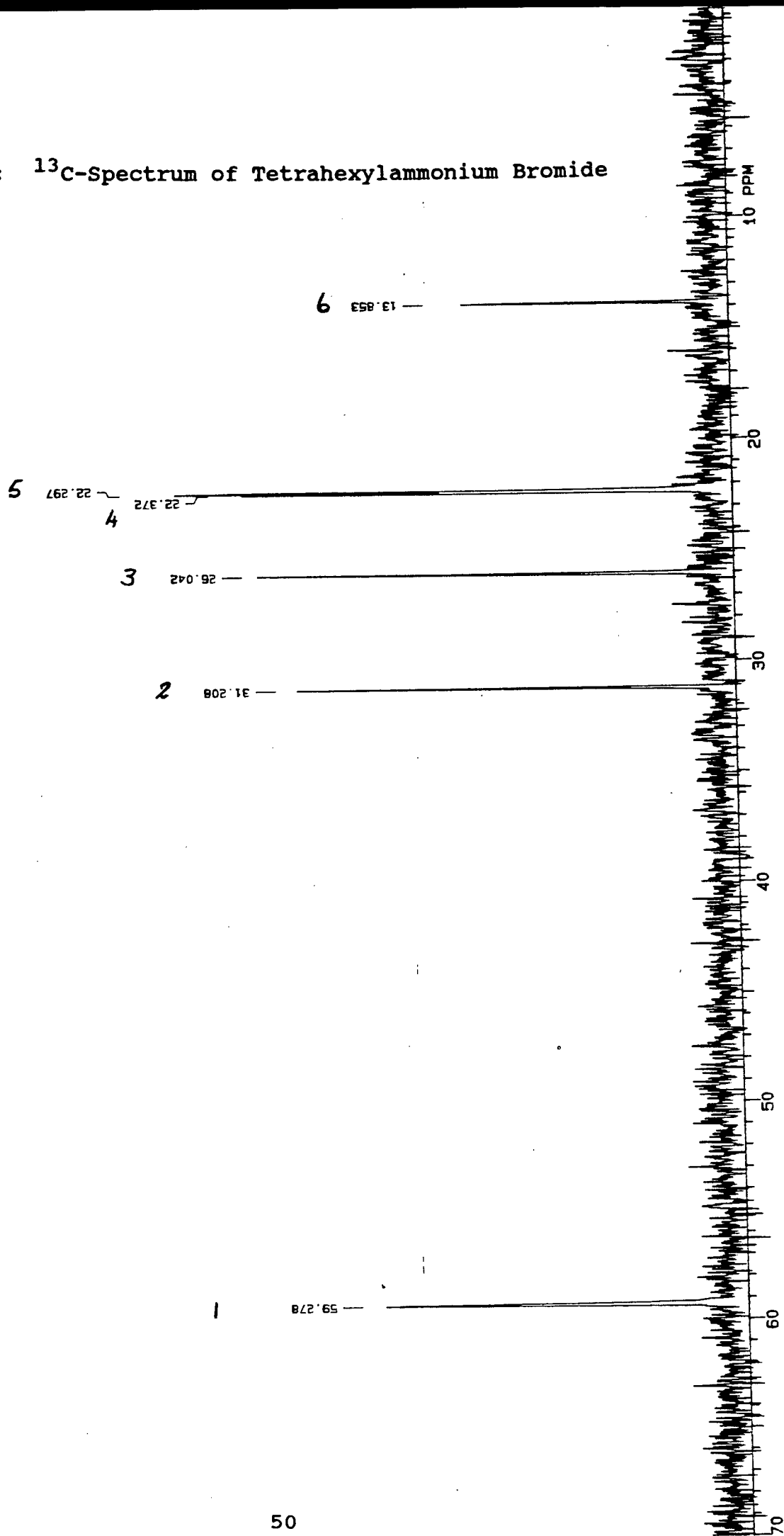


FIGURE 9: APT Plot of Tetrahexylammonium Bromide

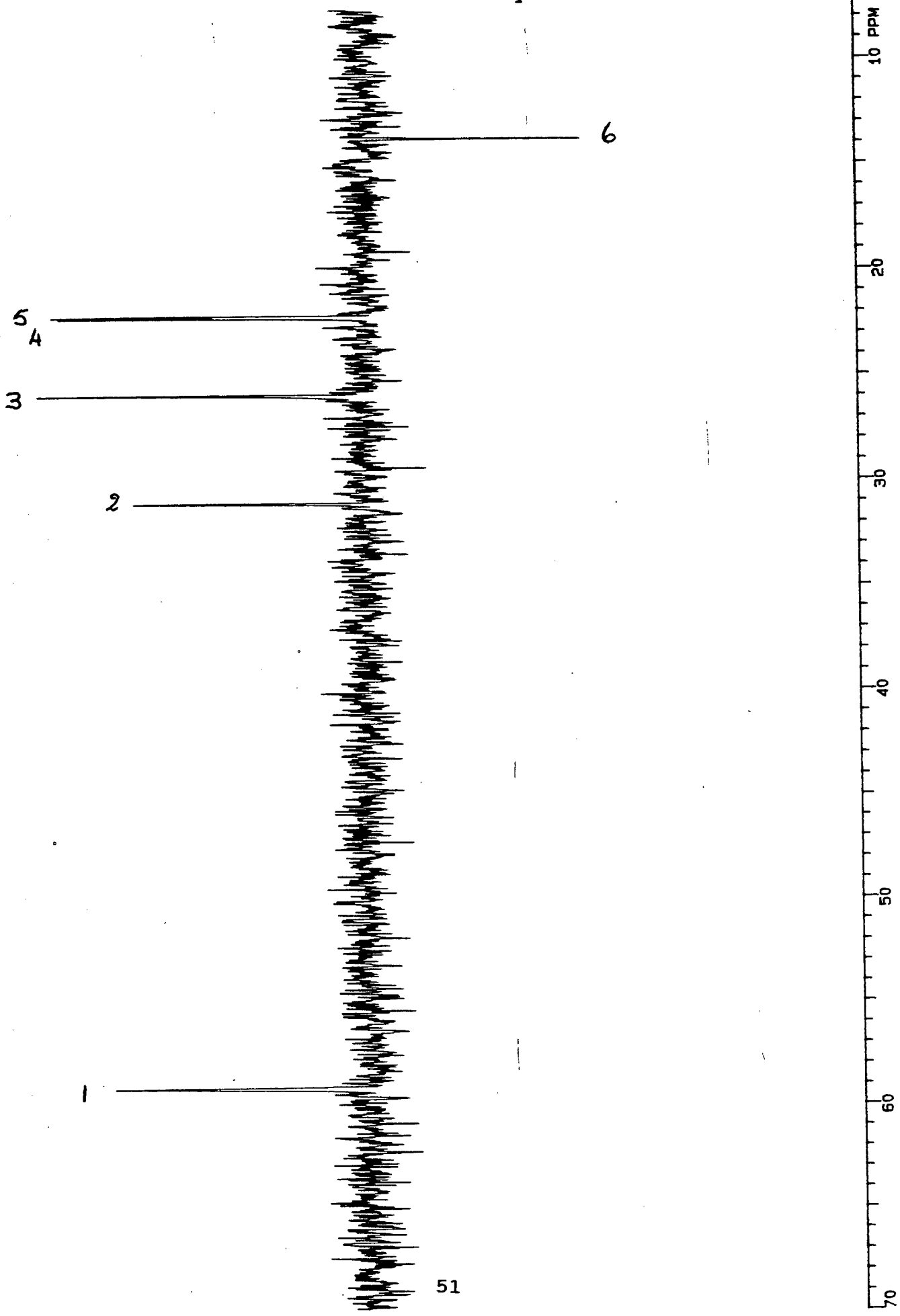
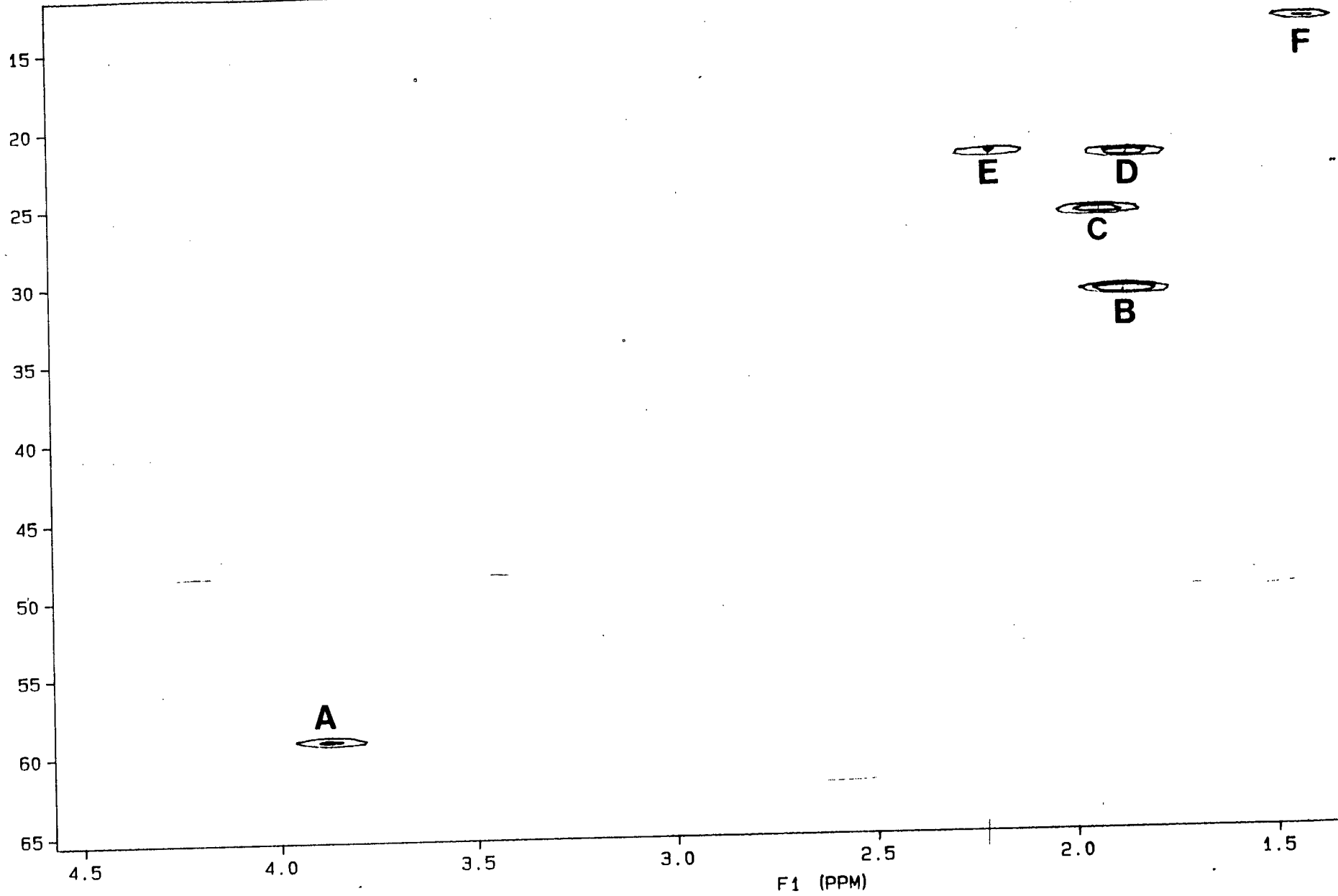
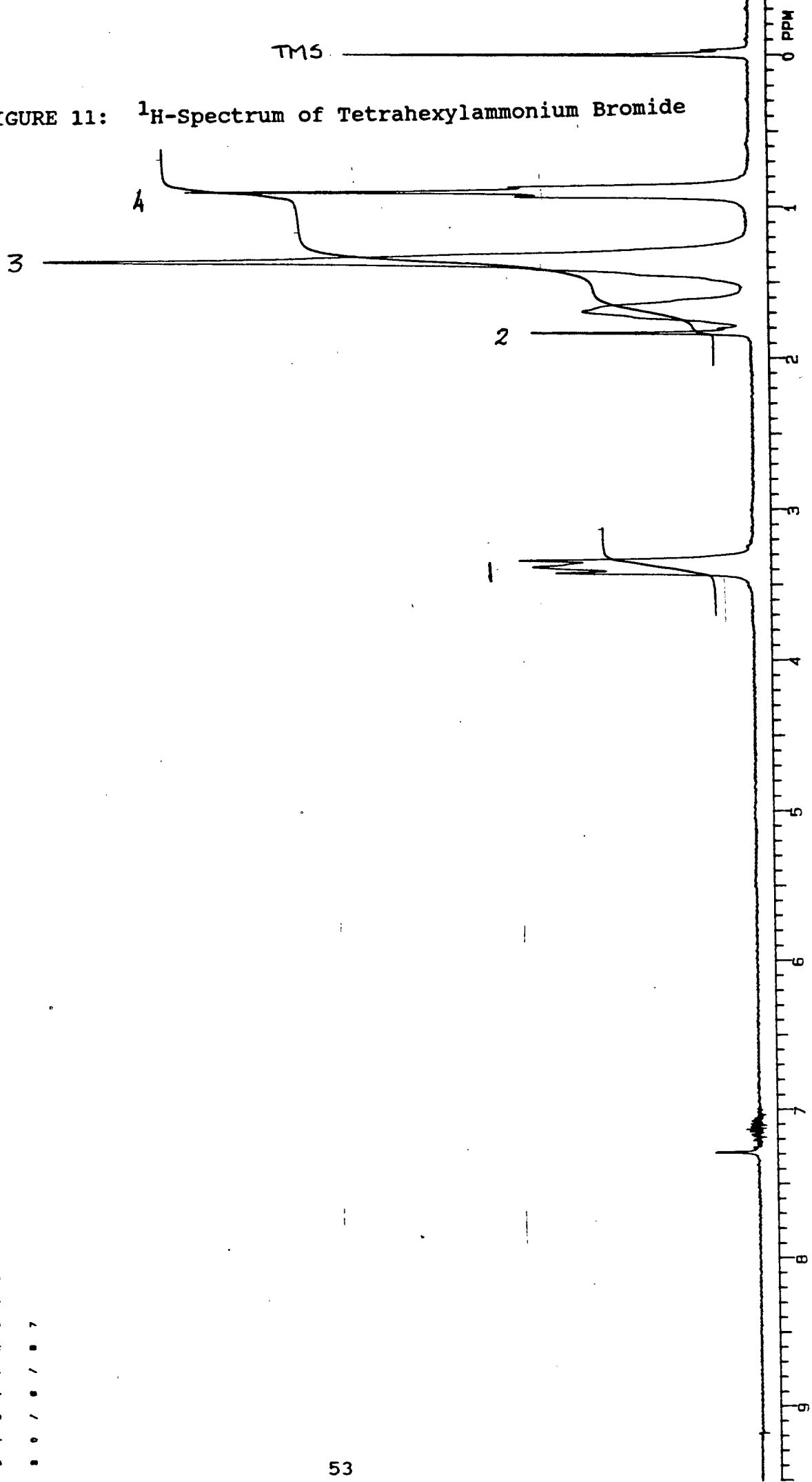


FIGURE 10: HETCOR Plot of Tetrahexylammonium Bromide



MEI DE
T E S T O N O R Y I M B P
S T D . P R O T O M
8 0 / 8 / 8 7

FIGURE 11: ^1H -Spectrum of Tetrahexylammonium Bromide



resonance has been assigned to carbon (a) (see fig.8) and therefore the 3.13 ppm resonance peak must result from the proton attached to this carbon atom. Similarly cross-peaks B, C, D, E, and F led to the assignment of the protons attached to carbons b, c, d, e, and f respectively. In this manner all the proton resonances were assigned. The ^1H - and ^{13}C - NMR assignments are tabulated in Table 3.

By comparison of the ^{13}C -spectrum of host(1a) with that of tetrahexylammonium bromide, peaks 1 to 6 (figure 12) were identified (results are tabulated in Table 4). This left the assignment of the host carbon atoms g to n still to be made. Using the APT experiment (fig. 13), a distinction could be made between carbon signals of $\text{CH}'\text{s}$, CH_2' and CH_3' 's. Thus the resonance peaks occurring at 31.8 ppm, 29.8 ppm, 29.0 ppm and 28.9 ppm result from CH_2 -carbon atoms, while those occurring at 18.5 ppm, 18.4 ppm, 16.0 ppm and 14.9 ppm are due to one CH - and three CH_3 -carbon atoms. Knowing that the boron atom has a negative charge and the more deshielded the carbon atom the lower the field at which it is observed to resonate, the assignment of these resonance peaks could be made (see Table 4).

Using a similar approach, the proton spectrum (figure 14) of host(1a) was assigned. The results are tabulated in Table 5.

TABLE 4: CARBON-13 ASSIGNMENTS FOR HOST (1a)

Peak no.	Position (ppm)	Assignment
1	59.05	a
2	31.07	b
3	25.89	c
4	22.31	d
5	21.95	e
6	13.76	f
7	28.93	g
8	29.1	h
9	31.81	i
10	18.6	j
11	14.99	k
12	29.88	l
13	18.43	m
14	15.99	n

TABLE 5: PROTON ASSIGNMENTS FOR HOST (1a)

Peak no.	Position (ppm)	Multiplicity	Integration	Assignment
1	3.13	broad multiplet	8 H	a
2	1.63	broad multiplet	14 H	b and m
3	1.38	multiplet	24 H	c, d and e
4	1.13	multiplet	4 H	h and i
5	0.7-1.0	multiplet	33 H	f, j, l and n
6	0.2	multiplet	3 H	k
7	0.05	multiplet	2 H	g

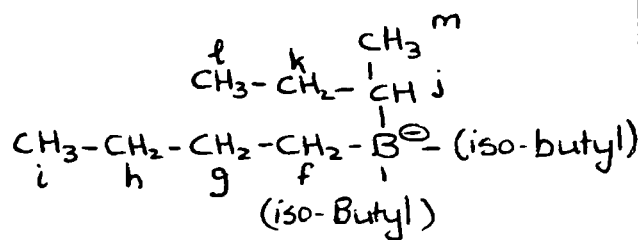
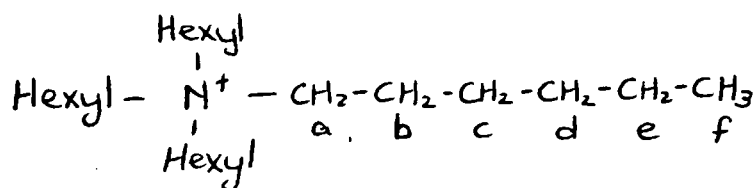
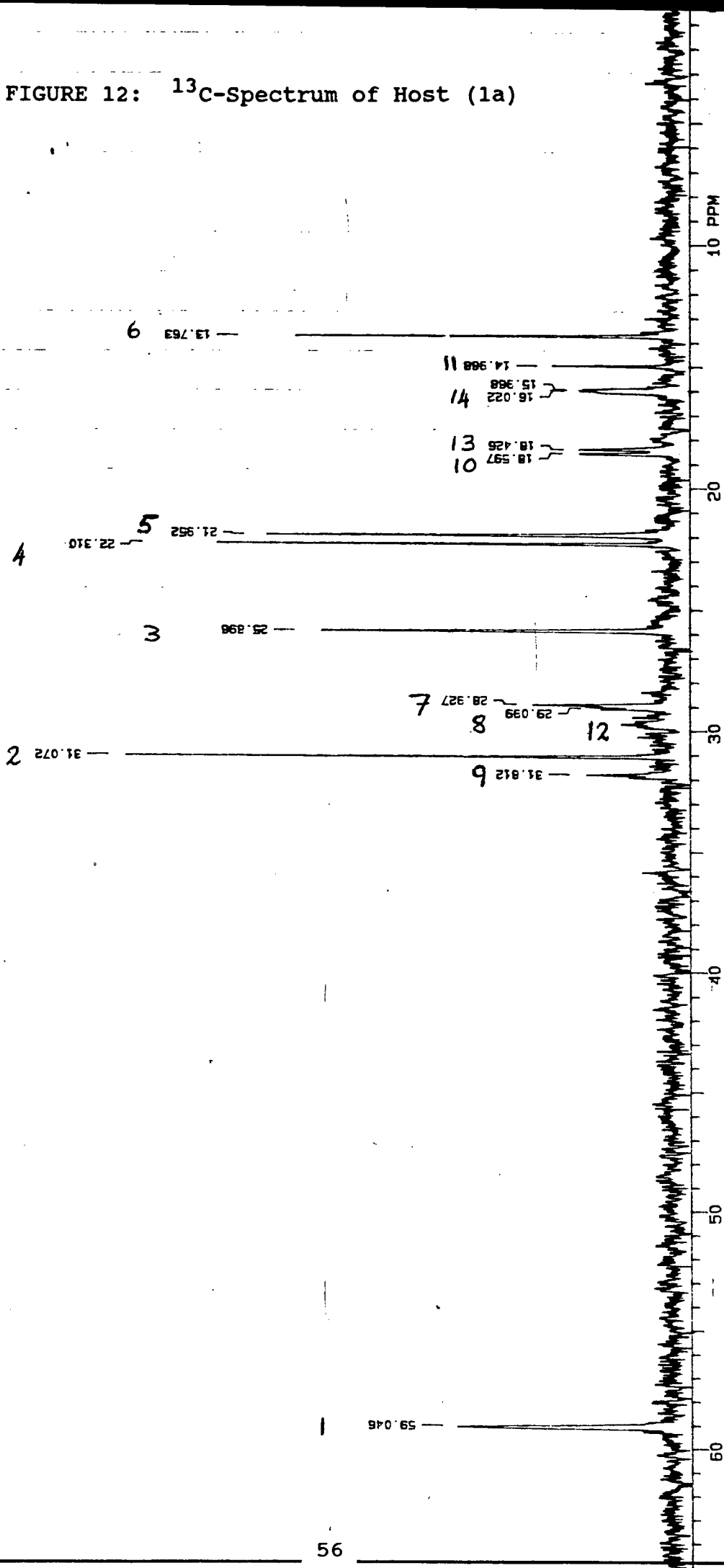


FIGURE 12: ¹³C-Spectrum of Host (1a)



Number _____
 File _____
 Date 28-08-87
 R. VYR 200

SAMPLE
 NAME: HEIDI
 HJ C-MEX
 CARBON-13
 28/8/87

Pulse Sequence: STD13C
 Tube OD: _____ mm
 Temp: _____ °C
 Solvent: CDCL3

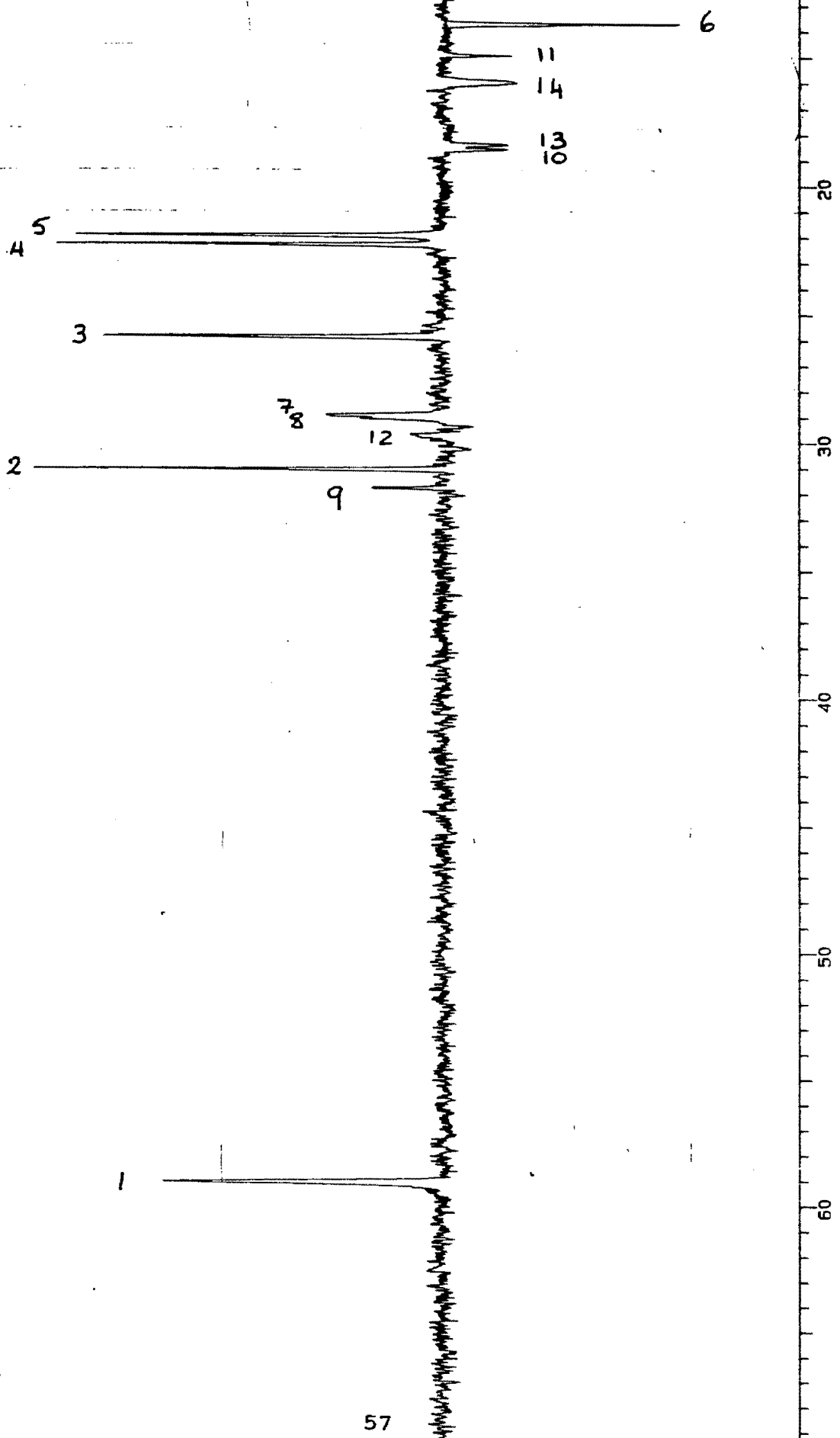
EXPERIMENT
 FN: 32 K RE: _____ sec CD: _____ sec
 LB: 1.000 Hz AF: _____ sec COD: _____
 Width: 3259.7 Hz/gram Start: 0 Hz/gram
 Reference: _____

PLOT/PROCESSING
 Nucleus: 13C
 Mode: VVV
 Modulator: Mod: S
 Pulse Width: 17.5 usec
 Offset: 170.2 Hz
 Power: 5 db
 Freq: 7700 Hz
 Power Mod: _____

DECOUPLE
 Nucleus: 13C
 Freq: 50 MHz
 Mode: 100 Hz
 Pulse Width: 100 usec
 Offset: 0 Hz
 Delay: 0 sec
 Transients: 1024

OBSERVE
 Nucleus: 13C
 Freq: 101.625 MHz
 Mode: 100 usec
 Pulse Width: 100 usec
 Offset: 0 Hz
 Delay: 0 sec
 Transients: 1024

FIGURE 13: APT Plot of Host (1a)



57

Number _____

File APT

Date 26-06-87

XL VXH 200

EXPERIMENT

Sample HE101 OIL (RU'NSR4) R'-HEXYL APT

Date 26/6/87

Pulse Sequence APT

Tube OD _____ mm

Temp _____ °C

Solvent CDCl3

PLT PROCESSING

FN _____

LB 1.000 Hz AF _____

Width 3259.7 Hz/ppm Shim 237.5 Hz/ppm

Reference _____

DECOUPLE

Nucleus 13C

Mod YNY

Modulation Mode S

Pulse Width 17.5 μsec

Offset 170.2 Hz

Power 5 dB

Freq 7700 Hz

Power Mod 47.0

OBSERVE

Nucleus 13C

Spec. Width 3996.8 Hz

Acq. Time 1.001 sec

Pulse Width 8.0 μsec

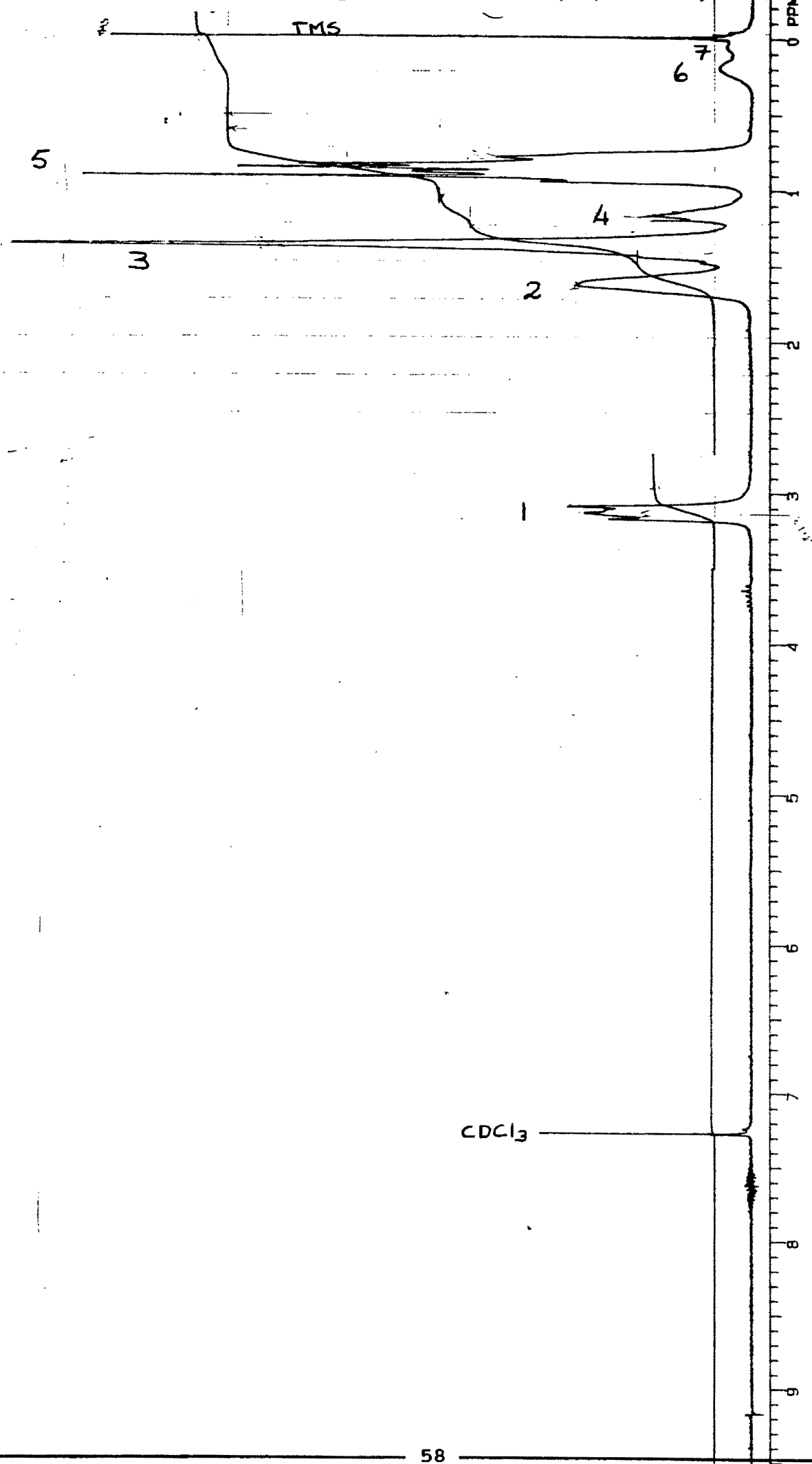
Transmit 6688

Power 50 mW

Offset 2500 Hz

Delay 0 sec

FIGURE 14: ¹H-Spectrum of Host (1a)

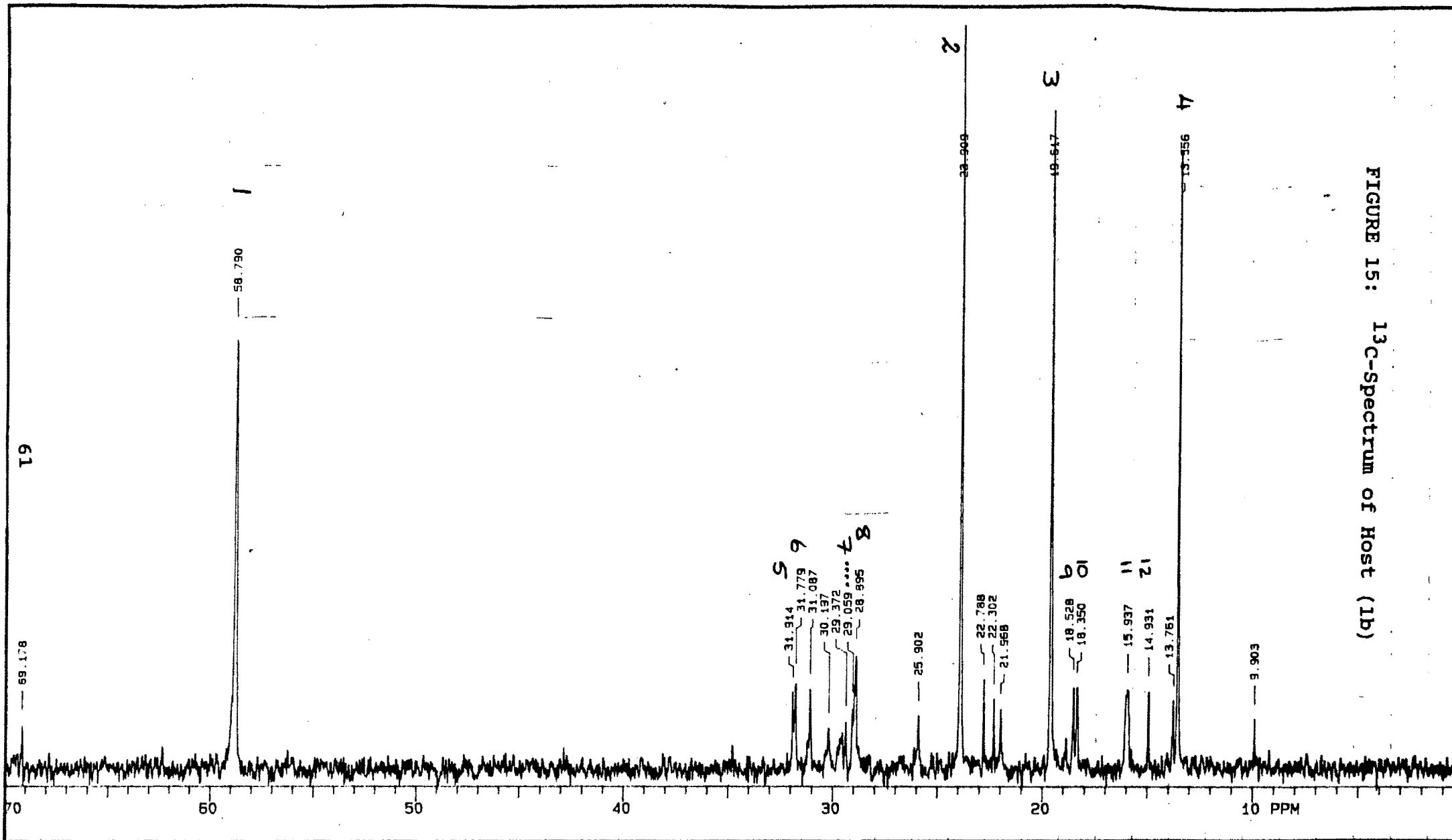


OBSERVE		Pulse Width: 16.0 μ sec		Transmit: 54	
Nuclei: 1.750	Freq: 200 MHz	Off: 1000 Hz	Delay: 0 sec		
Spec Width: 7000.0 Hz	Off: 1000 Hz	Delay: 0 sec			
Avg Time: 3.752 sec					
Pulse Width: 16.0 μ sec					
DECODE					
Nuclei: 1.750	Off: 170.2 Hz				
Mark: NNN	Power: 20 dB				
Modulation: 0	Prog: 200 Hz				
Pulse Width: 16.0 μ sec	Power Mark: 200 Hz				
PLOT/PROCESSING					
FN: 32	K RE: 0	sec CD: 0	sec		
IR: 0	Hz AF: 0	sec CD: 0	sec		
Width: 2000.8 Hz/gm	Start: 100.0	Hz/gm			
Reference: 0					
EXPERIMENT					
Pulse Sequence: ST01H	Tube OD: 0 mm	Temp: 0 $^{\circ}$ C			
SAMPLE	HEIDI				
HJ H-NEX					
STD. PROTON					
28/6/87					
Number: 000	File: H	Date: 26-08-87			
X-VXH 200					

Based on the assignments of Host 1a, the ^1H - and ^{13}C - spectra (figures 15 and 16) of Host 1b were assigned (see Table 7).

These spectra show more signals than are expected, this being due to the presence of impurities. Resonance signals resulting from the impurities overlap with the host signal making the assignment of the spectrum more difficult and it was therefore necessary to describe the position of resonance of some protons by means of a range of delta values.

FIGURE 15: ¹³C-Spectrum of Host (1b)



OBSERVE
 Nucleus 13.750 Freq. 50 MHz
 Spec. Width 20000.0 Hz
 Acq. Time 0.750 sec
 Pulse Width 15.0 μsec
 Offset 500 Hz
 Delay 1.000 sec
 Transients 640

DECOUPLE
 Nucleus 1.750 Offset 170.2 Hz
 Mode YNY Power 5 db
 Modulation Mode S Freq. 7700 Hz
 Pulse Width 17.5 μsec Power Mode 47.0

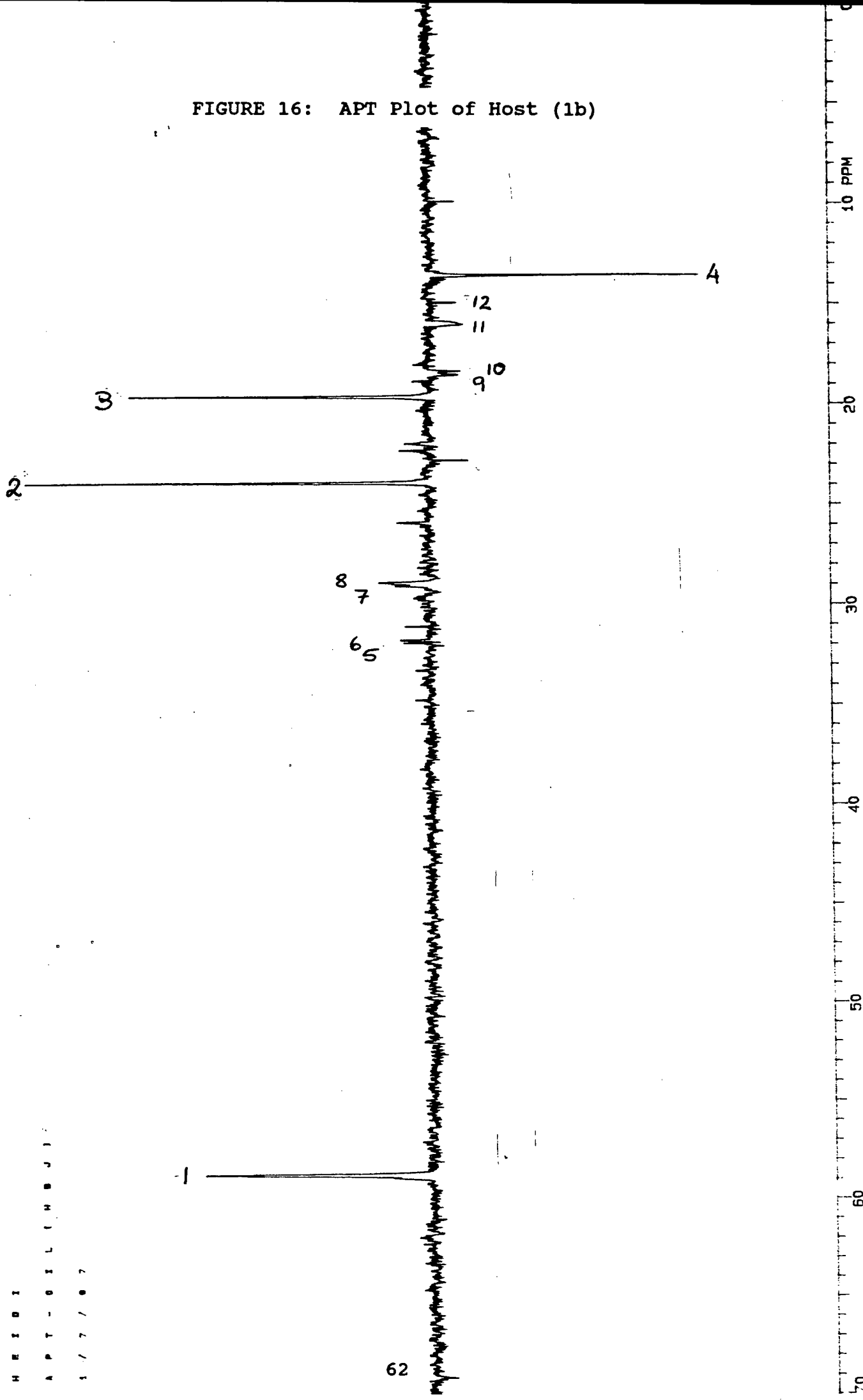
PLOT/PROCESSING
 FN 32 K RE ___ sec CD ___ sec
 LR 1.000 Hz AF ___ sec CCD ___
 Width 3524.9 Hz/ppm Start 0 Hz/ppm
 Reference _____

EXPERIMENT
 Pulse Sequence APT
 Tube OD ___ mm
 Temp ___ °C
 Solvent CDCl₃

SAMPLE
 HEIDI
 -OIL<HBJ>

Number _____
 File APT
 Date 26-08-87
 XL VXR 200

FIGURE 16: APT Plot of Host (1b)

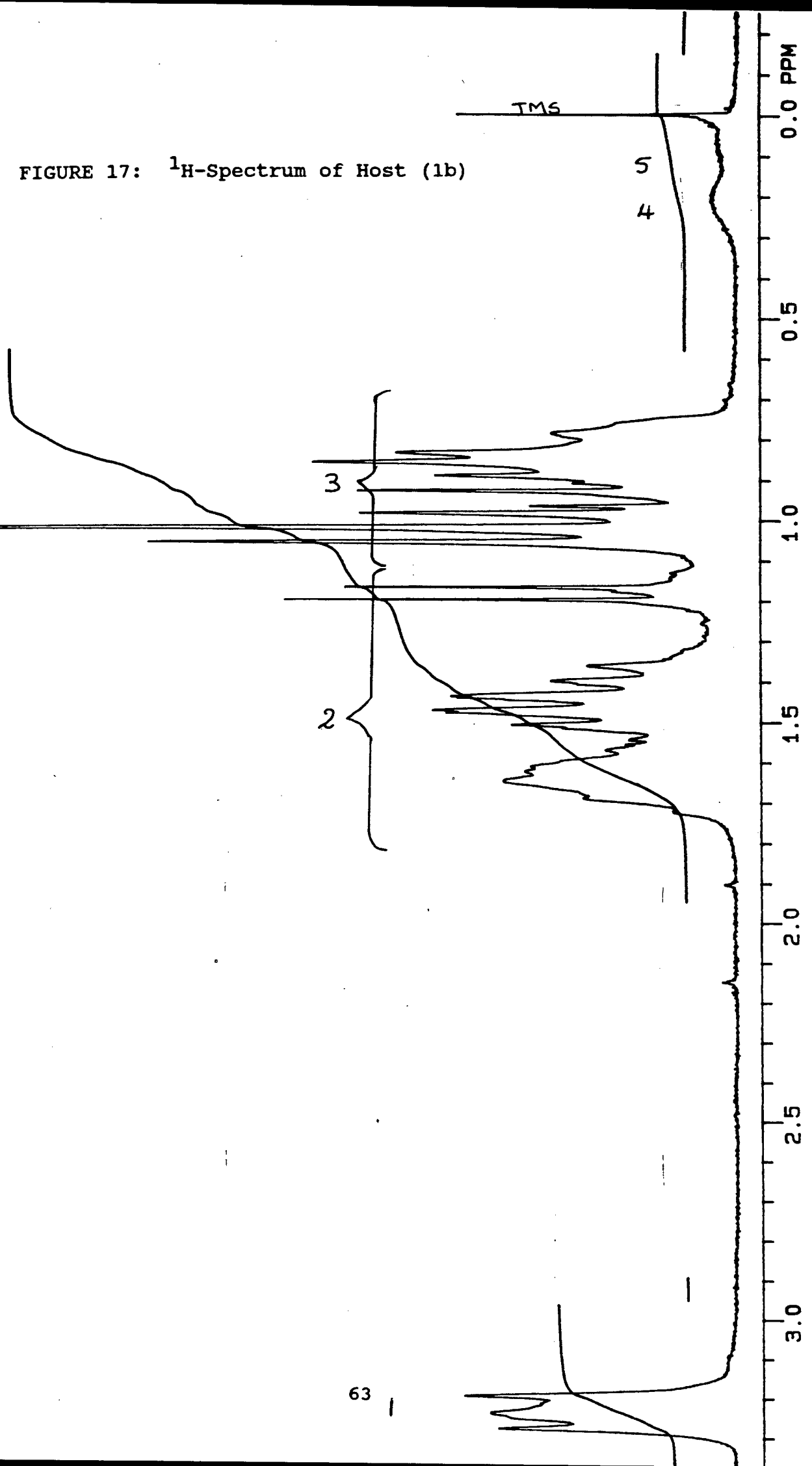


H E I O I

A P T - C O S I L C H B J I

1 / 7 / 0 7

FIGURE 17: ^1H -Spectrum of Host (1b)



CHAPTER 4 ANALYSIS OF LIQUID CLATHRATE COMPOSITION BY ^1H - N.M.R. SPECTROSCOPY

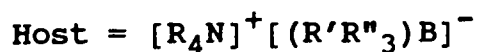
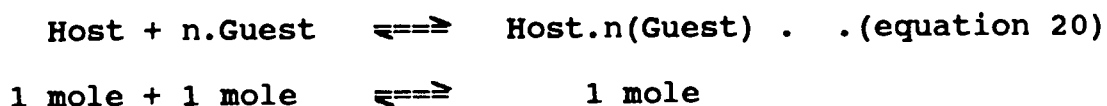
Liquid clathrates are inclusion compounds which form upon the interaction of hydrocarbon molecules (guests) with species related geometrically to $[\text{R}_4\text{N}]^+[\text{R}_4\text{B}]^-$ (hosts). The substance thus formed contains a certain maximum number of guest molecules and is immiscible with excess hydrocarbon. Preparation of a liquid clathrate, therefore, simply involves mixing parent compound with excess hydrocarbon. Upon gentle agitation at room temperature the two immiscible layers separate. Before examining trends it is important to discuss in detail one aspect of the behaviour. Each liquid clathrate is characterized by a maximum hydrocarbon-to-parent-compound ratio. In Table 8 (and henceforth) this value will be referred to as the G/H number (guest/host ratio) or "n" (the number of moles of guest clathrated per mole of host compound). The value is a constant for each system at a given temperature. Regardless of the amount of hydrocarbon present, the maximum G/H number cannot be exceeded. For example, if 17.5 mol of benzene are heated to 25°C with 1.0 mol of tetrahexylammonium (n-butyl)(tri-sec-butyl)boron, a liquid clathrate will result and it will appear as a pure solution. If 20.0 mol of benzene are placed in contact with 1.0 mol of the same host at 25°C , two immiscible liquids result (see Fig. 1, chapter 1). The composition of the lower layer in this experiment is

identical to that of the single phase in the previous example. The upper layer contains pure benzene. An equivalent result would be obtained if 1.0 mol of the above host were contacted with 100 mol of benzene.

Consideration should be given to the interaction of a parent compound with a quantity of hydrocarbon which is less than the maximum G/H. For the 'oily' parent complexes (see Chapter 2: 1.1.3 - Syntheses) any portion of hydrocarbon may be added up to the maximum G/H value, whereas a minimum threshold amount of guest usually exists for a solid clathrate¹.

2.1 The Behaviour of a Liquid Clathrate with Temperature Variation

A temperature study was made of liquid clathrates with four different aromatic guests to determine the effect of temperature on the G/H value, caused by any shift of the equilibrium constant for reaction (20) on varying temperature. The results obtained are listed in Table 8 and presented graphically (see fig.18).



Guest = n.hydrocabon

TABLE 8: TEMPERATURE STUDY

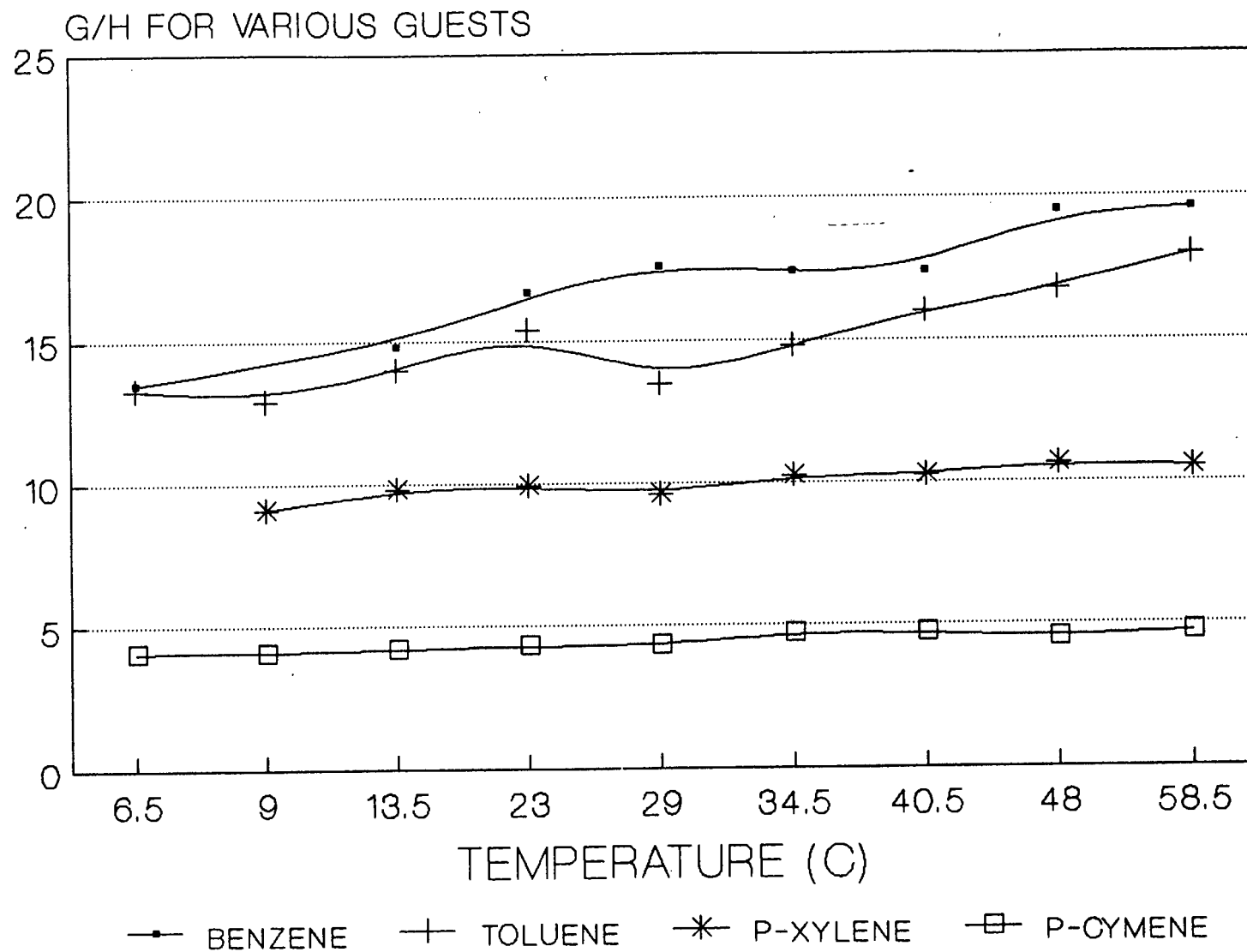
GUEST	TEMPERATURE (C)								
	6.5	9	13.5	23	29	34.5	40.5	48	58.5
BENZENE	13.5		14.8	16.7	17.6	17.4	17.4	19.5	19.6
TOLUENE	13.3	12.9	14	15.4	13.5	14.8	16	16.8	18
P-XYLENE		9.1	9.8	9.9	9.6	10.2	10.2	10.6	10.5
P-CYMENE	4.1	4.1	4.2	4.3	4.3	4.7	4.7	4.5	4.7

Table 8 Tabulation of G/H values for Host(1a) with different Guests at various Temperatures

Since one forms an associated compound of host and guest on the right-hand side of equation 20, one expects a decrease in entropy for this reaction.

The enthalpy term is expected to be small as only Van der Waals forces are involved in making the associated compound. Raising the temperature will have the effect of increasing the thermal motion of the molecules of the liquid clathrate and there will be a tendency to pull them apart. This will result in the equilibrium shifting to the left in equation 20.

FIGURE 18: RESULTS OF TEMPERATURE STUDY



Ideally then, one should be able to recover the unaltered free host material in this manner.

From the graphs it would appear as if temperature has little influence on the amount of guest material clathrated. The liquid clathrates are almost saturated with guest material at room temperature. There is a gradual increase in the value of G/H as the temperature is increased from 6.5°C to 58.5°C. On increasing the temperature above 74°C, the liquid clathrate formation, for H.n(G) (guest = benzene), was observed to break down and a pure solution of parent compound (1a) dissolved in excess aromatic (i.e. a single phase solution) formed. On increasing the temperature still further the same result was observed for the other liquid clathrates at 77°C, 82°C, and 86°C for guest = toluene, p-xylene and p-cymene respectively.

In an attempt to recover the host from the p-xylene clathrate, the clathrate layer was cooled. As the temperature was decreased, the G/H ratio decreased. It was hoped that the ratio could be decreased sufficiently to retrieve the host compound. This was not feasible as the whole solution freezes below a certain temperature, trapping the host (6°C in the case of H.np-xylene), and at slightly higher temperatures the host is still contaminated with a fairly high ratio of guest.

Thus, once the liquid clathrate has been formed (equ.20), the maximum G/H is essentially temperature independent up to the decomposition point of the liquid clathrate. The same

result was found by Atwood¹ for liquid clathrates with host species related geometrically to $M(Al_2R_6X)$. This surprising result may be attributed to the strength of the cation...anion interaction in the liquid clathrate.

2.2 Stoichiometry and Selectivity: As Determined from ¹H-N.M.R. Studies

The composition of liquid clathrate systems was studied at room temperature in order to gain some insight into the selectivity of these new host compounds. Table 9 tabulates the G/H ratios determined by ¹H-N.M.R. for the liquid clathrate systems $H_1.nG$ and $H_2.nG$, where H_1 and H_2 represent parent compounds (1a) and (1b) respectively and G the guest (see fig.19 for graphical presentation).

TABLE 9: SUMMARY OF G/H VALUES FOR H = 1a AND 1b

HYDROCARBON GUEST TYPE	HOST = 1a		HOST = 1b (25°C)
		MAX. G/H VALUES (AT 25°C)	MAX. G/H VALUES
BENZENE	1	17	9
TOLUENE	2	16	8
p-XYLENE	3	14	5
o-XYLENE	4	22	6
m-XYLENE	5		5
p-CYMENE	6	4	3
CYCLOHEXANE	7	3	
CYCLOHEXENE	8	6	2
DIOXANE (1,4)	9	15	
n-HEXANE	10	4	

**FIGURE 19: G/H VALUES FOR HOST(1a, 1b)
FOR VARIOUS GUESTS (see Table 9)**

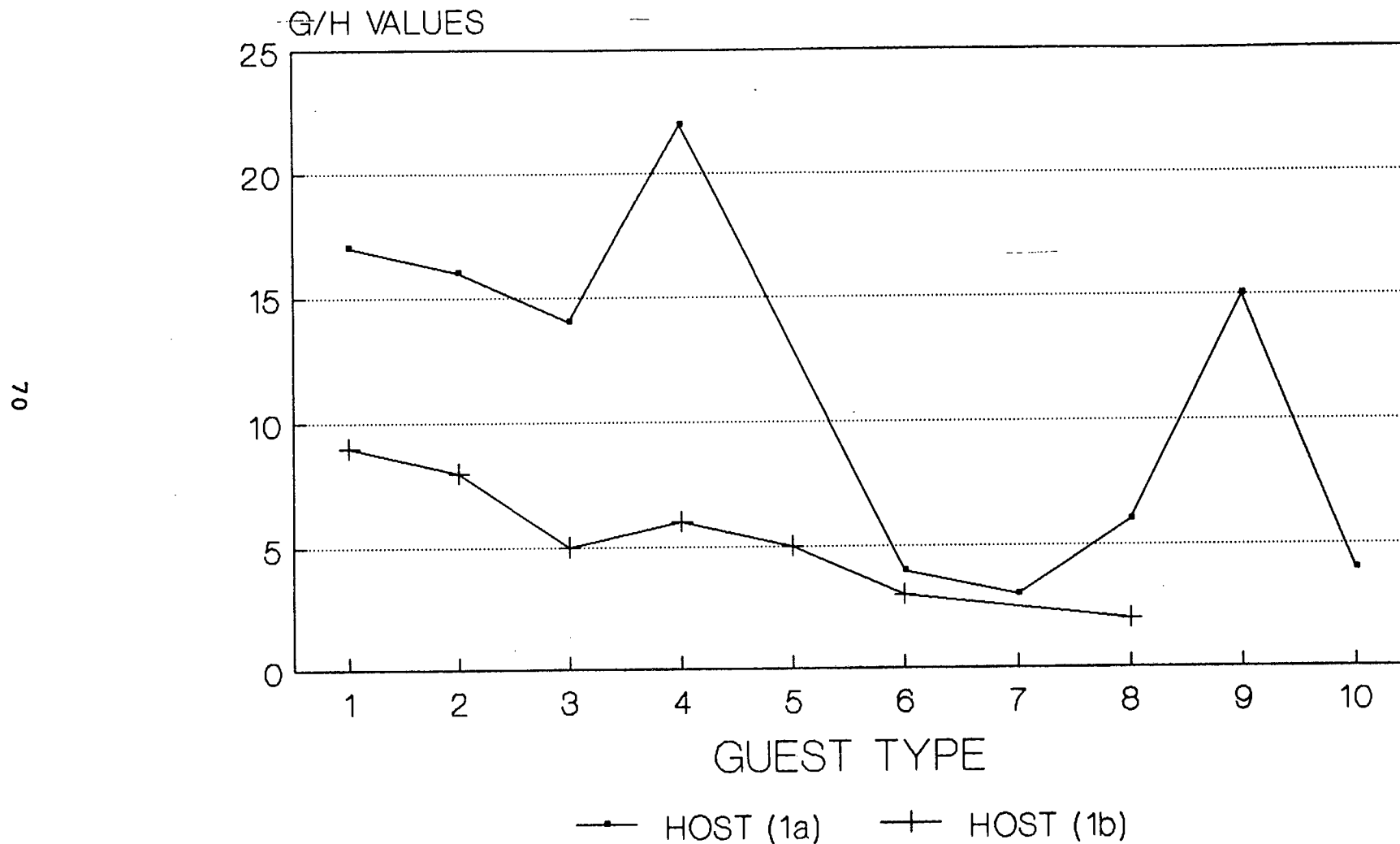
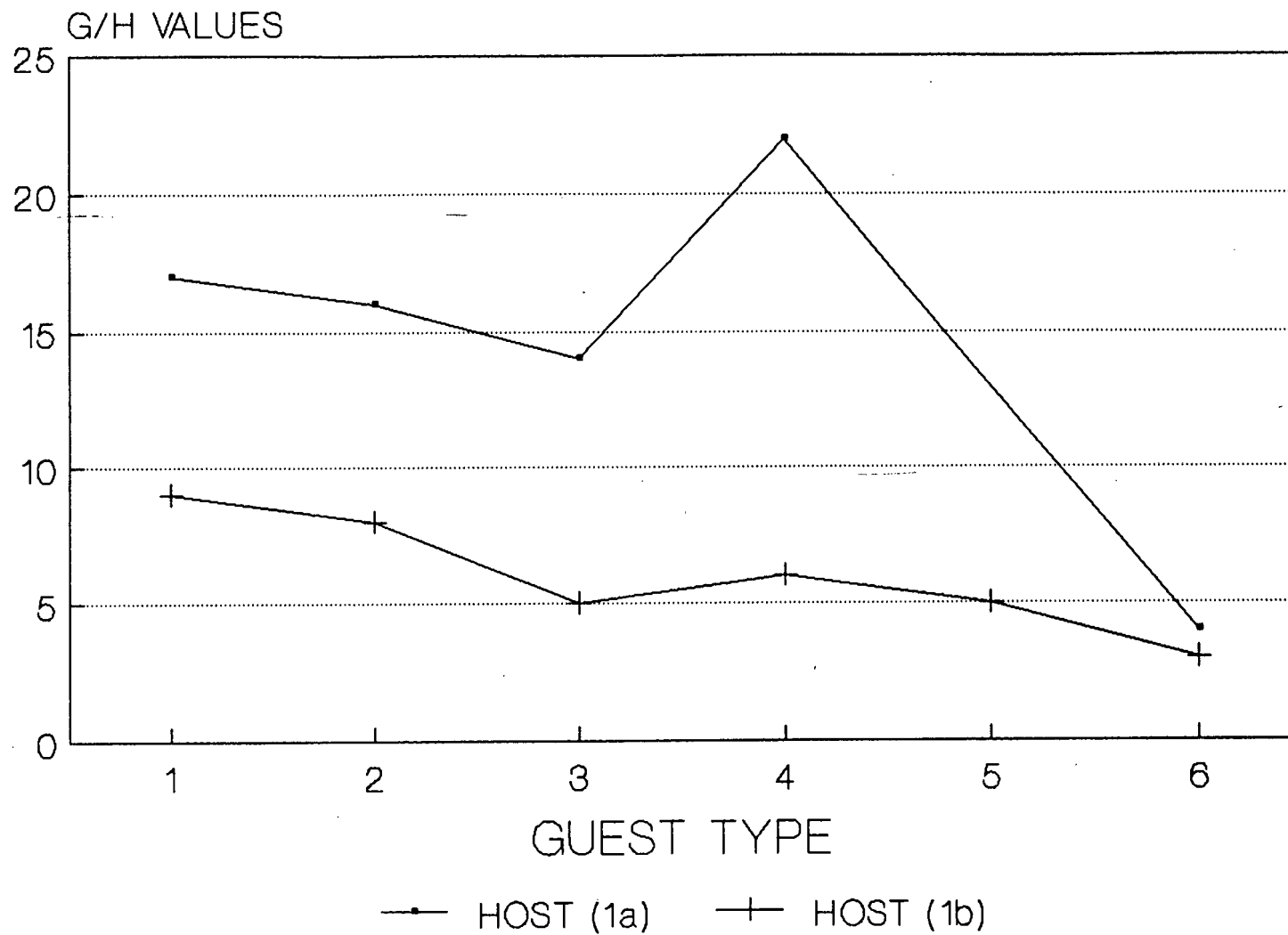


**FIGURE 20: G/H VALUES FOR HOST(1a,b)
WITH VARIOUS AROMATICS (see Table 9)**



Both parent compounds are observed to trap aromatic as well as aliphatic hydrocarbons (guest). The liquid clathrates prepared from parent compound (1b) are far less efficient than those of compound (1a), as indicated by the lower G/H ratios for the former liquid clathrates.

As found by Atwood¹, a careful analysis of the data in Table 9 reveals that liquid clathrates possess properties in common with solid state clathrates. It was observed that:

(1) for a given anion and aromatic /or aliphatic guest, the larger the cation, the larger the G/H ratio (see fig.19);
(2) for a given cation and anion, the larger the aromatic /or aliphatic guest, the smaller the G/H ratio (see fig. 19). It was also observed that for a given anion and cation:

i) the more aliphatic the guest is in character, the smaller G/H (i.e. the higher the aromaticity of the guest, the larger G/H). (Diagrammatically shown in fig.20);

ii) a polar guest does not form a liquid clathrate. This is illustrated by the guests Chlorobenzene, Bromobenzene and 1,2-dichloropropane not forming liquid clathrates (see Table 9);

Observations 1 and 2 were also observed for the liquid clathrates studied by Atwood¹. As stated by Atwood, it thus appears that each parent complex can be expanded to create cavities of a rather constant size.

TABLE 10: G/H VALUES FOR 2 COMPONENT GUEST SYSTEMS
(BASED ON EQUAL VOL'S OF GUEST)

G1	G2	A HOST = 1a		B HOST = 1b	
		H : n1G1 : n2G2 IN CLATHRATE		H : n1G1 : n2G2 IN CLATHRATE	
BENZENE	n-HEXANE	7	1	5	0.6
TOLUENE	n-HEXANE	5	1	3.7	1
P-XYLENE	n-HEXANE	5	2		
P-CYMENE	n-HEXANE	2	2		
BENZENE	P-XYLENE	5	4	5	2.5
TOLUENE	P-XYLENE	7	5	4	2.5
P-CYMENE	P-XYLENE	2	4	6.8	1
BENZENE	TOLUENE	4	9	4	3
BENZENE	P-CYMENE	7	3	4	1.5
TOLUENE	P-CYMENE	6	6	8	2
BENZENE	O-XYLENE			4.5	3
BENZENE	M-XYLENE			4	2.8

Further selectivity studies were undertaken by presenting the parent compounds (1a and 1b) with excess amounts of two-component guest samples, at room temperature (see equ.21).



G_1 and G_2 are aliphatic and/or aromatic guest.

These two-component mixtures of hydrocarbon, typically substituted benzenes and aliphatics, are representative components of raw coal. The extracting capability of the host material can thus be tested. G/H ratios are listed in Table 10 for the various two-component guest systems tested.

The results showed that if both aromatic and aliphatic hydrocarbon guests are added to the host, a liquid clathrate is formed which contains both types of guest. However, the presence of an aliphatic chain significantly reduces the clathrating capacity of the parent compound. This is evident from the fact that the sum of n_1 and n_2 is considerably less than the n (G/H value) obtained for the liquid clathrate where only aromatic guest is present. It is also apparent that there is competition between the two guests for occupation of sites around the host (indicated by the ratio of n_1 to n_2 , which (for example) is not 1:1 when an equal number of moles of G_1 and G_2 are added to host.

The preference of the parent compound (1a) for aromatic guest (G_1) as compared to an aliphatic one (G_2), namely n-Hexane, was also studied. Various mixtures of G_1 and n-Hexane, in known stoichiometric amounts, were prepared and the G/H ratios determined for each guest in the resultant liquid clathrate formed. The results of which are tabulated in Table 11.

The results clearly indicate a preference for the aromatic guest. This is also illustrated diagrammatically in figures 21, 22 and 23 for G_1 being benzene, toluene and p-xylene respectively. If the host compound unselectively clathrated guest material solely on the basis of the availability of sites around the host, then the experimental results (curved

plots in fig's. 21-23) would have coincided with the straight line on the graph.

Since the aromatic guest was taken up to a significantly larger extent by the host than the aliphatic guest, the Host may, in principle, be used to separate aromatic/aliphatic mixtures by repetitive clathration and separation of the entrapped guest.

TABLE 11: RESULTS OF THE AROMATIC-ALIPHATIC COMPETITION STUDY

MIXTURE OF HYDROCARBON IN KNOWN STOICHIOMETRIC AMOUNTS, AS PREPARED		STOICHEIOMETRY OF HYDROCARBON AFTER CLATHRATION		G/H VALUES DETERMINED BY H-NMR		% MOLE FRACTION OF AROMATIC GUEST CLATHRATED
G1=AROMATIC (MOLES)	n-HEXANE (MOLES)	G1=AROMATIC (MOLES)	n-HEXANE (MOLES)	TOLUENE (MOLES)	n-HEXANE (MOLES)	
1.0	0.0	1.00	0.00	16.0	0.0	100
0.8	0.2	0.74	0.26	9.5	1.6	85
0.5	0.5	0.49	0.51	3.6	2.1	63
0.3	0.7	0.27	0.72	2.2	3.2	41
0.1	0.9	0.10	0.90	0.6	3.2	16
0.0	1.0	0.00	1.00	0.0	4.0	0
G1=AROMATIC MOLES	n-HEXANE (MOLES)	G1=AROMATIC MOLES	n-HEXANE (MOLES)	BENZENE (MOLES)	n-HEXANE (MOLES)	
1.0	0.0	1.00	0.00	18.0	0.0	100
0.8	0.2	0.72	0.28	12.3	2.4	83.8
0.5	0.5	0.46	0.54	4.5	2.4	65.6
0.3	0.7	0.26	0.73	2.5	2.8	47
0.1	0.9	0.08	0.93	1.0	2.9	25.6
0.0	1.0	0.00	1.00	0.0	4.0	0
G1=AROMATIC MOLES	n-HEXANE (MOLES)	G1=AROMATIC MOLES	n-HEXANE (MOLES)	p-XYLENE (MOLES)	n-HEXANE (MOLES)	
1.0	0.0	1.00	0.00	9.8	0.0	100
0.8	0.2	0.77	0.23	8.8	1.5	85.4
0.5	0.5	0.44	0.56	6.2	2.9	62.6
0.3	0.7	0.25	0.75	2.0	2.7	42.2
0.1	0.9	0.09	0.91	0.5	2.2	17.3
0.0	1.0	0.00	1.00	0.0	4.0	0

FIGURE 21: COMPETITION EXPERIMENT
G1-BENZENE; G2-n-HEXANE; H-1a

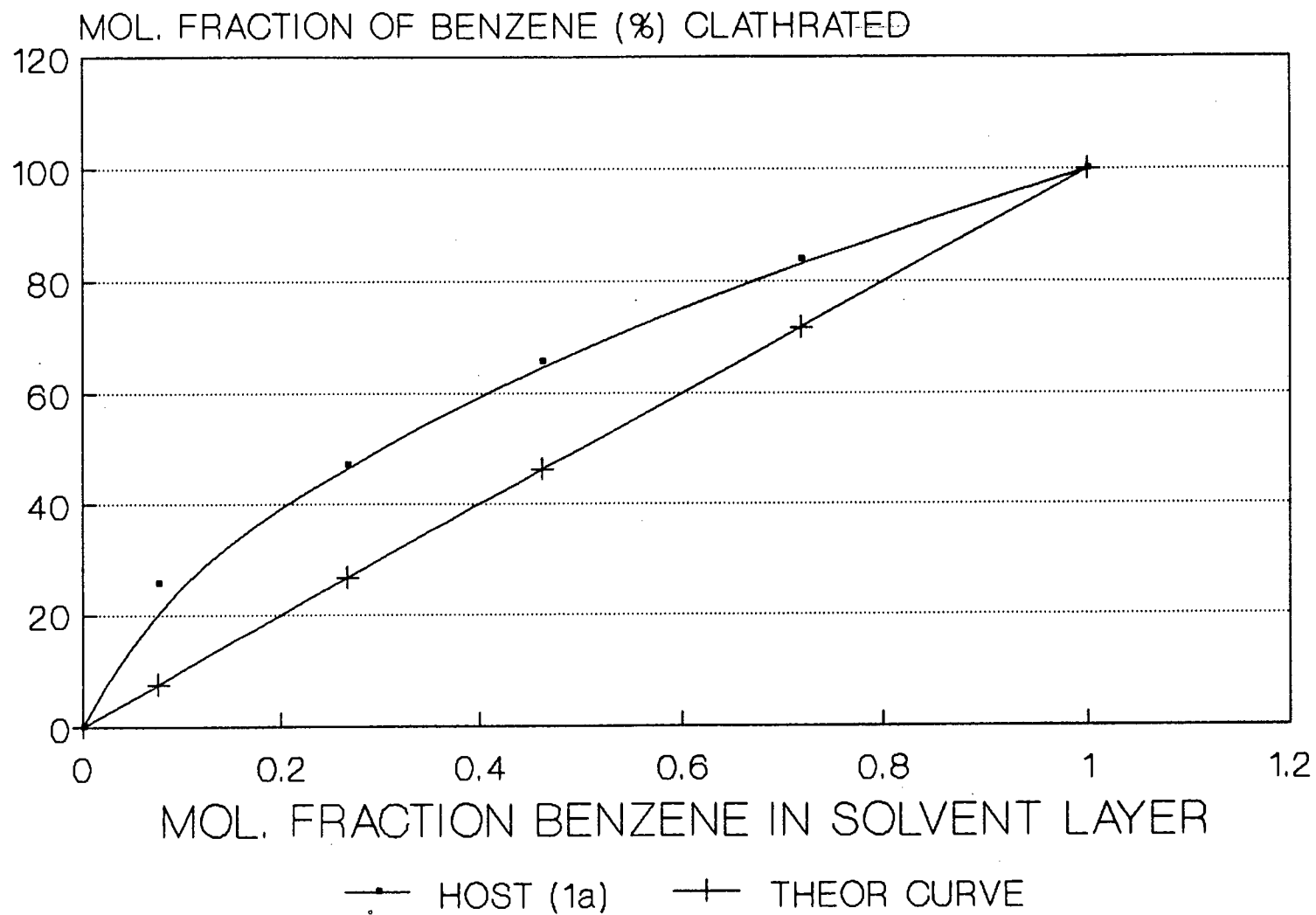


FIGURE 22 COMPETITION EXPERIMENT
G1-TOLUENE; G2-n-HEXANE; H-1a

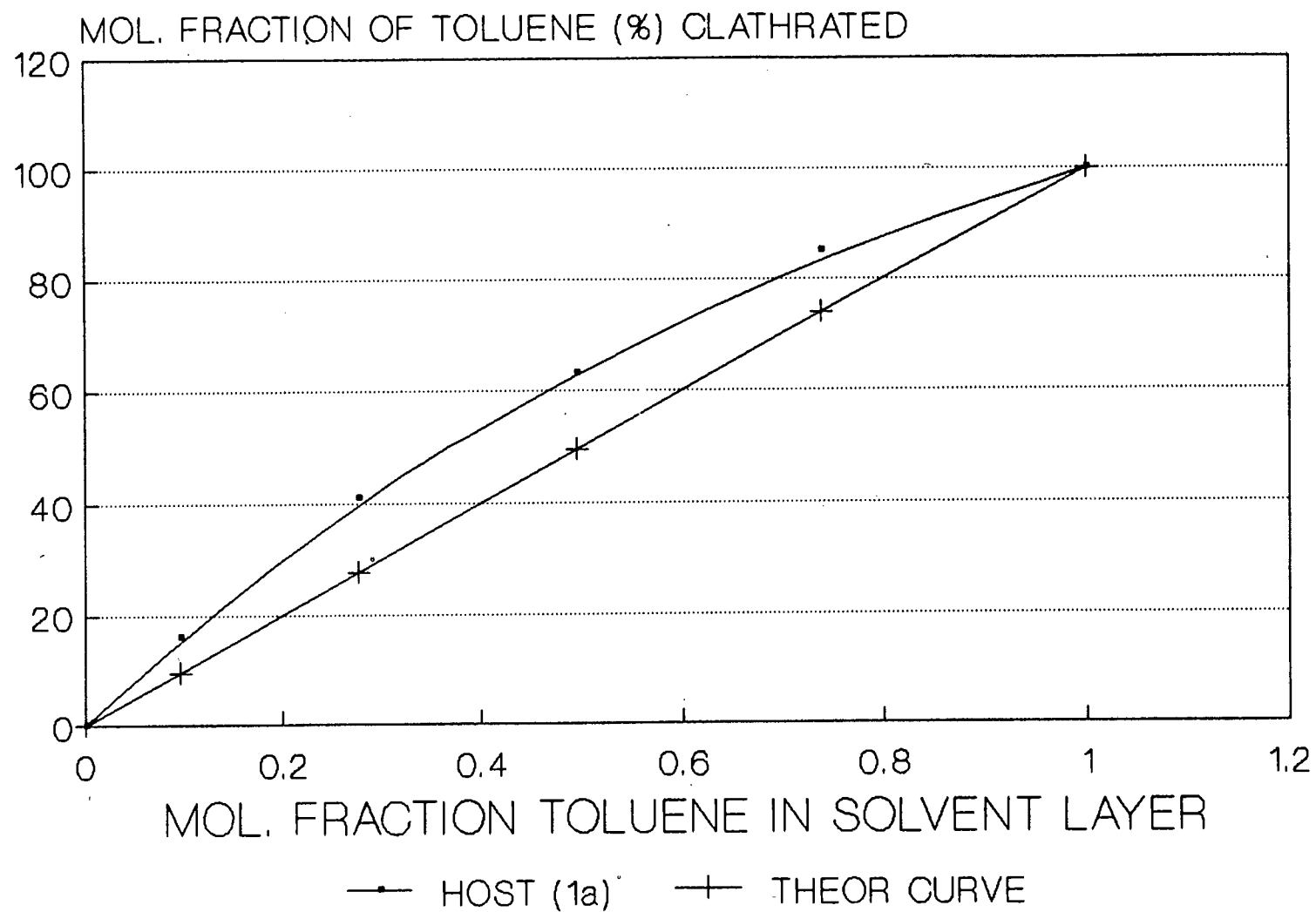
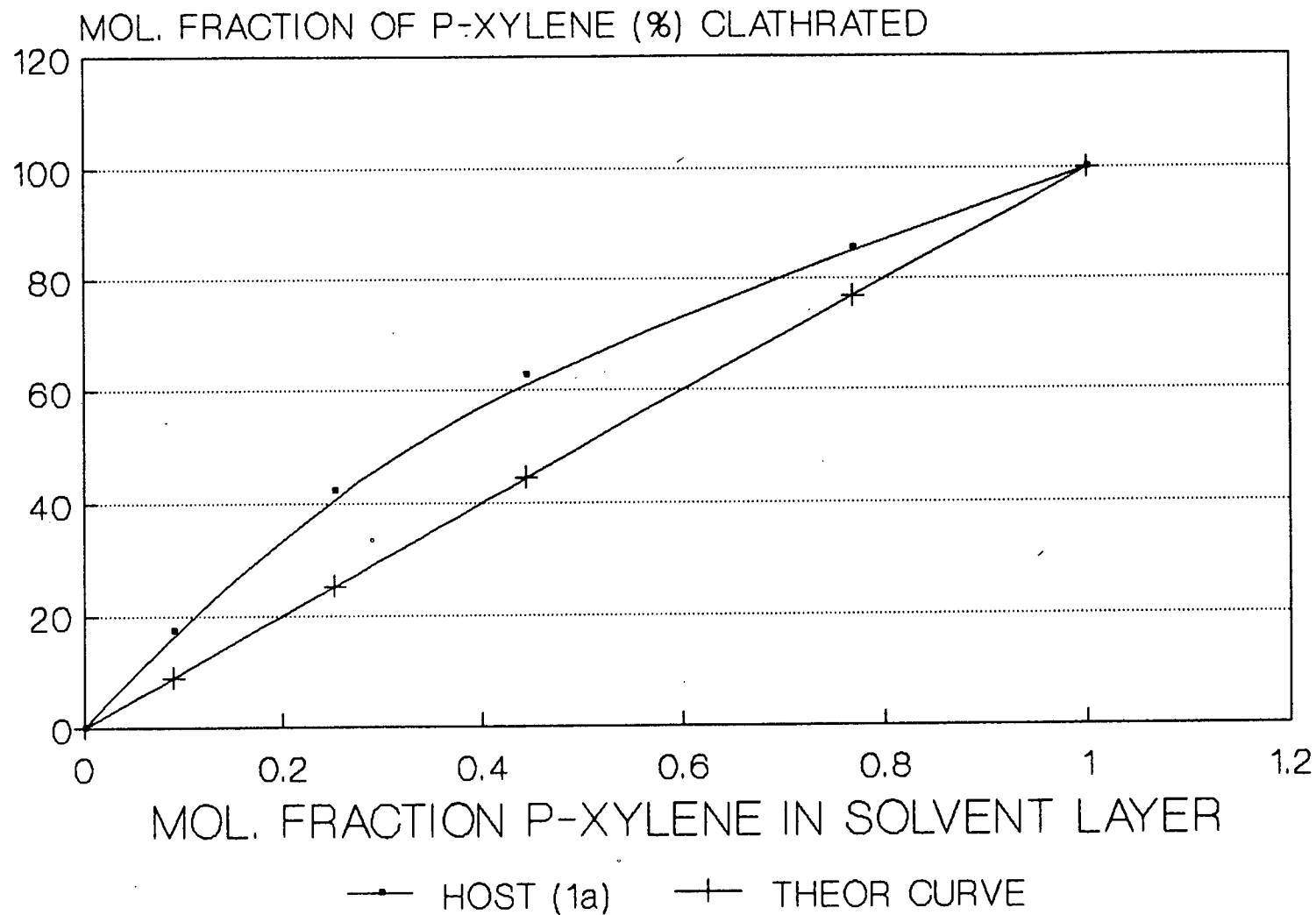


FIGURE 23: COMPETITION EXPERIMENT
G1-P-XYLENE; G2-n-HEXANE; H-1a



3.1 Thermal Analysis

The liquid clathrates of parent compound 1a, with aromatic guest, were studied using the techniques of Differential Thermal(DT)- and Thermogravimetric(TG)- Analysis. These experiments were performed on the parent material, the guest and the liquid clathrate formed on the addition of the host and guest. It was observed, from the TGA and DTA plots of Guest, Host.nGuest and Host (figures 24-33), that (i) the Host decomposes in a single step at approx. 320°C; (ii) The guest is released from the Host in a single step at a temperature which is dependant on the guest clathrated (see Table 12 and Fig's. 26-29).

TABLE 12: TEMPERATURE AT WHICH GUEST IS RELEASED
HOST = 1a

GUEST	FURNACE TEMP AT WHICH GUEST IS RELEASED (°C)	SAMPLE TEMP AT WHICH GUEST IS RELEASED (°C)
BENZENE	73-77	52 - 56
p-XYLENE	140-145	98-103

The TGA and DTA curves of the Guest and Host.nGuest were analyzed and the enthalpy of vaporization calculated for the guest: (i) alone and (ii) clathrated. The difference in enthalpy calculated for (i) and (ii) would give the energy of clathration between the guest and host (see equ.22).

$$\Delta H_{\text{vap}}(\text{G in H.nG}) = \Delta H_{\text{vap}}(\text{free guest}) + \Delta H_{\text{clathration}} \quad (\text{equ.22})$$

TGDTA OF BENZENE

N₂ 30ML/MIN. 10 DEG/MIN.

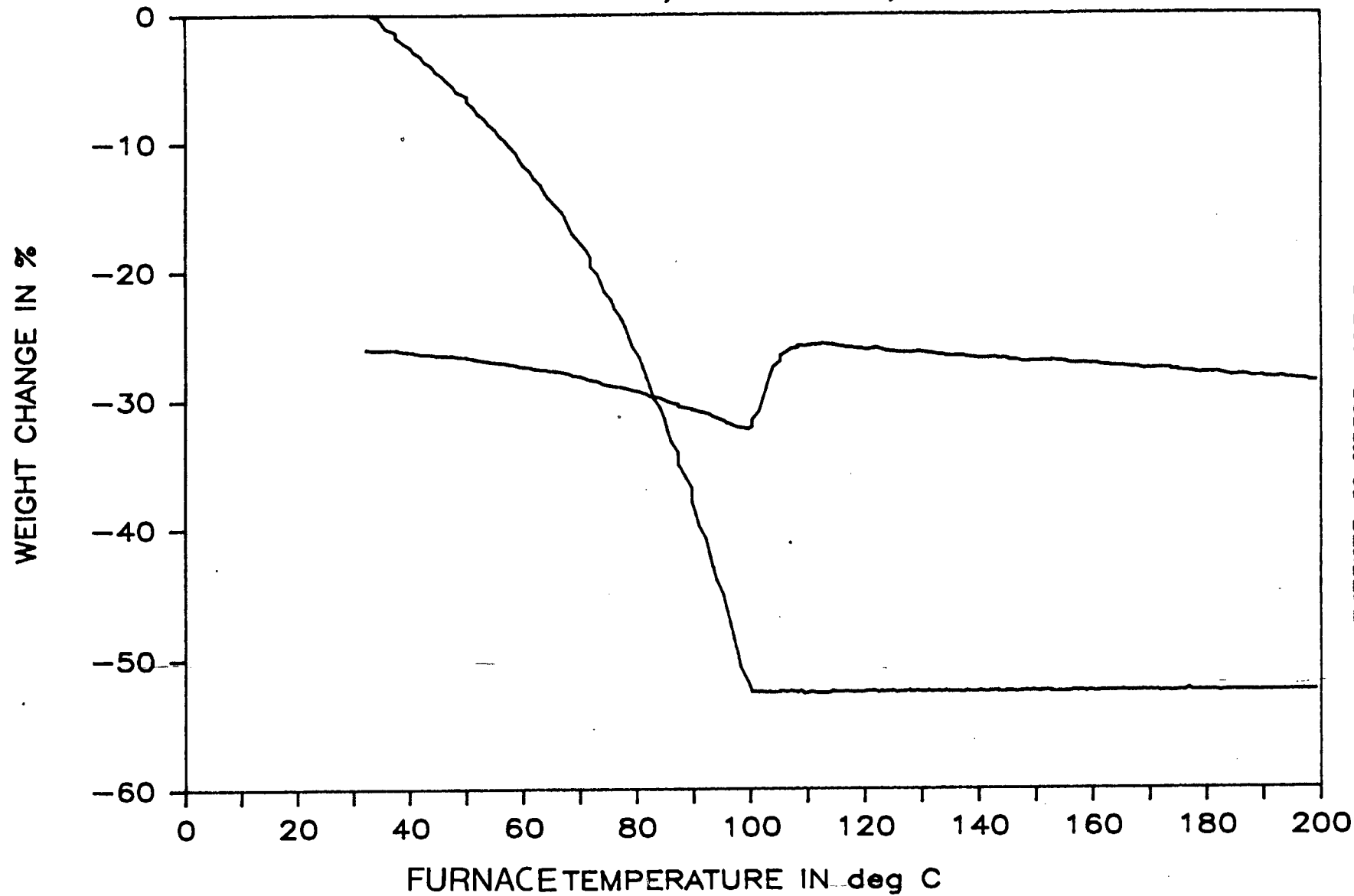


FIGURE 24: TGDTA OF BENZENE

DTA OF BENZENE

N2 30ML/MIN. 10DEG/MIN.

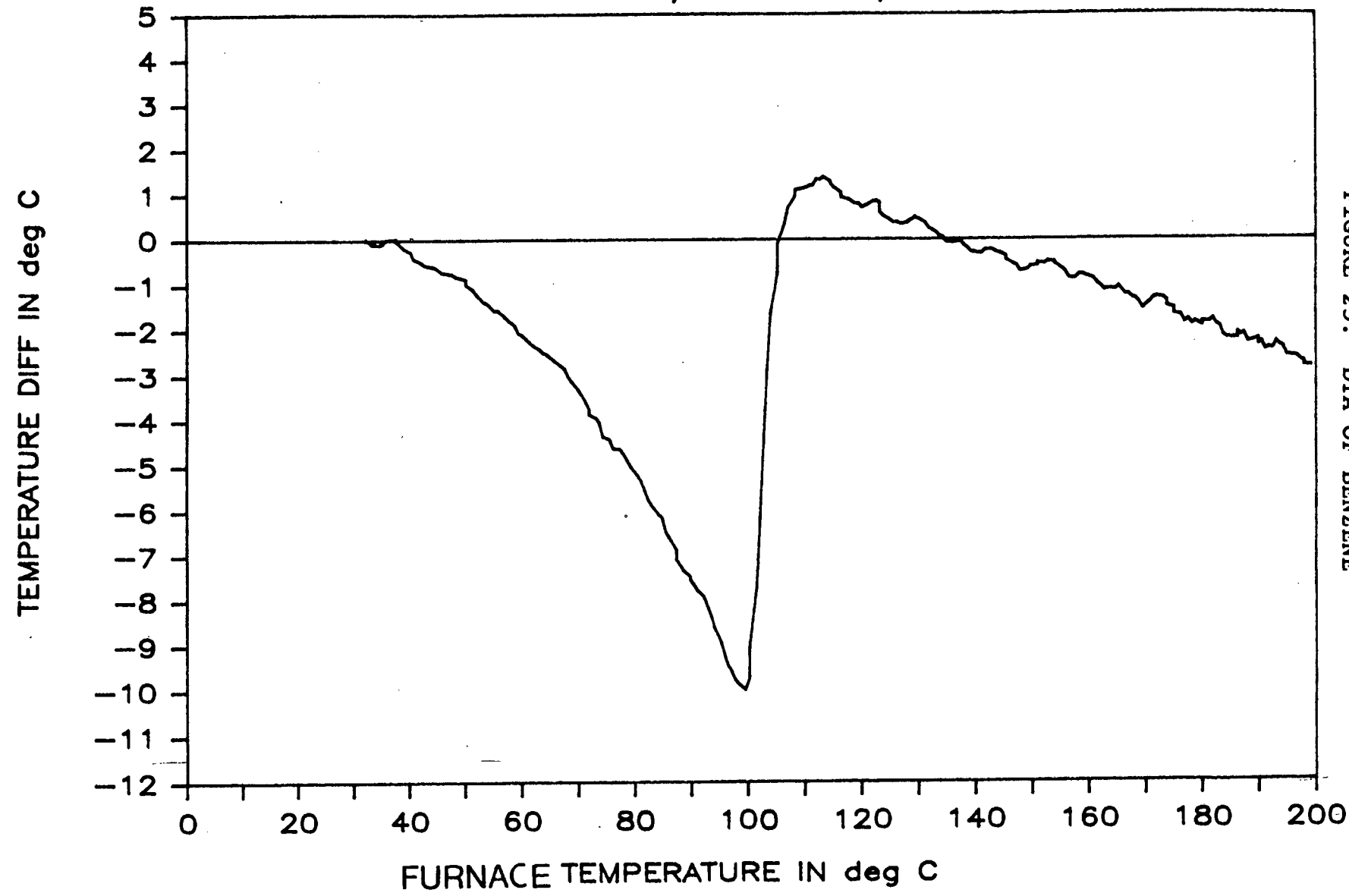


FIGURE 25: DTA OF BENZENE

DTA OF P-XYLENE.

N2 AT 30 ML/MIN. 10 DEG/MIN.

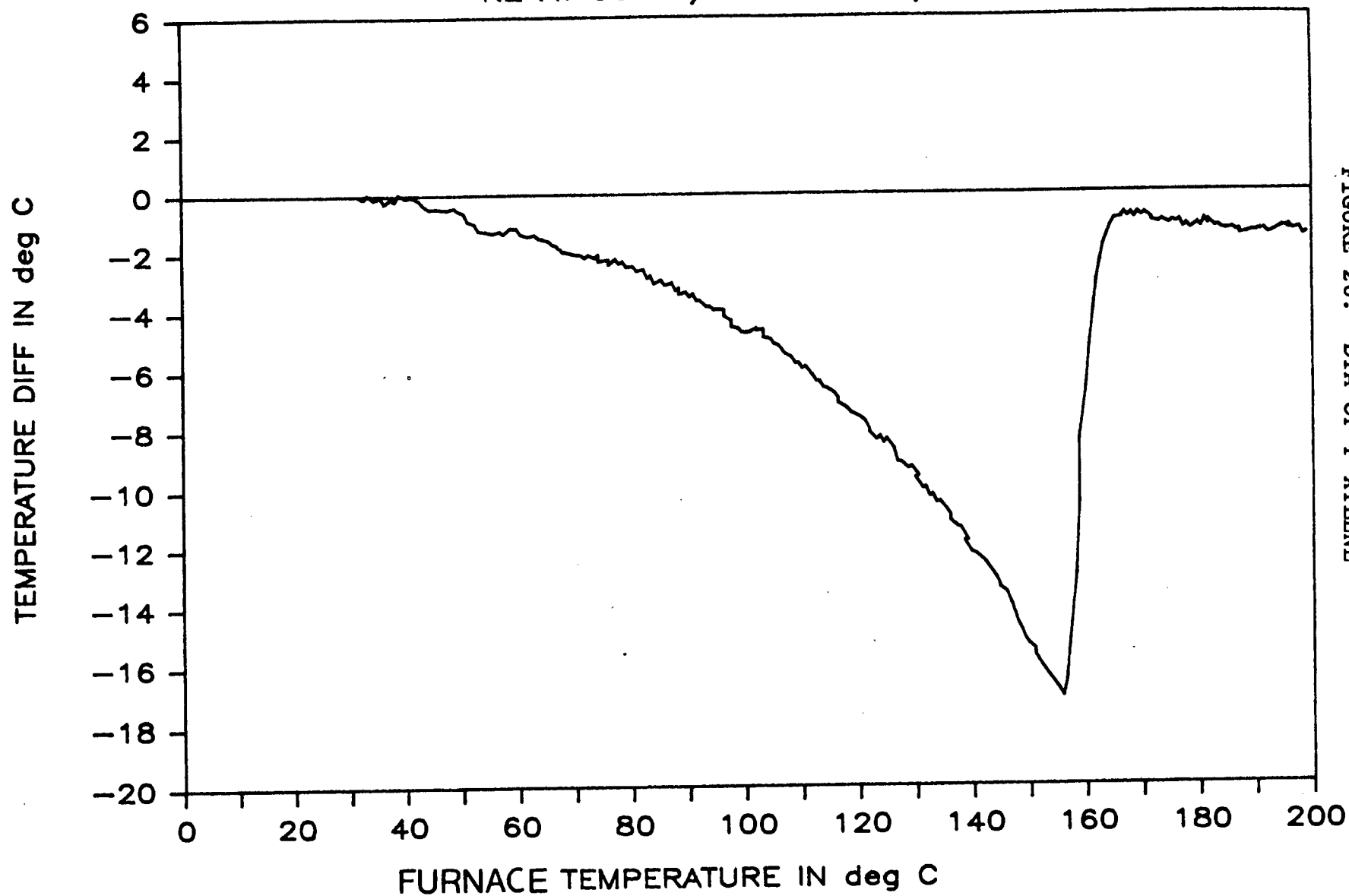


FIGURE 26: DTA OF P-XYLENE

TGDTA OF P-XYLENE

GAS FLOW; N₂ 30ML/MIN. 10DEG/MIN.

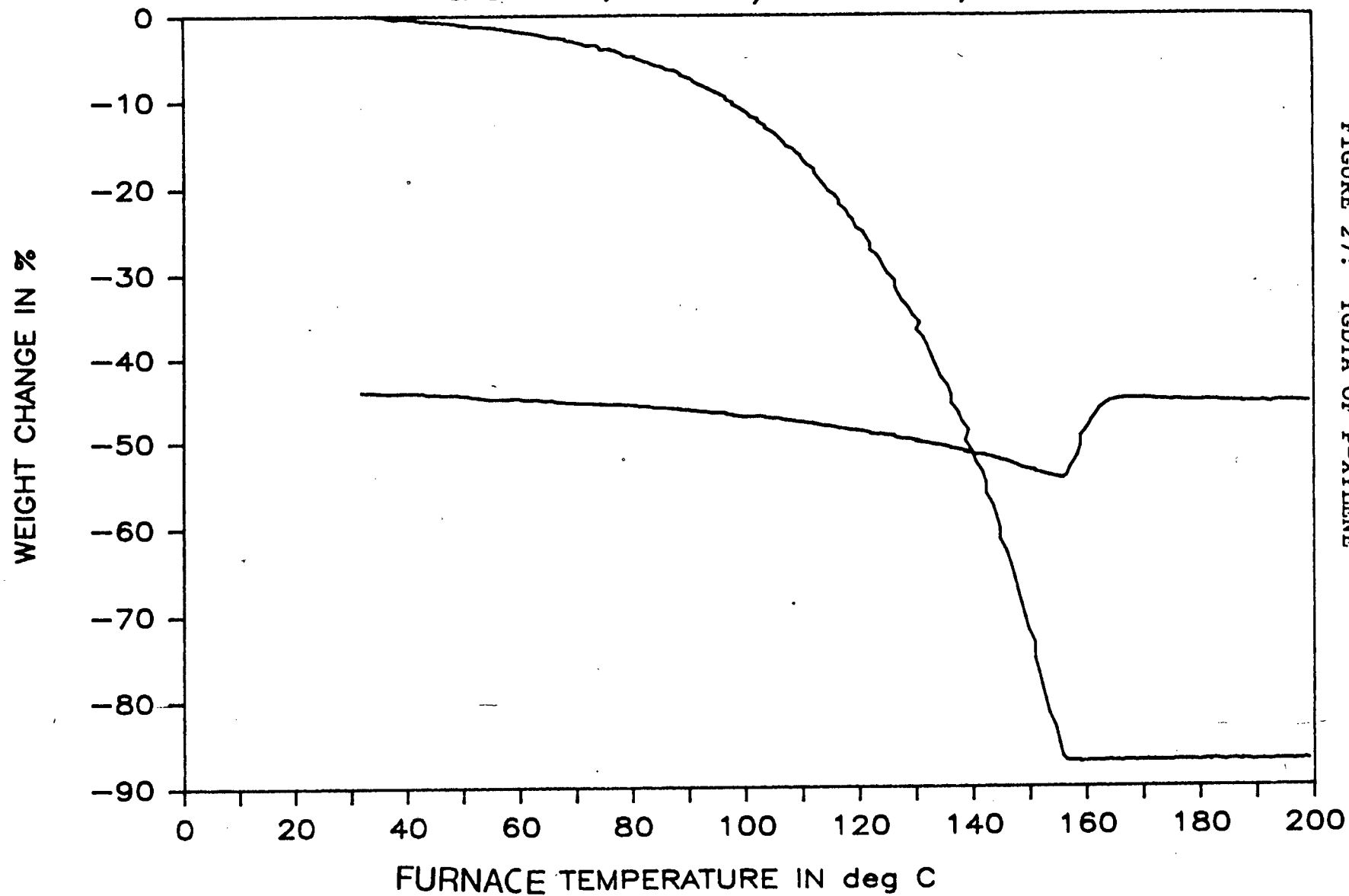


FIGURE 27: TGDTA OF P-XYLENE

DTA OF BENZENE & HOST.

N2 30ML/MIN. 10 DEG/MIN.

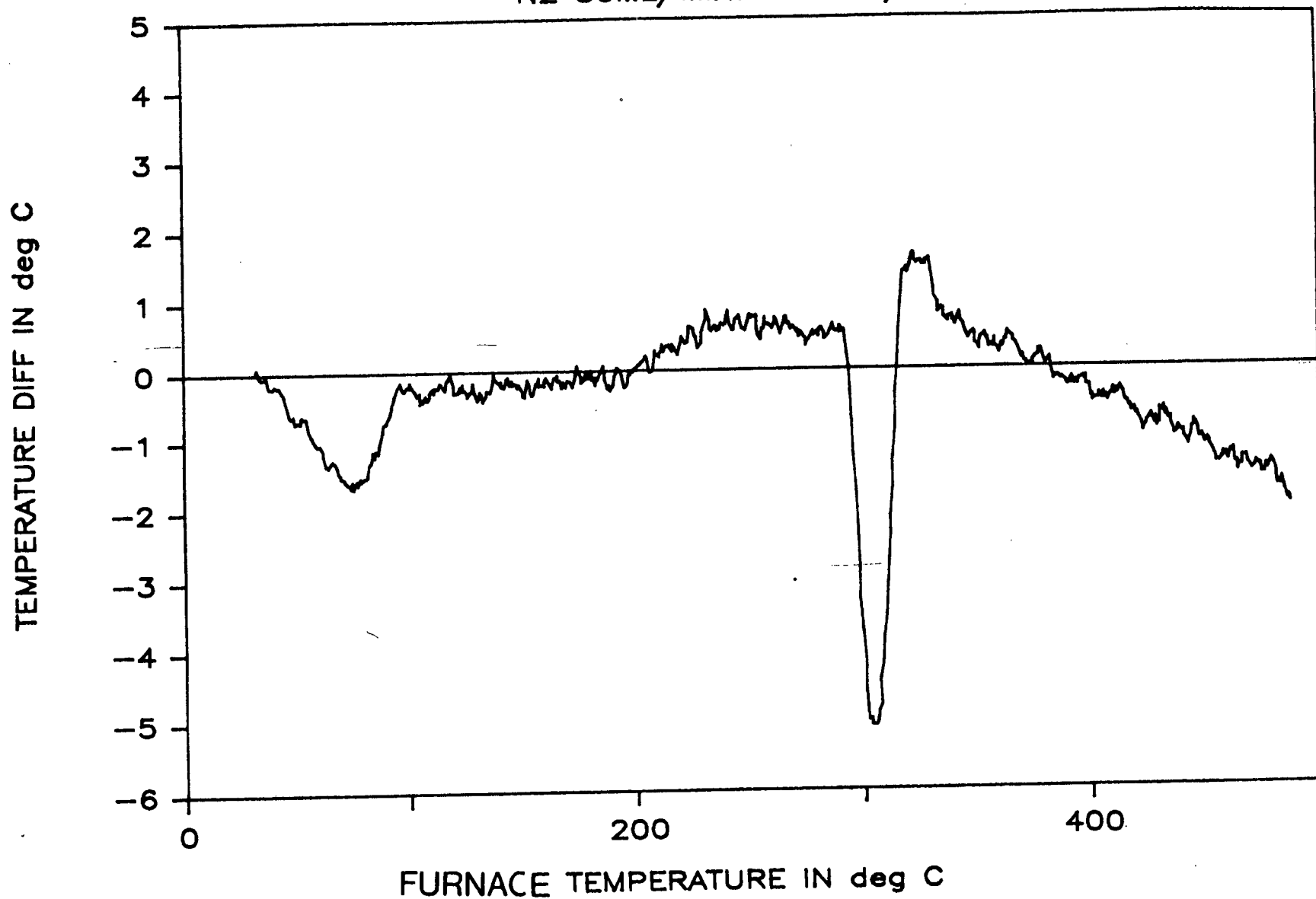
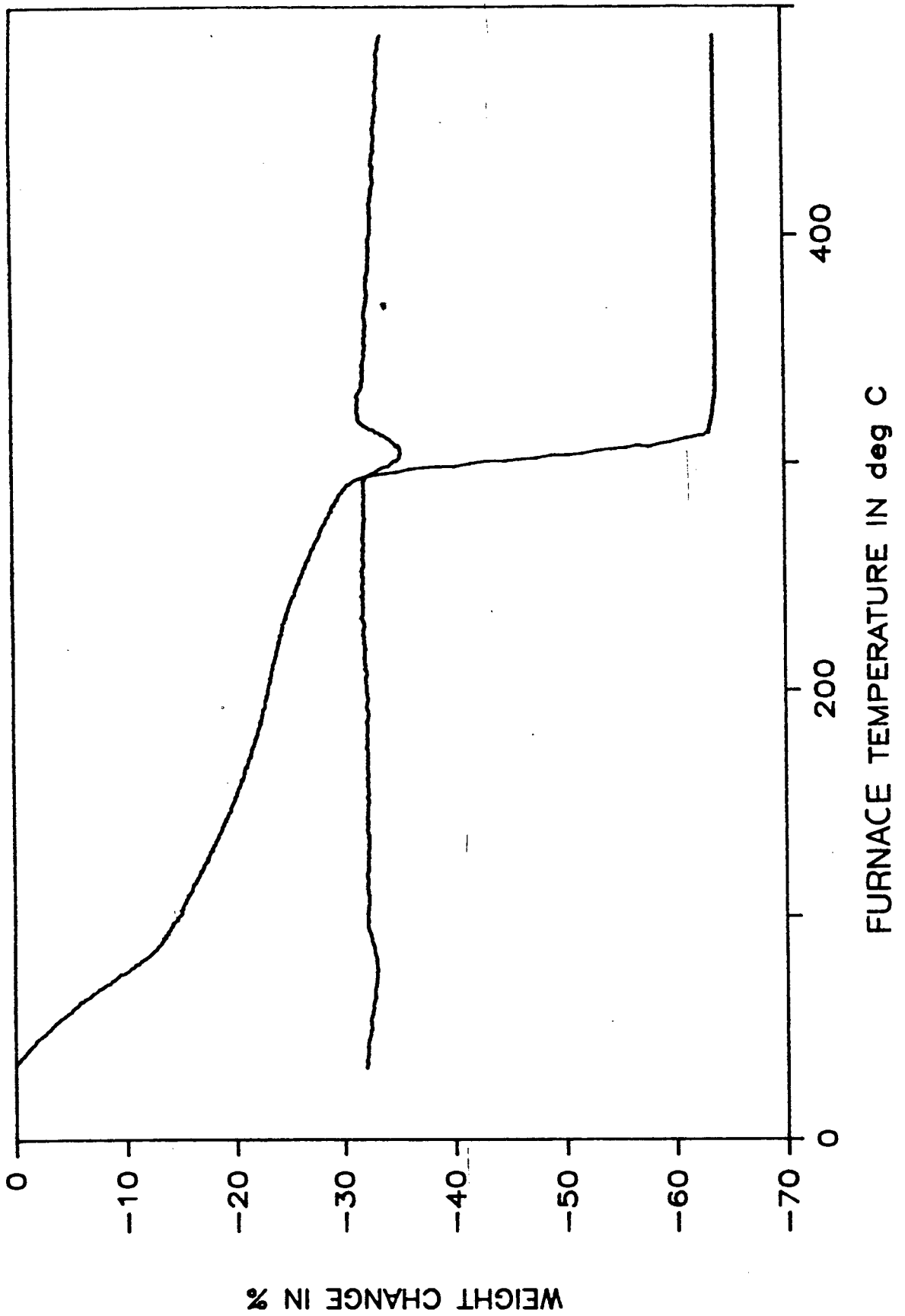


FIGURE 28: DTA OF HOST(1a) .n(BENZENE)

TGDTA OF BENZENE & HOST.

FIGURE 29: TGDTA OF HOST(1a).n(BENZENE)



R4-PX, 30 to 500C @10C/min in N2

DTA Graph

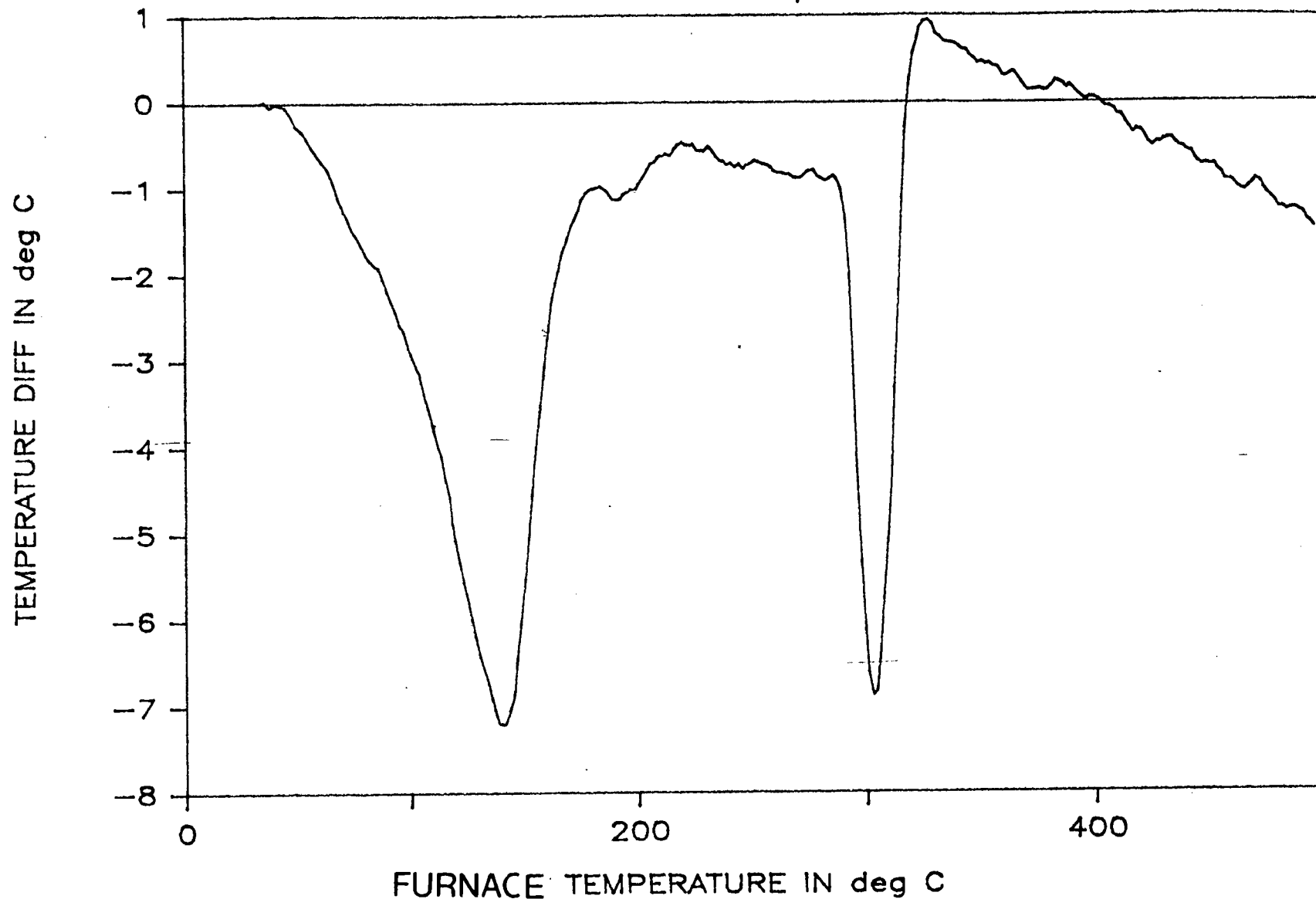


FIGURE 30: DTA OF HOST(1a).n(P-XYLENE)

R4-PX, 30 to 500C 10C/min in N2

TG Graph

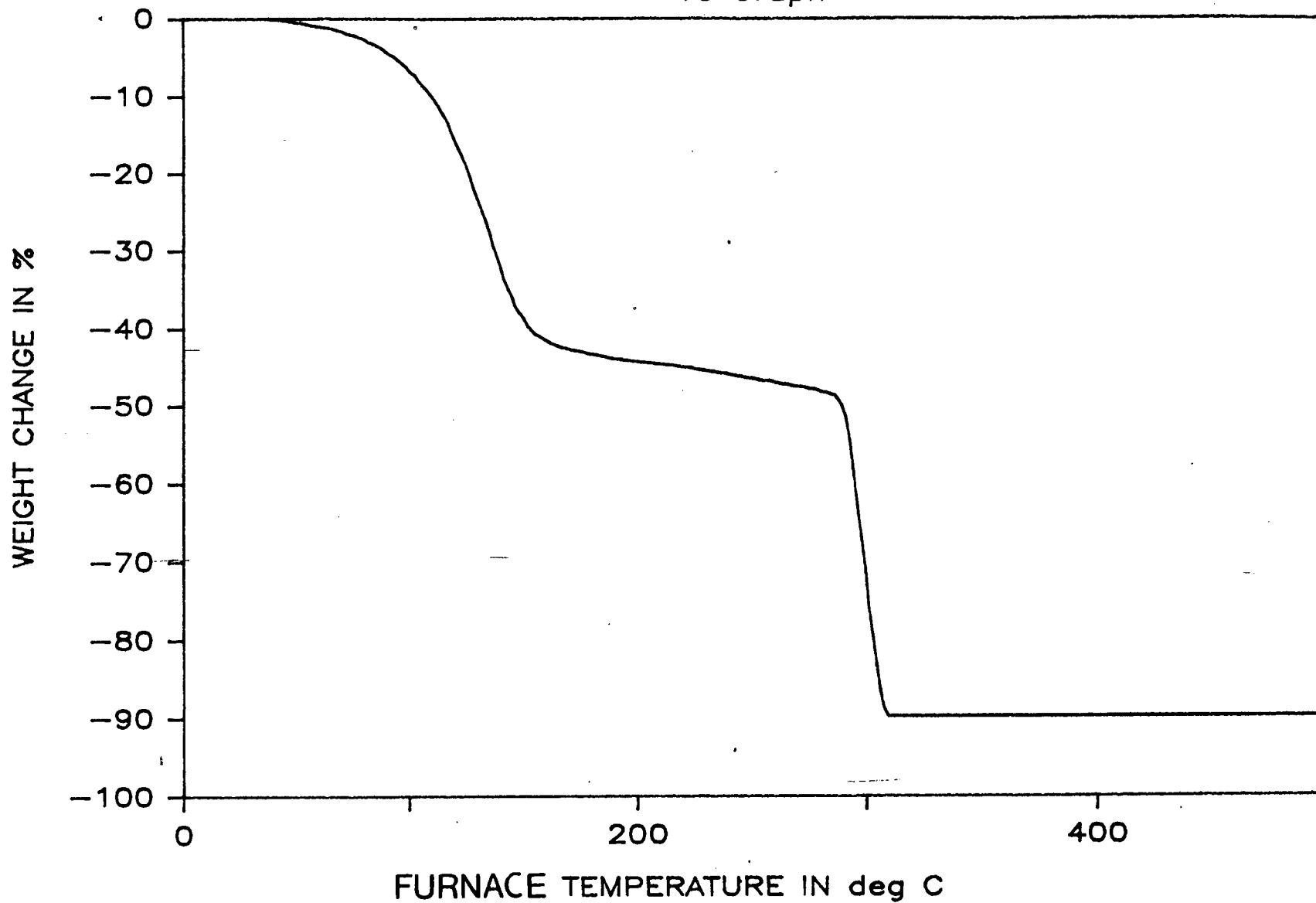


FIGURE 31: TG GRAPH OF HOST(1a).n(P-XYLENE)

R4NBR4, 30 to 500C @10C/min in N2

DTA Graph

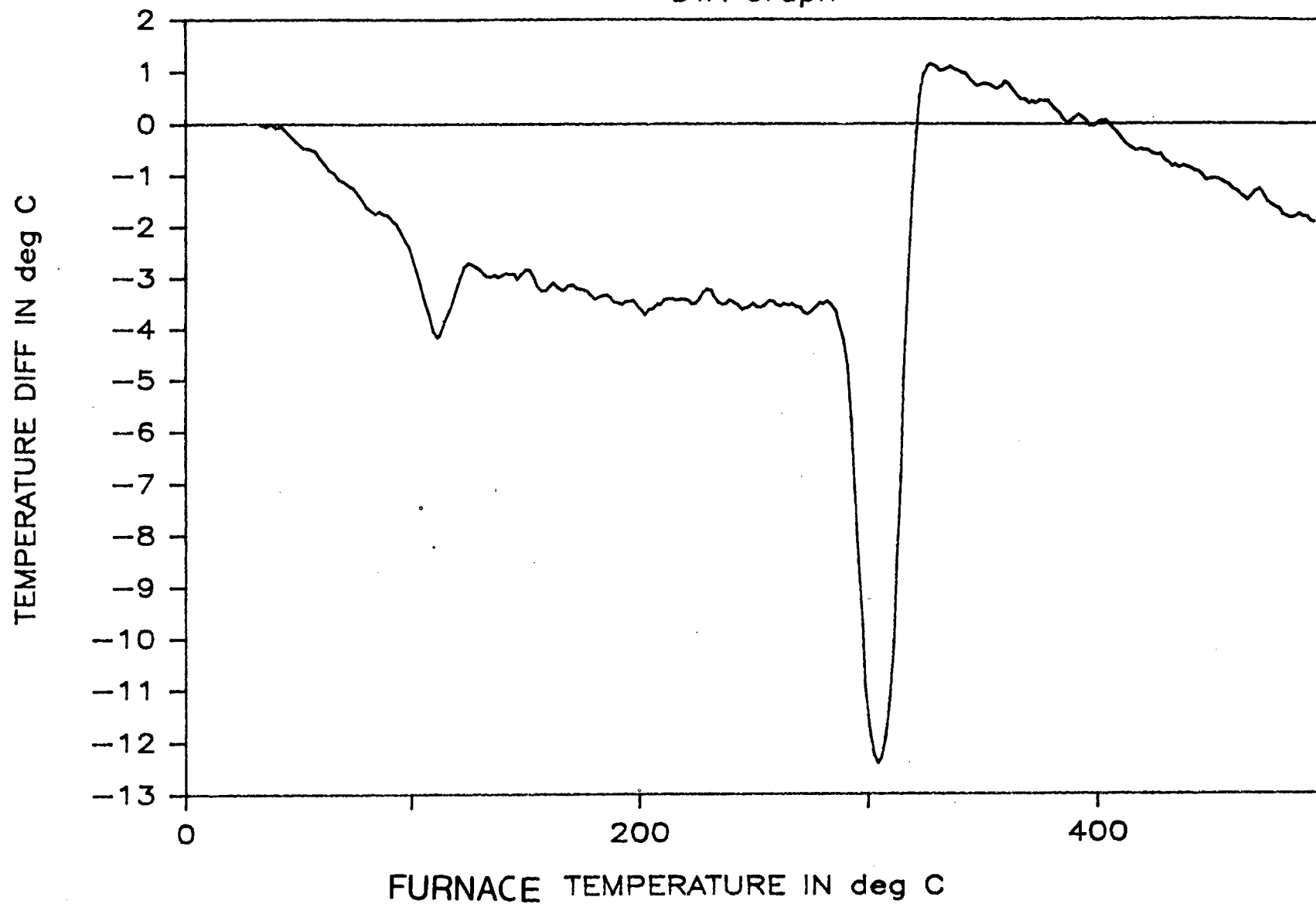


FIGURE 32: DTA OF HOST (1a)

R4NBR4 30 to 500C @10C/min in N2

TG-DTA Graph

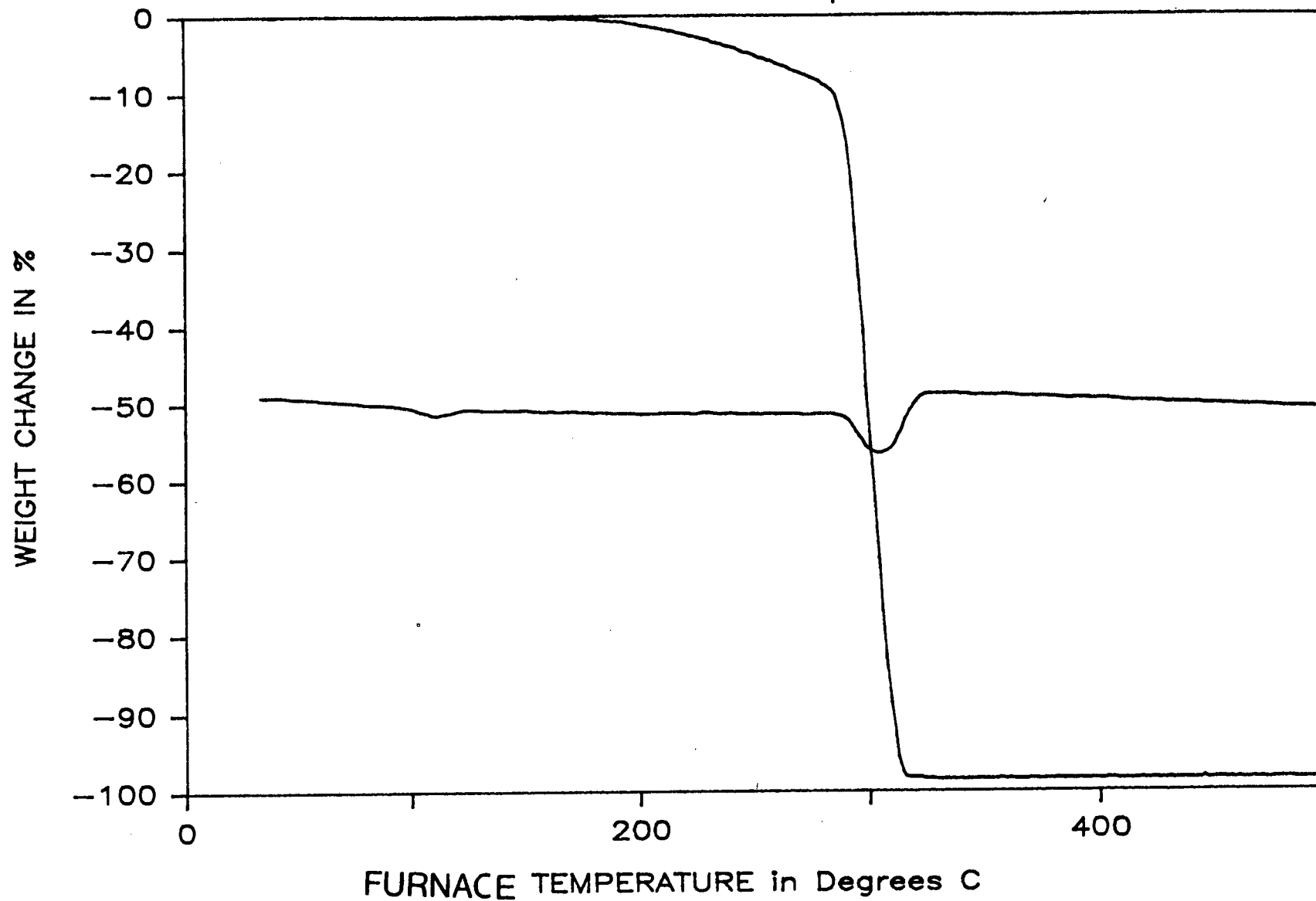


FIGURE 33: TGDIA OF HOSF (1a)

The values of ΔH_{vap} (enthalpy of vaporization) calculated from the DTA and TGA curves for guests compared favorably with theoretical values⁸ (see Table 13). However, when one compares ΔH_{vap} for H.nG and free G, it was found that their values were the same, within the error of measurement. This would imply that there is no energy of clathration, which is not possible. This observation can be explained in terms of the clathration energy being of a very small magnitude and the technique of using TGA and DTA curves not being sufficiently sensitive to detect the small difference in energy for free guest compared to clathrated guest. Since it was observed (as already discussed) that the guest is released in a single step (at a temperature characteristic of the guest) from the liquid clathrate, at a temperature which is lower than that at which the Host decomposes, it is evident that the Host material can be retrieved (unchanged) from the liquid clathrate. The parent material can, therefore, be regenerated for re-use by raising the temperature of the liquid clathrate to just above that temperature at which the guest evaporates from the clathrate.

Table 13 Tabulation of Theoretical and Calculated Enthalpy's for various guests.

GUEST	ΔH THEOR	ΔH EXPERIMENTAL (kJ/mol)
BENZENE	33.8	34.08
TOLUENE	35.9	35.78
P-XYLENE	41.04	42.2

3.2 Determination of Enthalpy using the Isosteniscope Experiment

In a further effort to determine the Energy of Clathration for the liquid clathrates, the Isosteniscope experiment was used. Samples of liquid clathrates (using parent material 1a, and various aromatic guests) were prepared and the vapor pressures of (i) the pure guest and (ii) the liquid clathrates were measured at various temperatures (see Table 14).

TABLE 15: TABULATION OF THEORETICAL AND CALCULATED ENTHALPY VALUES FOR BENZENE (ISOSTENISCOPE EXP.)

GUEST	ΔH (theor.) (kJ/mol)	ΔH (calc.) (kJ/mol)
BENZENE	33.80	34.08

$H_{calc.} + E_{clathration}$ for H.nG (H = 1a; G = benzene) = 32.5 kJ/mol

The enthalpy calculated for free guest, from a plot of $\ln(P)$ versus $1/T$, (P=vapor pressure; T=temperature; see figure 34) compared favorably with literature values²³ (see table 15):

$$\Delta H_{(clathrate)} = \Delta H_{(guest)} + \Delta H_{(clathration)} \quad \dots (\text{equation 23})$$

The enthalpy calculated for the liquid clathrate (fig.35) was found to be the same as for the guest in the absence of host. Since the enthalpy of clathration for pure guest can be determined to within 2 KJ/mol (comparing experimental and theoretical values of enthalpy) using the Isosteniscope experiment, it was concluded that the energy of clathration for the liquid clathrates must be less than 2 Kilojoules. The Isosteniscope is, therefore, not sufficiently sensitive to determine the energy of clathration of liquid clathrates.

TABLE 14: VAPOR PRESSURES MEASURED AT VARIOUS TEMPERATURES

 BENZENE

T (K)	1/T X10E-3(K)	Pvapor [mmHg]	LnP
292.0	3.425	76.95	4.33
297.4	3.363	101.45	4.61
300.0	3.333	115.45	4.74
302.0	3.311	127.05	4.84
304.5	3.284	140.95	4.95
307.5	3.252	158.95	5.07
310.0	3.226	173.95	5.16
312.5	3.200	192.95	5.27
316.0	3.165	218.45	5.39
318.0	3.145	239.95	5.48

HOST(1a).nBenzene

T (K)	1/T X10E-3(K)	Pvapor [mmHg]	LnP
291.5	3.431	76.05	4.33
293.8	3.404	90.05	4.49
296.0	3.378	101.05	4.63
299.0	3.345	114.55	4.74
302.0	3.311	129.05	4.86
305.0	3.279	146.55	5.00
310.8	3.218	183.05	5.21
314.0	3.185	207.55	5.34

FIGURE 34: PLOT OF $\ln P$ VERSUS $1/T$
FOR BENZENE

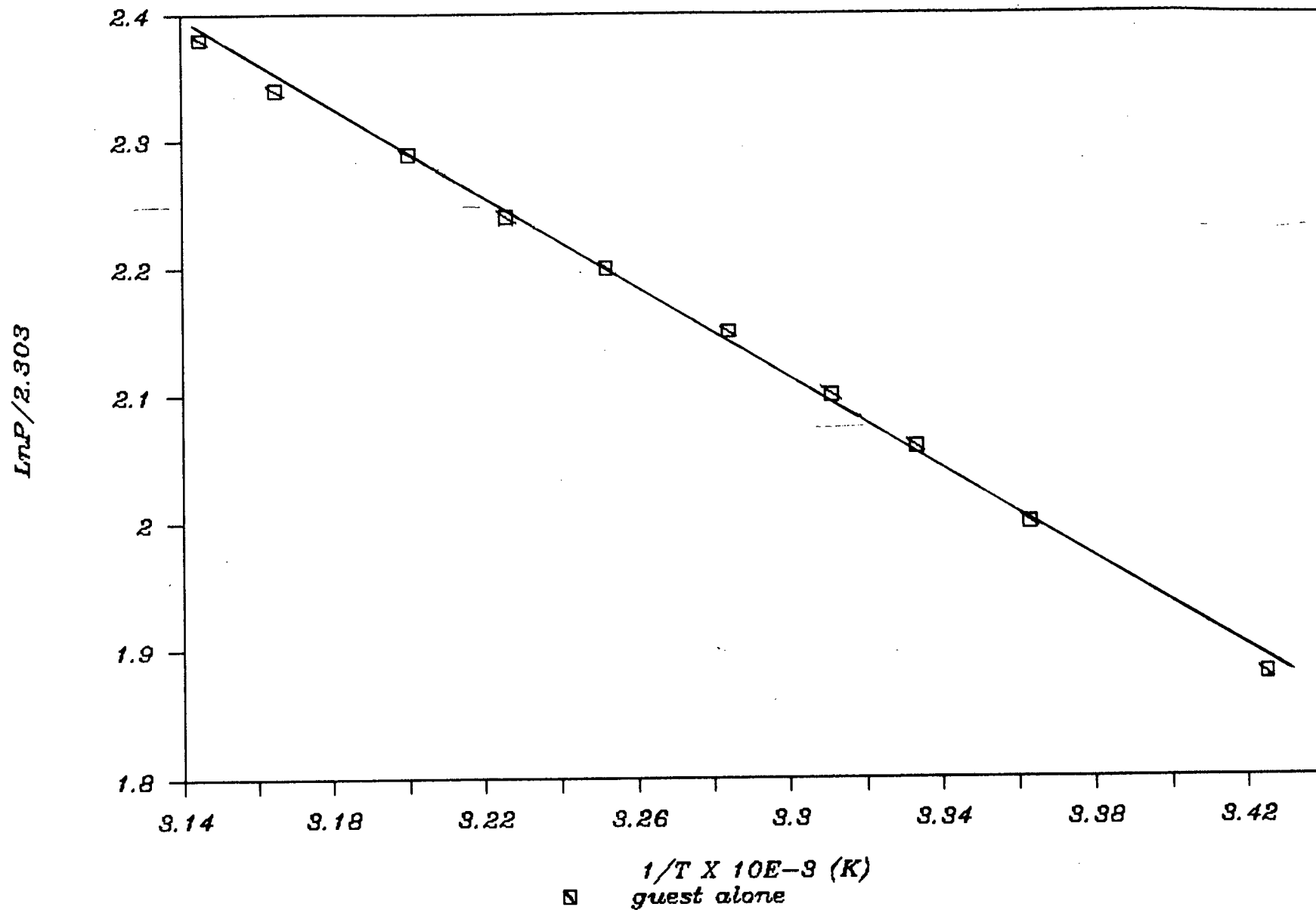
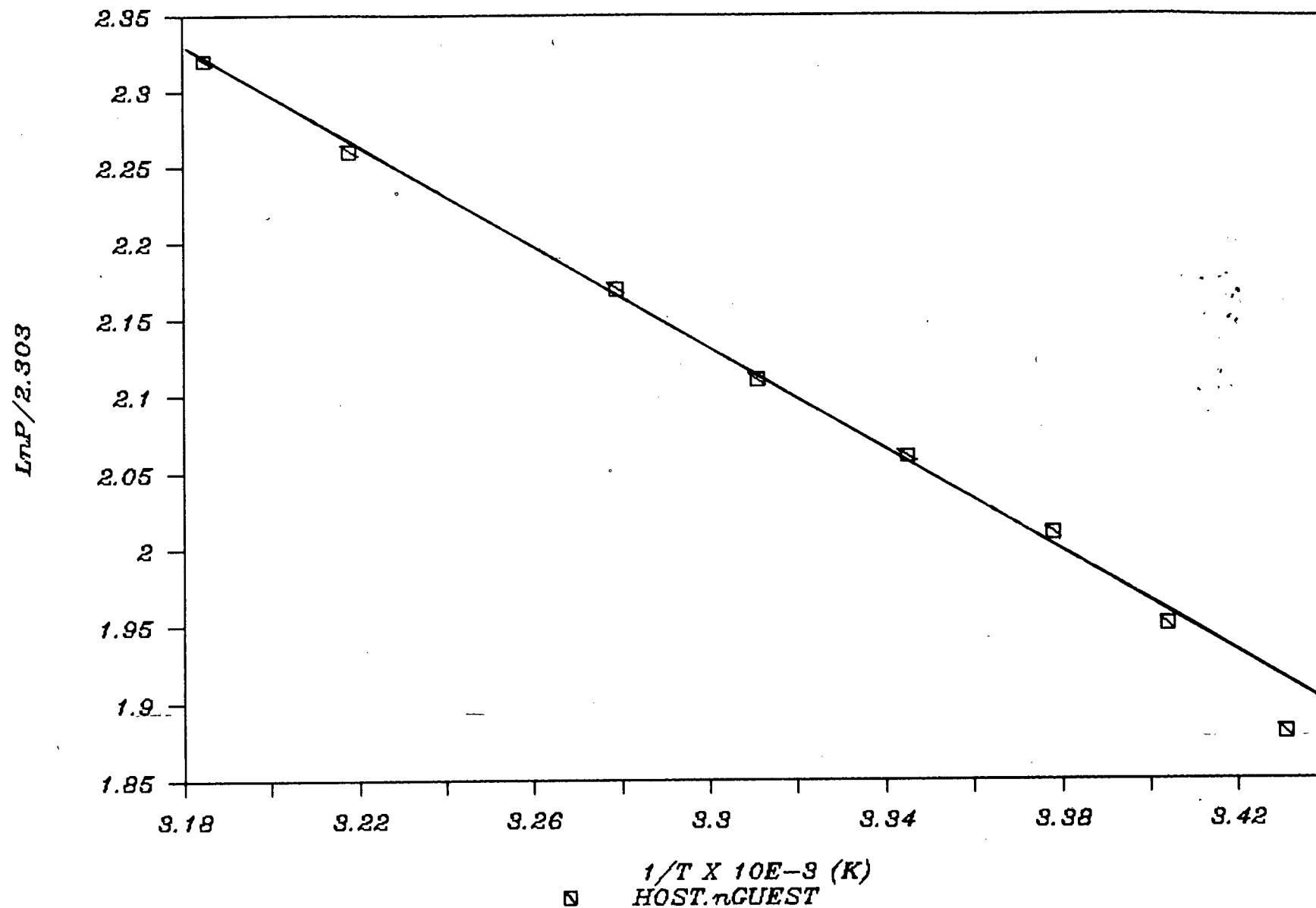


FIGURE 35: PLOT OF $\ln P$ VERSUS $1/T$

FOR HOST.nGUEST



CHAPTER 6: DETERMINATION OF STABILITY CONSTANTS

In the growing field of host-guest chemistry, which mimics biological complexation, several researchers have studied the stability of complexes formed in solution and in the solid state⁴⁴.

This study compared the strength of complexation between the parent compound (1a) and aromatic guest. Due to the rapid equilibrium of complexation, ¹H-NMR titrations provided quantitative determination of the binding between the host and guest (200 MHz, T=303°K, TMS peak taken as reference). Concentrations of host and guest were chosen to vary the percentage of complexation from about 10% to 80%. The association constants of the liquid clathrates were determined using a computer-assisted procedure. Table 16 gives the observed maximum chemical shifts ($\Delta\delta_{\text{max,obs.}}$) of the host proton whose signal can be best observed over the entire titration, the observed chemical shift of this proton at saturation binding ($\delta_{\text{sat.}}$), and the minimum value of the association constants (K_a).

TABLE 16: THE MINIMUM VALUES OF THE CALCULATED STABILITY CONSTANT OBSERVING THE SHIFT OF THE HOST CH₂ SIGNAL

GUEST	$\Delta\delta_{\text{max obs}}$	$\delta_{\text{sat.}}$	MIN. K_a calc.
BENZENE	0.570 ppm	1.035 ppm	1000 (l/mol)
TOLUENE	0.465 ppm	0.926 ppm	500

The chemical shifts of the host proton being monitored during the titration are listed in Table 17 and the calculated concentrations of H.nG for various values of K are listed in Table 18. The results tabulated in Tables 17 and 18 are depicted graphically in figures (36 and 37) and (38 and 39) respectively.

The plot of TG versus chemical shift is seen to approach, asymptotically, a maximum TG value which corresponds to a maximum n (which had been determined independently in a previous study). Using a titration point close to this maximum, theoretical values of TG as a function of K (chosen) were calculated. These results are shown in figures 38 and 39 for benzene and toluene respectively. In the case of toluene it is clear that for $K > 500$, $TG_{\text{theor.}}$ is equal to $TG_{\text{experimental}}$ and hence this value represents the minimum K necessary to explain the experimental results. It is not possible, using these results, to determine a maximum value for K. Similarly, K_{minimum} for benzene is equal to 1000.

The minimum values of K_a are observed to be very large, as expected on inspection of the plots of chemical shift of host versus total concentration of guest (see fig's. 36-37).

TABLE 17: CHEMICAL SHIFT OF THE HOST PROTONS ON TITRATION WITH G

MASS OF HOST = .117g (1.9698 X 10E-4 mol)
 GUEST = BENZENE

VOLUME G (ul)	TOTAL VOL (ul)	MOL G (X 10 ³)	[TH]	[TG]	CHEMICAL SHIFT
635	201	2.2659	0.6416	3.5683	0.8070
685	251	2.8229	0.5948	4.1210	0.8750
735	301	3.3852	0.5543	4.6057	0.9270
785	351	3.9475	0.5190	5.0287	0.9610
835	401	4.5099	0.4879	5.4011	0.9810
885	451	5.0722	0.4604	5.7313	1.0100
935	501	5.6345	0.4358	6.0262	1.0250
985	551	6.1968	0.4136	6.2912	1.0300
1035	601	6.7592	0.3937	6.5306	1.0350

MASS OF HOST = .220 g (3.7039 X 10E-4 mol)
 GUEST = TOLUENE

VOLUME G (ul)	TOTAL VOL (ul)	MOL G (X 10 ³)	[TH]	[TG]	CHEMICAL SHIFT
185	562	1.7799	0.6590	3.1670	0.7600
235	612	2.2597	0.6050	3.6920	0.8230
285	662	2.7405	0.5590	4.1400	0.8510
335	712	3.2213	0.5200	4.5240	0.8800
385	762	3.7020	0.4860	4.8580	0.9040
435	812	4.1828	0.4560	5.1510	0.9140
485	862	4.6636	0.4300	5.4100	0.9230
535	912	5.1444	0.4060	5.6410	0.9260

TABLE 18: CALCULATED VALUES OF [H.nG] FOR VARIOUS CHOSEN VALUES OF K

GUEST = BENZENE

n = 16.6; (use is made of titration point 9, see Table 12)

K (1/mol) CHOSEN	[H] (g/mol) CALCULATED	[G] (g/mol) CALCULATED	[H.(16.6)G] (g/mol) CALCULATED
100	2.7E-24	0.2740	2.022
200	3.1E-27	0.2097	2.644
300	5.6E-29	0.1795	3.089

GUEST = TOLUENE

n = 13.9; (use is made of tirtation point 8, see Table 12)

K (1/mol) CHOSEN	[H] (g/mol) CALCULATED	[G] (g/mol) CALCULATED	[H.(13.9)G] (g/mol) CALCULATED
1	3.00E-03	1.27E+00	0.0896
11	6.70E-07	2.27E-01	0.2433
100	3.20E-11	5.19E-02	0.3278
200	2.20E-12	3.15E-02	0.3417
300	5.70E-13	2.32E-02	0.3477
400	2.40E-13	1.85E-02	0.3512
500	1.30E-13	1.93E-03	0.3534
1000	3.10E-14	8.57E-03	0.3587

FIGURE 36: PLOT OF CHEMICAL SHIFT OF

HOST PROTONS ON TITRATION WITH BENZENE

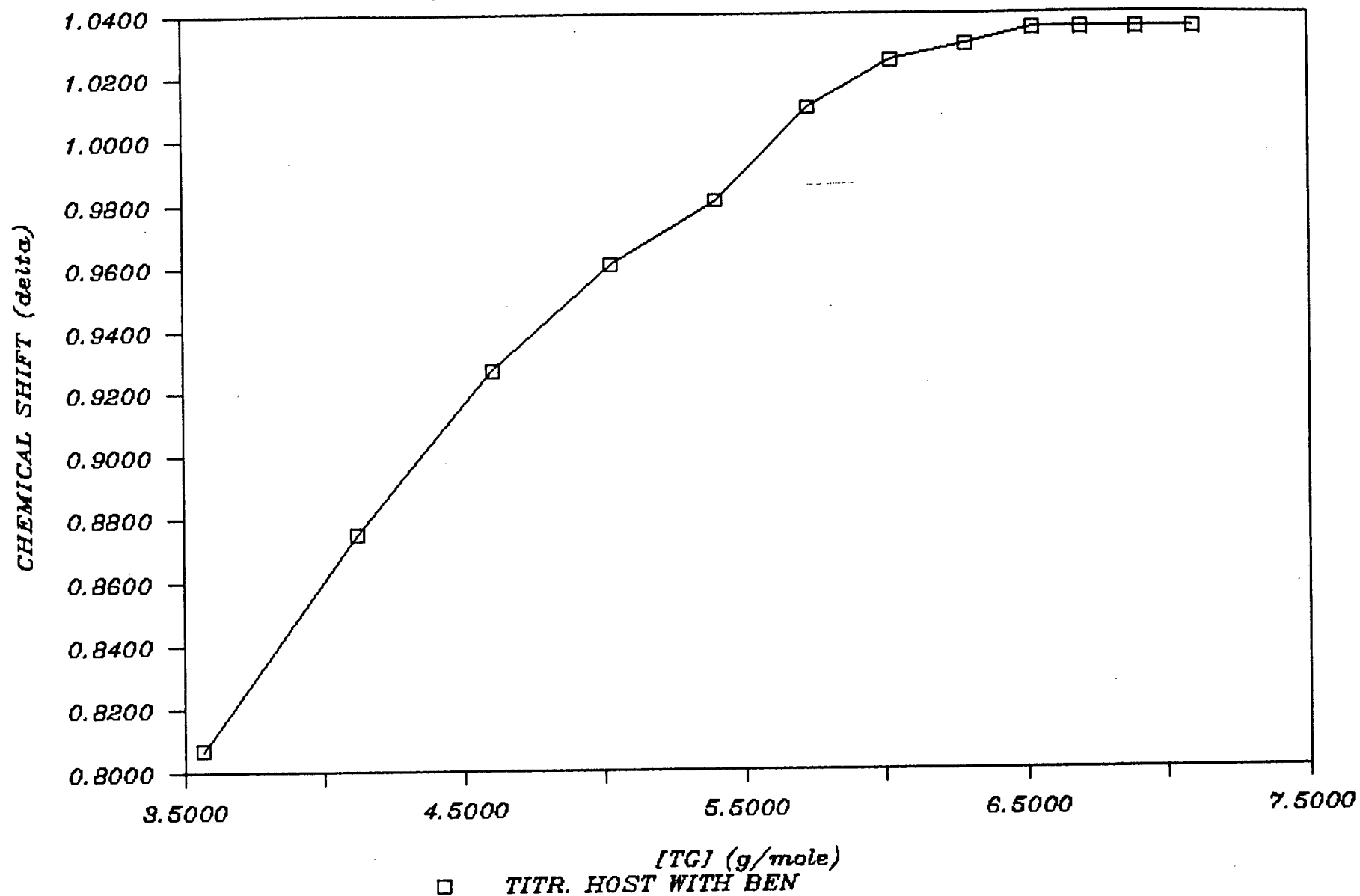


FIGURE 37: PLOT OF CHEMICAL SHIFT OF
HOST PROTONS ON TITRATION WITH TOLUENE

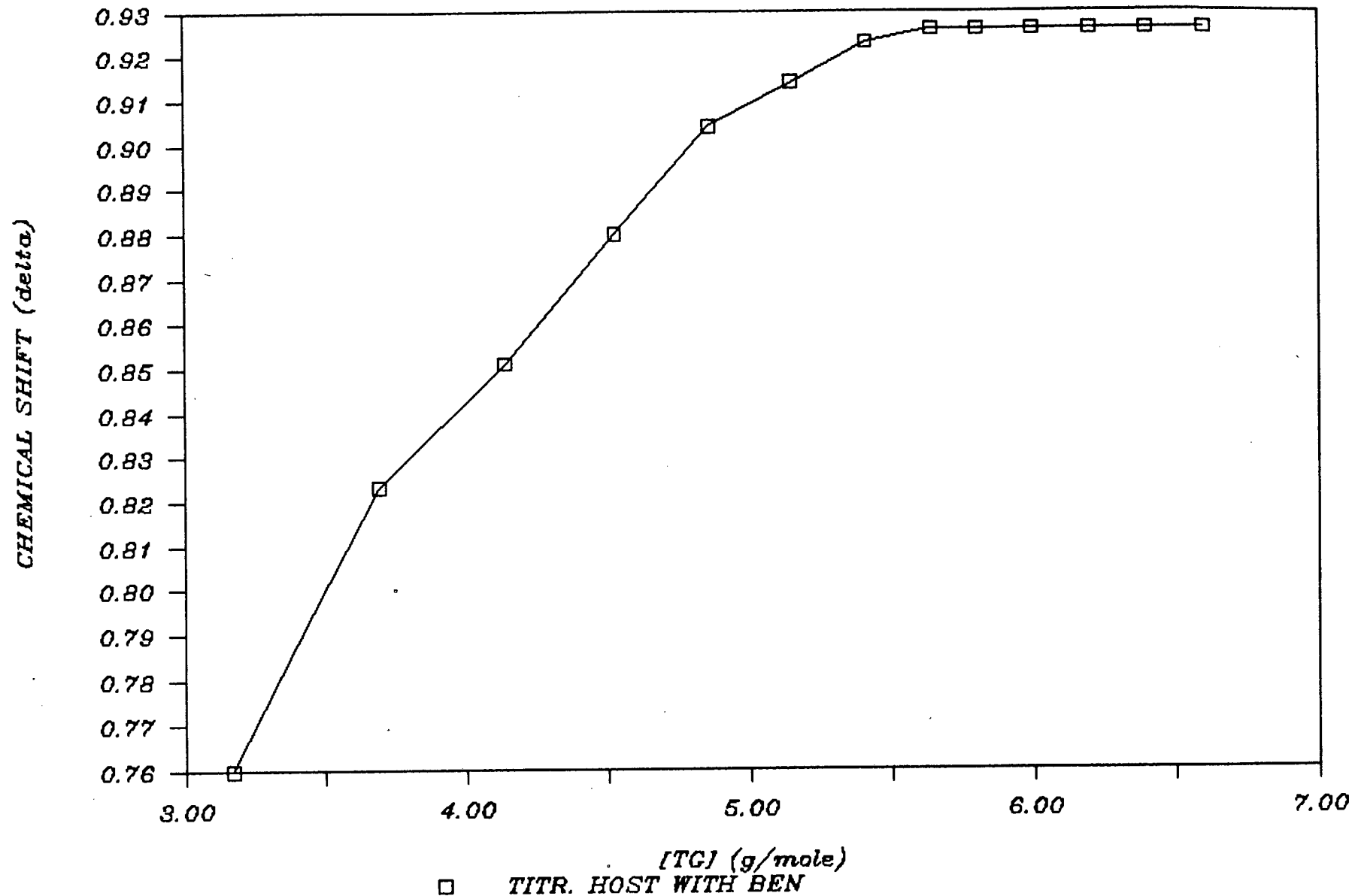


FIGURE 38: A plot of [H.n(Benzene)] versus K (chosen)

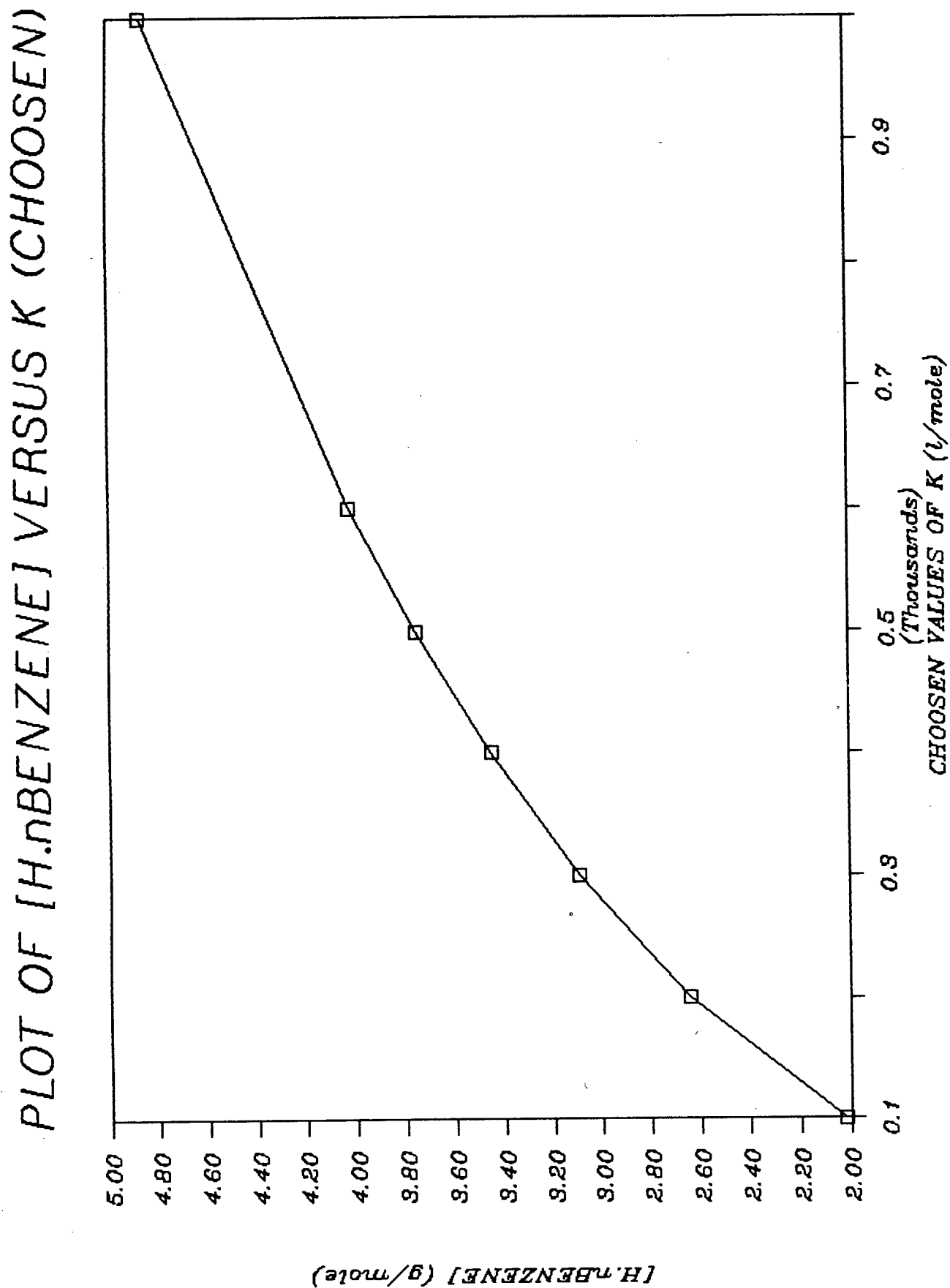
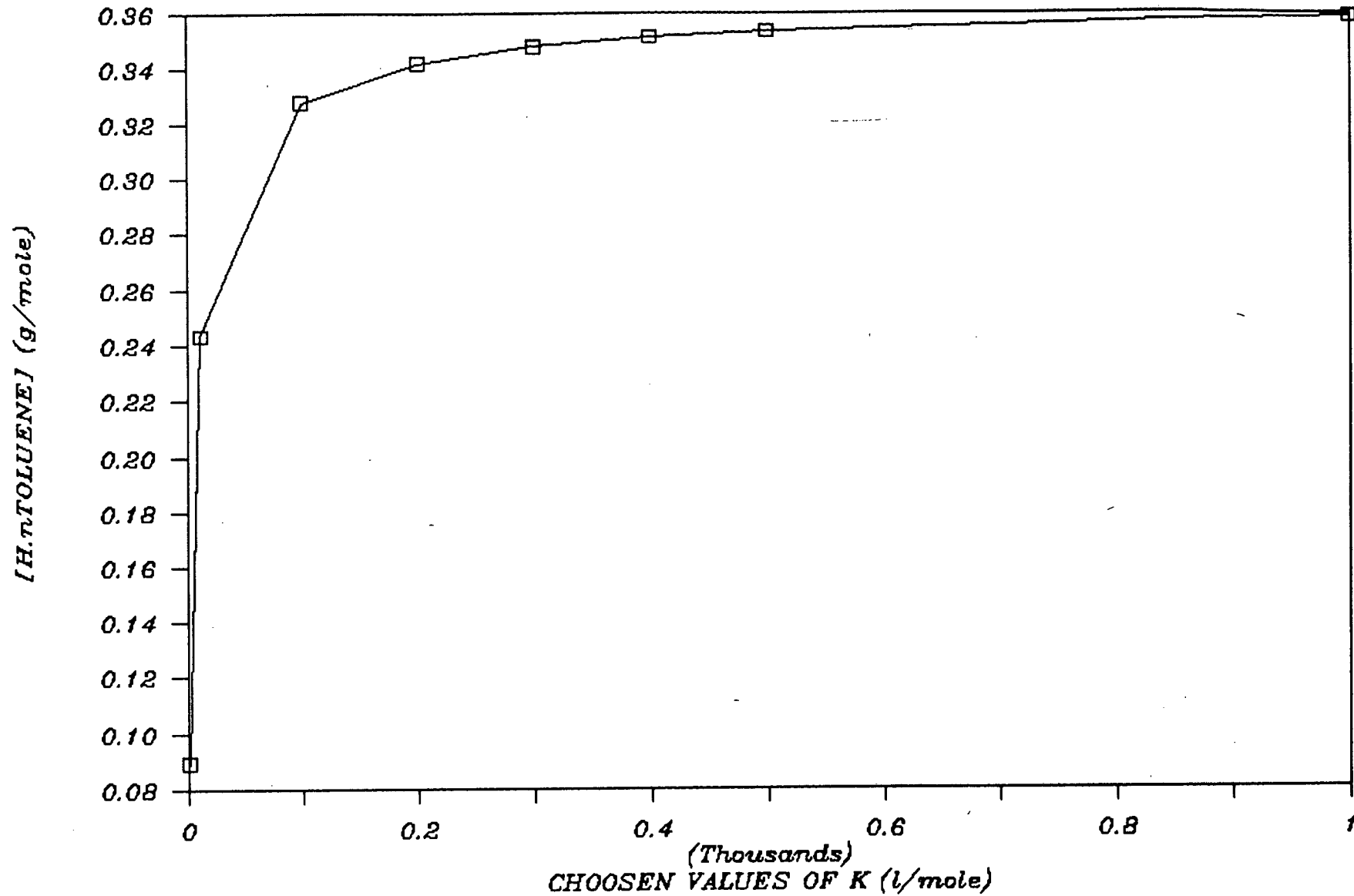


FIGURE 39: PLOT OF [H.nTOLUENE]
VERSUS K (CHOSEN)



CHAPTER 7 LIQUID CLATHRATE STRUCTURE DETERMINATION FROM NUCLEAR OVERHAUSER ENHANCEMENT (NOE) EXPERIMENTS

Experiments based on the nuclear Overhauser effect (nOe) occupy a special place in the repertoire of modern NMR methods. It is the only technique that does not depend on the presence of scalar coupling for its operation. Instead, the interaction involved is the direct magnetic coupling between nuclei (the dipolar coupling), which does not usually have any observable effect on spectra recorded in solution. The nOe provides an indirect way to extract information about this dipolar coupling, which in turn can be related to internuclear distances and molecular motion. Measurements of these parameters for molecules in solution are hard to obtain by other means, making the nOe an extremely important phenomenon.

The nOe, an aspect of nuclear relaxation, is a change in intensity of one resonance when the transitions of another are perturbed in some way. The mechanisms which drive relaxation are related to molecular motion, which is clearly random and, for a large molecule (more than about 20 atoms), may be extremely complex⁴⁵.

5.1 The Origin of The Nuclear Overhauser Effect

The nOe is a change in the intensity of one NMR resonance when the transitions of another resonance are perturbed. The 'perturbation' of interest will be saturation, which is to say that one eliminates the population difference across some transitions (by irradiating them with a weak rf field), while observing signals from others. The nOe is thus a manifestation of the attempt of the total system to stay at thermal equilibrium. Suppose the normal intensity of a resonance (i.e. that observed at thermal equilibrium and without perturbing the system) is I_0 . Then if the intensity observed while saturating some other related resonance (and waiting for the new equilibrium to be established) is I , the nOe is defined as:

$$\eta_i(s) = (I - I_0)/I_0 \quad \dots\dots(\text{Equation 24})$$

This expression is often multiplied by 100 to make the figure a percentage. $\eta_i(s)$ indicates that this is the nOe at nucleus 'i' when nucleus 's' is saturated.

5.2 Application of NOE Experiments to liquid clathrates

In order to obtain structural information on liquid clathrates, as regards the orientation of the guest in the

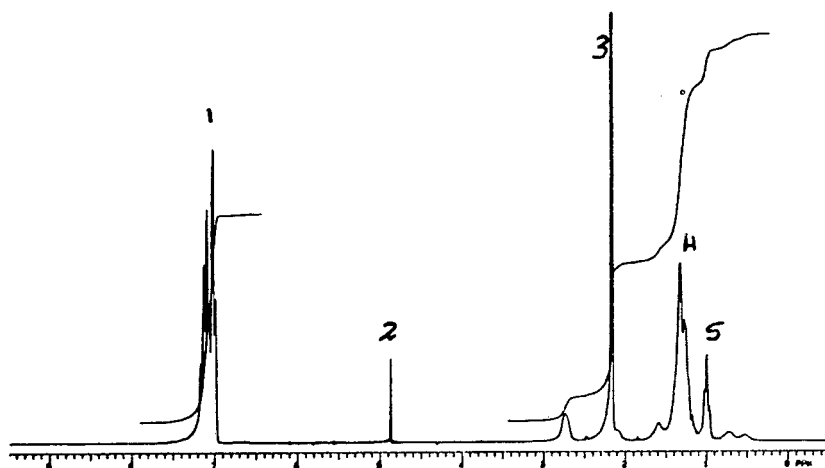
clathrate and the internuclear distance between the guest and host, nOe experiments were performed on a series of liquid clathrates formed from parent compound (1a) and aromatics.

The results of the nOe experiment performed on the liquid clathrate with toluene as guest are tabulated in Table 19.

Position of irradiation	% nOe Observed
1	2 : 4.4%
	4 : 2.6%
	5 : 4.3%
3	1 : 2.1%
4	1 : 5.0%
	2 : 2.9%
5	1 : 6.0%
	3 : 3.3%

Table 19: Results of the nOe exp. performed on H.n(Toluene)

Figure 40: Spectrum of H.n(Toluene)



A difference peak was observed for the methyl protons of toluene (3 in figure 40) when the CH₃-protons on the cation of the host were irradiated. No nOe, however, was observed at this position when the CH₂-protons were irradiated. From this it is evident that the methyl of toluene is orientated towards the CH₃'s (i.e. away from the cationic nitrogen centre of the host). NOE is also observed between the aromatic protons of the toluene and the CH₂'s and CH₃'s of the cation, the effect being larger in the latter case. This indicates that the aromatic protons of toluene are situated closer to the CH₃-protons than the CH₂-protons of the cation. One expects to see nOe between the methyl and aromatic protons of toluene, and this was observed.

The internuclear distance (r) between the protons being irradiated and the protons whose signal is enhanced, under ideal conditions, is given by:

$$\eta \propto 1/r^6 \quad \dots\dots(\text{Equation 25})^{45}$$

Thus

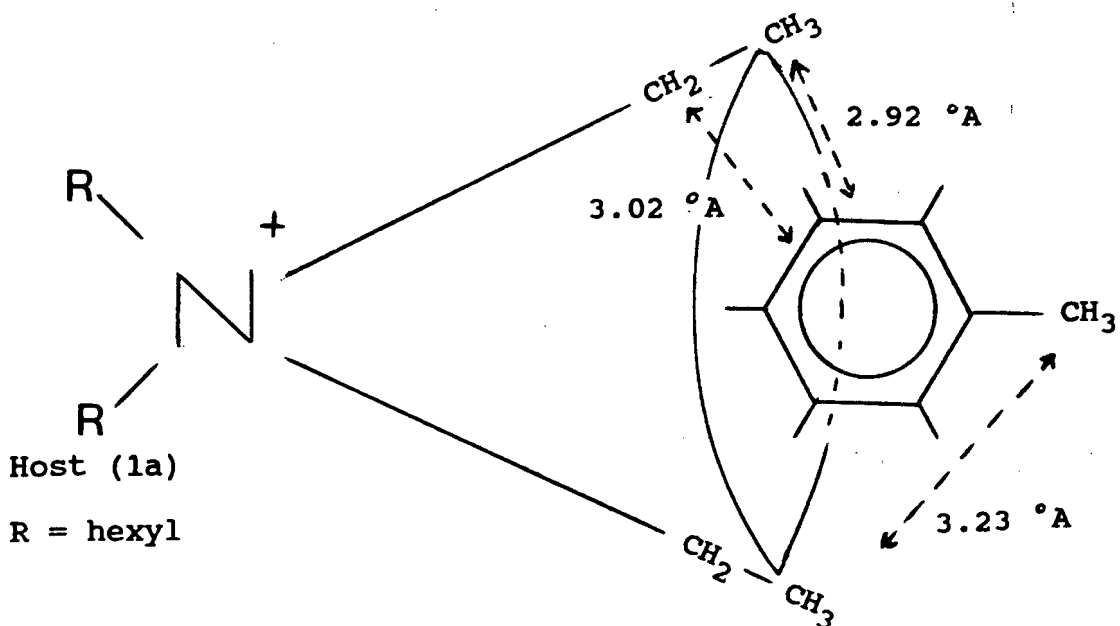
$$1/\eta = K \times r^6 \quad \dots\dots (\text{Equation 26})$$

gives the relationship between nOe and the internuclear distance. K is a constant and depends on the molecule being studied and its molecular motion. An average value of 'r' can be determined for the internuclear distance between the aromatic and methyl protons of toluene (see fig.41). Since nOe was observed between these protons, the approximate value of K for this liquid clathrate system can be

TABLE 20: TABULATION OF CALCULATED INTERNUCLEAR DISTANCES BETWEEN THE CH2- AND CH3- PROTONS OF THE HOST CATION AND THE GUEST PROTONS

	Host CH2-Protons	Host CH3-Protons
Aromatic Protons of Toluene	3.02	2.92
Methyl Protons of Toluene	no nOe obs.	3.23
CH2's attached to the N of the Host	3.3	
Aromatic Protons of p-Cymene	3.36	3.77
Methyl Protons attached to the p-cymene ring	3.77	
Aromatic Protons of Xylene	3.49	3.79
Methyl Protons of p-xylene	3.89	4.34

Figure 42: Diagram of H.nG (G = toluene) as determined from nOe results.



The guest is located between the arms of the cation of the host molecule. The internuclear distance between the host and guest being given by a cone (see fig. 42).

The calculated average distance between the methyl and aromatic protons of toluene, using the results of the nOe experiment, yielded a value of 3.08 °A. This compared favourably with the average distance calculated from the model (fig.41), from which the value of K is calculated.

The liquid clathrates, with p-Cymene as guest, were also studied using nOe, the results of which are tabulated in Table 21 (Also see fig.43).

FIGURE 43: ^1H -Spectrum of H.n(p-Cymene)

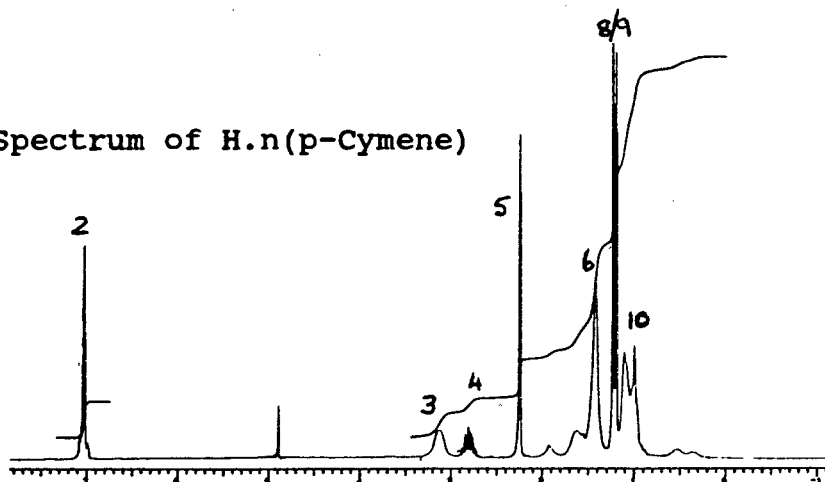


Table 21: Results of the nOe exp. performed on H.n(p-Cymene)

Position of Irradiation	nOe Observed
2	4 5 small 8 and 9
4	2 8 and 9
5	2 : 2.5%
6	2 : 3.8% 5 : 1.9%
8	2 4
9	2 4
10	2 : 1.9%

Only a very small difference peak is observed for the aromatic protons of p-cymene on irradiating the CH_3 's of the cation. Difference spectra are obtained for the protons of the methyl attached to the aromatic ring of p-cymene when the CH_2 protons of the cation are irradiated. However, no nOe is observed at the protons of the two methyls on the opposite side of the aromatic ring of p-cymene. This indicates that the p-cymene guest is orientated such that the one methyl group is orientated towards the host and the

two methyl groups, on the opposite side of the ring, are orientated away from the host. One expects to observe nOe between the two methyls of p-cymene and the adjacent -CH, and also between the methyl attached to the ring and the ring protons. This was observed. The weaker nOe signals between guest and host observed in the case of p-cymene guest, compared to toluene guest, is indicative of larger distances between the host and guest molecules (see fig.45) in the former liquid clathrates.

As described above, the average distance between the methyl protons (of the methyl attached to the ring) and the aromatic protons of p-cymene can be determined (see fig.44) and hence the value of K determined from equation 26, for the host.n(p-cymene) liquid clathrate system. The value of K was found to be $1.80 \times 10^{-4} (\text{Å}^{-6})$. From the measured nOe's, the distances between the guest and host were calculated (see Table 20). This is also illustrated in figure 45. The cone formed by the arms of the cation (of host), which contains the guest molecules, is observed to be displaced so that the guest is observed to be further from the apex of the cone when compared to the result obtained for the toluene guest.

Figure 44: Diagram of p-Cymene, used for the calculation of

$r_{ave.}$

$$1/(r_{ave.})^{-6} = 0.25[2(3.02 \text{ \AA})^{-6} + 2(5.14 \text{ \AA})^{-6}]$$

$$\therefore r_{ave.} = 3.37 \text{ \AA}$$

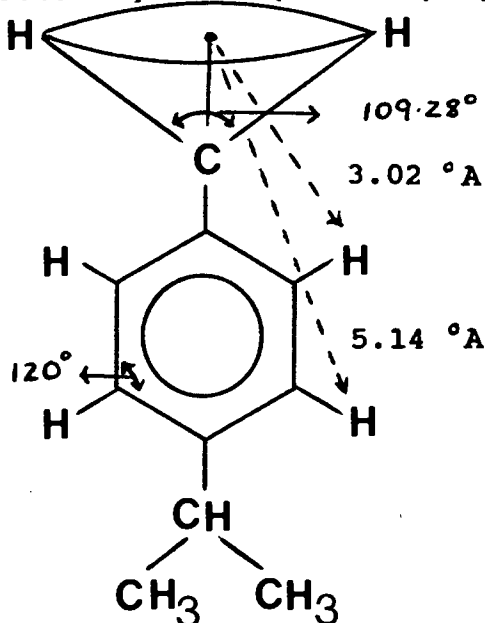
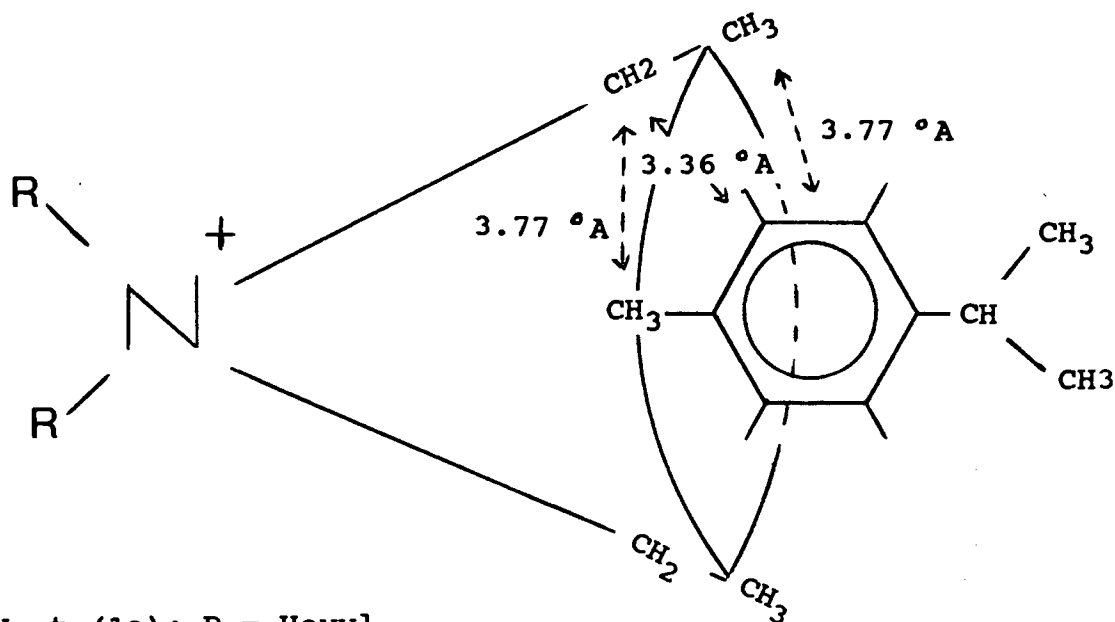


Figure 45: Diagram of H.n(p-Cymene) as determined by nOe.



Host (1a); R = Hexyl

In order to obtain further structural information, liquid clathrates, using p-xylene as guest, were also studied.

Table 22 tabulates the results of the nOe experiments (also see fig. 46).

Figure 46: Spectrum of H.n(p-Xylene)

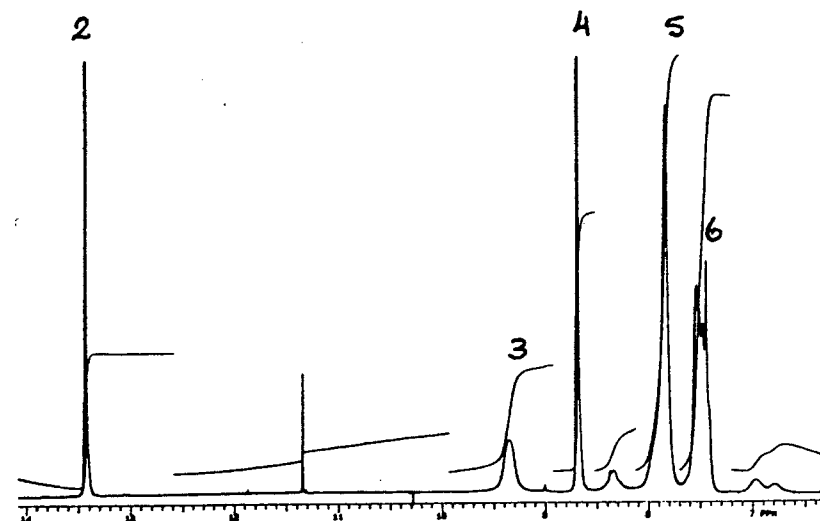


Table 22: Results of the nOe exp. performed on H.n(p-Xylene)

Position of Irradiation	%nOe observed
2	4 : 2.9%
4	2 : 5.5%
5	2 : 4.4%
	4 : 2.3%
6	2 : 2.7%
	4 : 1.2%

A Difference peak is observed for the methyl protons of p-xylene when either the CH₂- or CH₃- protons of the host cation are irradiated. This is anticipated, since there is a methyl on either side of the aromatic ring of p-xylene and from the previous discussion of the results obtained from the study of other clathrates, the p-xylene is expected to

be orientated with one methyl group directed towards, and the other away, from the nitrogen centre of the cation (of host). As before, the nOe which one expects between the aromatic and adjacent methyl proton of p-xylene, is observed. The nOe observed between the aromatic protons of the guest and the protons of the CH₂'s (cation of host) is less than that observed for toluene guest, but more than that for the p-Cymene guest. The same trend is observed when the CH₃'s of the cation are irradiated (see Table 23). From this it is deduced that the guest is found further from the nitrogen cation centre as one changes the guest from toluene to p-xylene to p-cymene.

An average value of 'r' (the internuclear distance between the methyl and aromatic protons of p-xylene) was calculated (see fig. 47) and a value of $1.24 \times 10^{-4} (\text{\AA}^{-6})$ obtained for K, using equation 26. Hence, the internuclear distances between the host and guest were calculated from the measured nOe's, using equ. 26 (see Table 20 for tabulation of results). The results of the distance determinations are illustrated diagrammatically in figure 48.

Figure 47: Diagram of p-Xylene (used to calc. $r_{ave.}$)

$$1/(r_{ave.})^{-6} = 0.25 [2(3.02 \text{ \AA})^{-6} + 2(5.14 \text{ \AA})^{-6}]$$

$$\therefore r_{ave.} = 3.37 \text{ \AA}$$

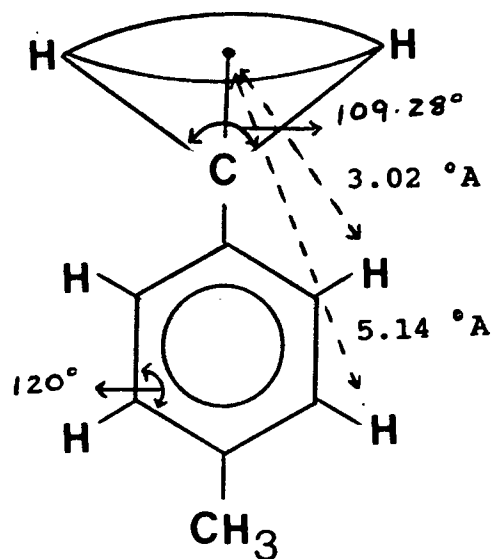


Figure 48: Diagram of H.n(p-Xylene) as determined from nOe results.

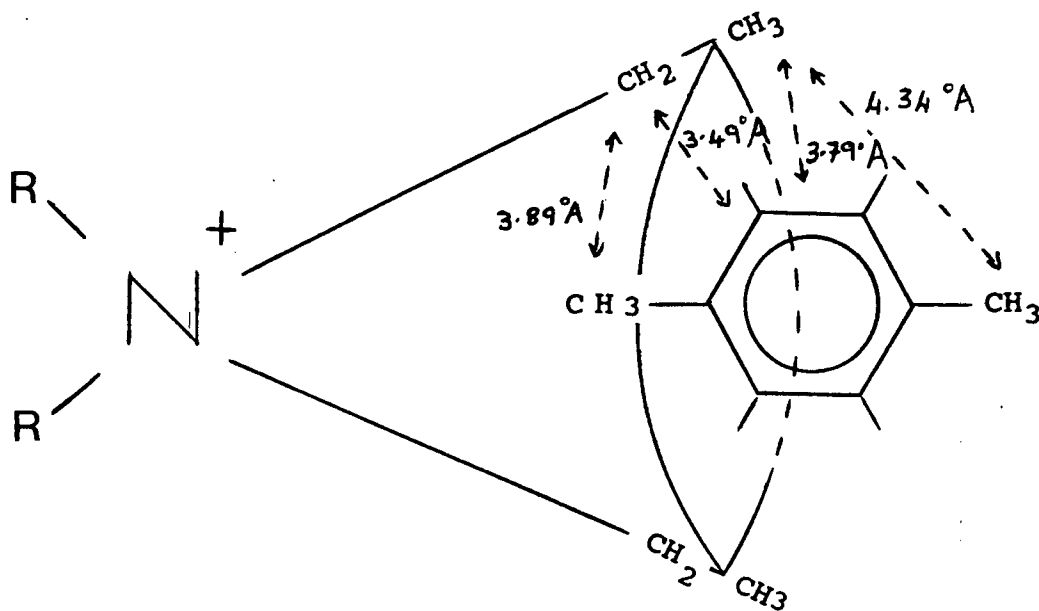


Table 23: Tabulation of Calculated nOe 's Observed between the CH_2 - and CH_3 - Protons of the host cation and the Guest Protons.

HOST CATION	Methyl (toluene)	Aromatic (toluene)
Irradiating CH_2 's	-	5
Irradiating CH_3 's	3.3	6.03
	Methyl (p-xylene)	Aromatic (p-xylene)
Irradiating CH_2 's	2.3	4.4
Irradiating CH_3 's	1.2	2.7
	Methyl (p	Aromatic (p-cymene)
Irradiating CH_2 's	1.9	3.8
Irradiating CH_3 's	-	1.9

Considering the results tabulated in Table 23, it is evident that the observed nOe between the host and guest decreases as one goes across the series: guest = toluene, p-xylene, p-cymene. This implies that, on going across the series, the guest molecules are situated further from the nitrogen centre of the cation (of the host). This would also imply that there would be a less efficient packing of the guest molecules and, therefore, less guest able to pack around the host as one goes from left to right across the series. If one considers the change in the size of the guest molecules: toluene, p-xylene, p-cymene, it would be expected that more toluene would be clathrated, since it is the smallest guest molecule. This is found to be the case, as indicated by the values of n obtained for H.nG : $n = 14-15$ for Toluene; $n = 9-11$ for p-xylene; $n = 4-5$ for p-cymene.

CHAPTER 8: CRYSTALLOGRAPHIC ANALYSIS OF CLATHRATES

The liquid clathrate from parent compound (1a) and cyclohexene was prepared, as previously described. On allowing this clathrate to stand (contained in a vial), it was observed that crystals formed, after approx. 7 months, as the guest slowly evaporated. A crystallographic study of the liquid clathrate host was thus conducted.

The tetrahexylammonium (isobutyl)(tri-sec-butyl)borate parent compound (host) was expected to be disordered. This was found to be the case and an attempt was made to model the anion (borate ion) as a disordered sphere by replacing it with a calculated group scattering factor.

In order to obtain further information about the behavior of liquid clathrates a comparison was made between the crystal structure of parent compound (1a) (which forms liquid clathrates when added to hydrocarbons) and a geometrically similar compound, tetrahexylammonium tetraphenylborate (which does not show liquid clathrate behavior).

The light-orange monoclinic-shaped crystals of 1a were identified by micro-analysis and NMR. This also gave evidence that the guest, cyclo-hexene, had been desorbed. It must be stressed that the quality of the crystal was

poor, as indicated by the small number of good reflections obtained (discussed below).

6.1.1 Preliminary X-Ray Analysis of Parent Compound (1a)

A monoclinic space group was revealed by oscillation and Weissenberg photography. The approximate cell parameters obtained from the photographs were: $a = 19.5 \text{ \AA}$, $b = 6.4 \text{ \AA}$, $c = 22.0 \text{ \AA}$, $\beta = 98^\circ$ and $z = 4$.

From the Weissenberg photographs, the conditions for non-extinction of reflections were determined as

$$hkl : h + k = 2n$$

$$h0l : l = 2n \text{ (} h = 2n \text{)}$$

$$0k0 : k = 2n$$

These systematic absences are indicative of the space groups Cc or $C2/c$ ⁴⁶.

6.1.2 Intensity Data Collection

The diffractometer data set, obtained on an Enraf-Nonius CAD4 diffractometer (MoK α radiation, $\lambda = 0.7107 \text{ \AA}$), contained 1958 unique reflections collected within the range

$1^\circ < 2\theta < 25^\circ$. Of these, 978 had $I_{rel} > 2\sigma I_{rel}$, and constituted the "observed" data.

Accurate cell parameters determined by least squares analysis and other relevant crystal data are listed in Table 24.

Table 24: Crystal Data

Molecular formula	$C_{40}H_{80}NB$
Molecular weight	$593.962 \text{ gmol}^{-1}$
Space group	Cc
a	$20.21(8) \text{ \AA}$
b	$6.70(6) \text{ \AA}$
c	$23.77(5) \text{ \AA}$
β	$98.0(3)^\circ$
v	3184 \AA^3
ρ_c	1.24 gcm^{-1} for $z = 4$
$\mu(\text{MoK}\alpha)$	0.33 cm^{-1}
F(000)	1328.00
Scan mode	w-2 θ
Scan width (in w ($^\circ$))	$(1.05 + 0.35\tan\theta)^\circ$
Scan speed	variable
Aperture width	$(1.25 + 1.05\tan\theta) \text{ mm}$
Crystal Dimensions	$(0.16 \times 0.31 \times 0.47) \text{ mm}^3$

6.1.3 Attempted Solution and Refinement of the Parent compound (1a) Structure

Solution was attempted in the non-centrosymmetric space group Cc, using the Direct Methods package of SHELXS-86⁴⁷. The position of the nitrogen atom and all the carbon atoms on the cation were found, and refined using SHELX-76⁴⁸. It was necessary to place some of the carbon atoms (of the cation) at a site occupancy of 0.5, owing to disorder in the molecule. A smear of electron density was observed for the atoms of the anion and the position of the boron could not be found. After inserting all the positions of the atoms of the cation and calculating structure factors, the subsequent least-squares refinement yielded a value of 17.5% for the conventional Residual Factor (R), (the number of parameters being equal to 147). Attempts to solve the structure in either the P1 or $\bar{P}1$ space groups (having obtained a further primitive triclinic data set), yielded far higher values of R, and no further information about the positions of the atoms on the anion was obtained from this treatment. Hence work on the Cc data set was continued.

A Difference Fourier map, obtained from a structure factor calculation based on the positions of the atoms of the cation, revealed the borate anion to be disordered. A spherically averaged group scattering factor was calculated by modelling the disordered borate anion as totally

TABLE 25: Fractional atomic coordinates ($^{\circ}\text{A}$)
and Thermal Parameters ($^{\circ}\text{A}^2$)
with e.s.d.'s in parentheses for Host (1α).

ATOM	X/A	Y/B	Z/C	U11	ATOM	X/A	Y/B	Z/C	U11
R1	.3600	-.7831	-.6100	.0595	C431	.4706	-1.1203	.0890	.0898
	.0000	.0040	.0000	.0071		.0044	.0126	.0039	.0238
C11	.3522	-.6028	.0242	.1055	C44	.5225	-1.1551	.1231	.1538
	.0026	.0064	.0024	.0125		.0037	.0101	.0032	.0248
C12	.3294	-.5766	.0740	.0840	C45	.5682	-1.3538	.1459	.2684
	.0027	.0063	.0028	.0117		.0044	.0136	.0043	.0342
C13	.2969	-.5484	.1192	.1949	C51	.6826	.4279	.0369	.1223
	.0043	.0137	.0042	.0356		.0036	.0112	.0033	.0285
C14	.2980	-.3964	.1538	.1160	C52	.5341	.9212	-.0566	.0737
	.0029	.0077	.0029	.0159		.0032	.0096	.0032	.0192
C15	.2560	-.3271	.2005	.2271	C53	.6236	.7615	-.0085	.0262
	.0048	.0144	.0042	.0370		.0020	.0042	.0020	.0069
C16	.2555	-.1592	.2260	.3384	C54	.6814	.0961	.0262	.0878
	.0060	.0175	.0050	.0550		.0027	.0077	.0029	.0168
C21	.3959	-.7458	-.0581	.1185	C55	.5949	.2547	.0002	.0661
	.0030	.0100	.0029	.0193		.0024	.0072	.0027	.0131
C22	.3941	-.6855	-.1028	.1443	C56	.6881	.0803	-.0047	.0855
	.0037	.0114	.0037	.0253		.0027	.0073	.0028	.0164
C24	.4333	-.4344	-.1946	.1829	C57	.5212	.5771	-.0365	.0335
	.0043	.0120	.0040	.0286		.0022	.0040	.0022	.0075
C31	.3271	-.9709	-.0444	.1216	C58	.5243	.9048	-.0210	.3239
	.0034	.0097	.0028	.0203		.0054	.0176	.0054	.0598
C32	.2766	-.9707	-.0825	.1572	C59	.6928	.4078	.0148	.0700
	.0034	.0095	.0035	.0215		.0031	.0089	.0033	.0179
C33	.2212	-1.1041	-.1170	.2249	C60	.5957	.2425	-.0282	.1103
	.0042	.0125	.0036	.0277		.0032	.0105	.0032	.0260
C34	.1749	-1.1458	-.1471	.2895	C62	.5587	.7423	-.0310	.0274
	.0048	.0140	.0043	.0362		.0021	.0045	.0021	.0068
C35	.1487	-.2992	-.1615	.3046	C42	-.0533	.5202	.0650	.1270
	.0054	.0169	.0051	.0414		.0030	.0090	.0032	.0173
C41	.4300	-.8200	.0244	.1464	C25	.9283	.2860	.7919	.1977
	.0029	.0085	.0029	.0173		.0039	.0116	.0036	.0257
C38	.1287	-1.4724	-.1768	.2915	C23	.4069	.5638	.8588	.1996
	.0044	.0144	.0041	.0384		.0040	.0119	.0038	.0275
C432	.5092	-.9869	.0972	.0691	C26	.4578	-.2705	-.2608	.2088
	.0039	.0121	.0038	.0221		.0040	.0130	.0042	.0302
					C46	.6232	-1.2288	.1707	.4450
						.0049	.0152	.0042	.0441

spherically disordered⁴⁹. The borate anion was then inserted in the centre of the observed high electron density cloud, where the anion was anticipated to be. The subsequent treatment of the cation atoms and the anion model using SHELX76 gave an R value equal to 45.4%. Applying fractional site occupancy to the anion model and subsequent refinement resulted in the lowering of the R value to 42.0%. Thus, trying to model the disorder of the anion as totally spherically disordered proved to be unsuccessful.

We realise that the structure cannot be considered to be solved, but since some structural information was obtained from this study, its discussion has been included.

The structure of the host molecule (1a) was therefore only obtained for the cation. The proposed structure of the host cation, from the information obtained from the crystallographic analysis, is shown diagrammatically in figure 49. A view of the four cations in the unit cell is shown in projection down the y-axis (see figure 50).

The final atomic coordinates of the cation, with corresponding thermal parameters, are listed in Table 25. Lists of observed and calculated structure factors are presented in Appendix VI(a).

After the final cycle of refinement an analysis of variance was calculated (Table 28), but we recognise that little

TABLE 28: ANALYSIS OF VARIANCE

a) By parity groups

Group	ggg	ugg	gug	ugg	ggg	ugu	guu	uuu	All
N	353	0	0	192	145	0	0	288	978
V	578	0	0	486	472	0	0	461	512

b) As a function of sin(theta)

sin(theta)	0.00 - 0.14	0.14 - 0.18	0.18 - 0.21	0.21 - 0.23	0.23 - 0.26	0.26 - 0.28	0.28 - 0.30	0.30 - 0.32	0.32 - 0.34	0.34 - 0.43
N	105	110	90	92	130	99	87	92	89	84
V	1010	593	544	402	337	406	405	343	294	258

c) As a function of (F/Fmax)

(F/Fmax)	0.00 - 0.16	0.16 - 0.17	0.17 - 0.19	0.19 - 0.20	0.20 - 0.22	0.22 - 0.24	0.24 - 0.27	0.27 - 0.32	0.32 - 0.39	0.39 - 1.00
N	129	73	143	61	105	89	88	105	88	97
V	380	349	375	370	423	504	587	456	524	926

d) As a function of Miller index

Miller index	0	1	2	3	4	5	6	7	8	9	10	11	12	13	REST
h	0	1	2	3	4	5	6	7	8	9	10	11	12	13	REST
N	38	72	78	74	86	60	76	60	66	62	49	48	43	40	126
V	699	582	685	564	664	533	535	440	464	403	392	434	448	396	273
k	0	1	2	3	4	5	6	7	8	9	10	11	12	13	REST
N	126	223	200	172	127	78	45	7	0	0	0	0	0	0	0
V	828	5223	460	474	379	294	267	133	0	0	0	0	0	0	0
l	0	1	2	3	4	5	6	7	8	9	10	11	12	13	REST
N	83	67	72	69	78	62	68	60	59	51	60	47	48	30	124
V	427	504	944	567	633	552	420	398	420	424	445	372	385	396	367

N = No. of reflections in the group

V = 100[M (F - F) / N] where M = total no. of reflections

FIGURE 49: The Proposed Structure of Host (1a) shown in projection down the y-axis

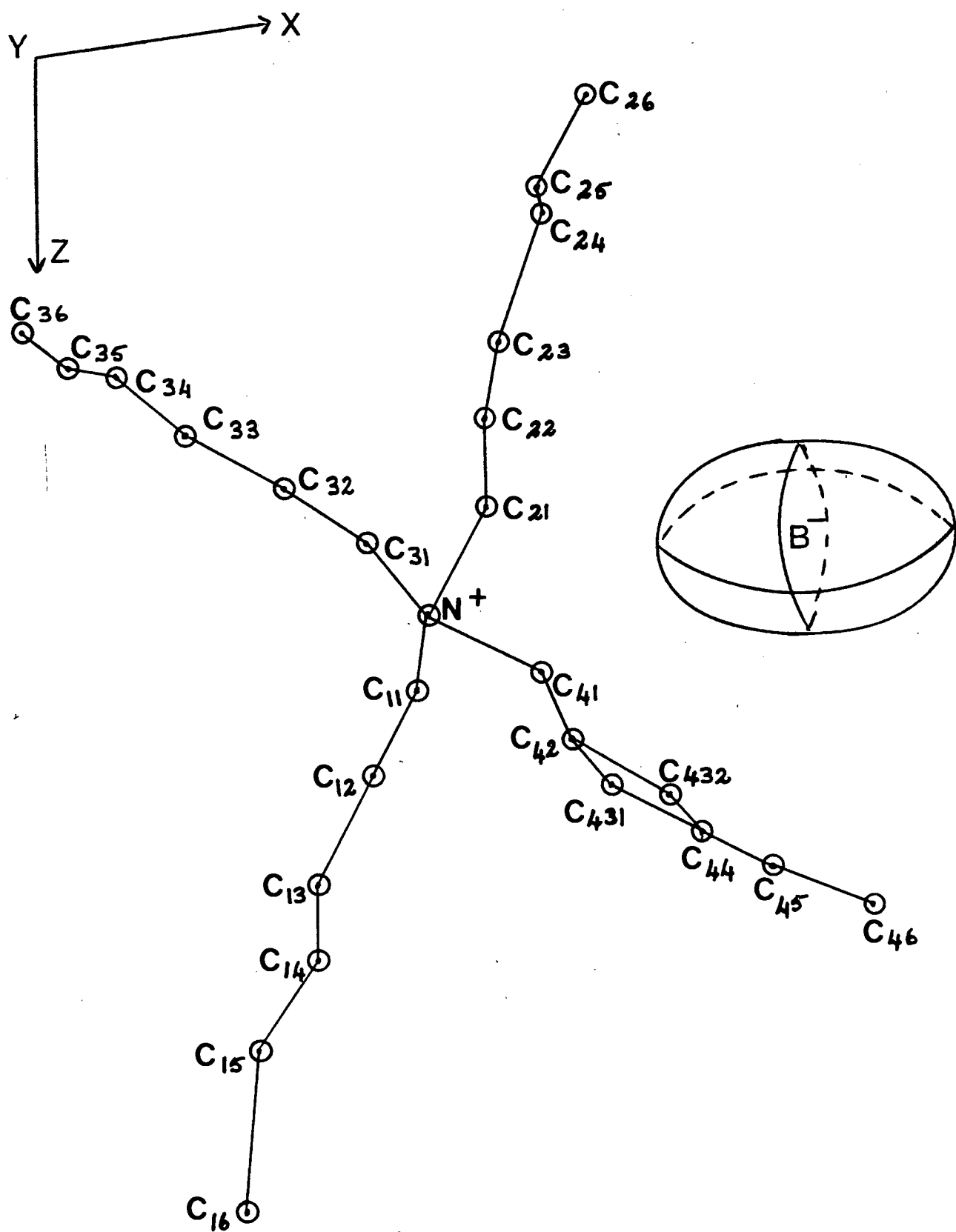


FIGURE 50



FIGURE 51

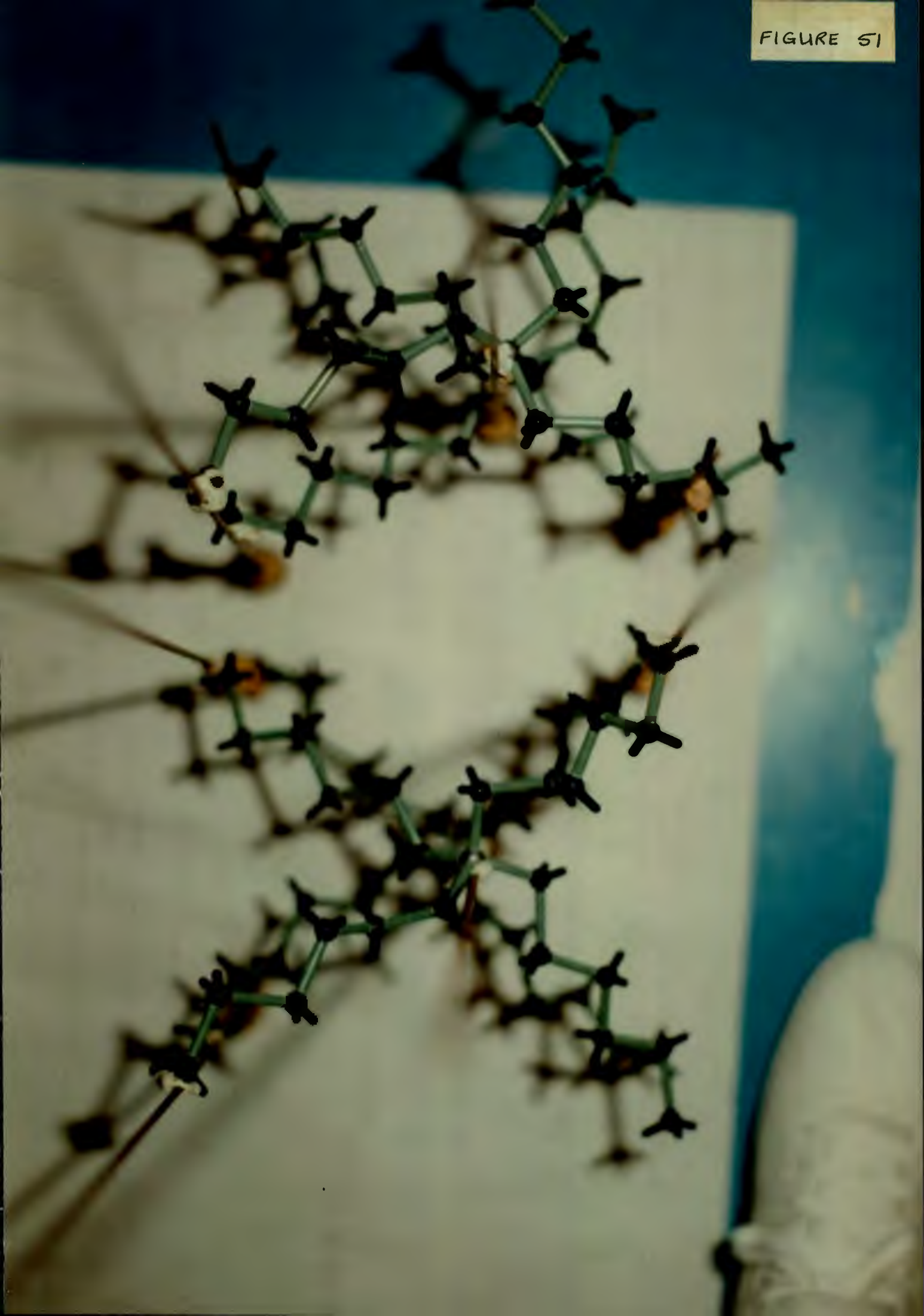
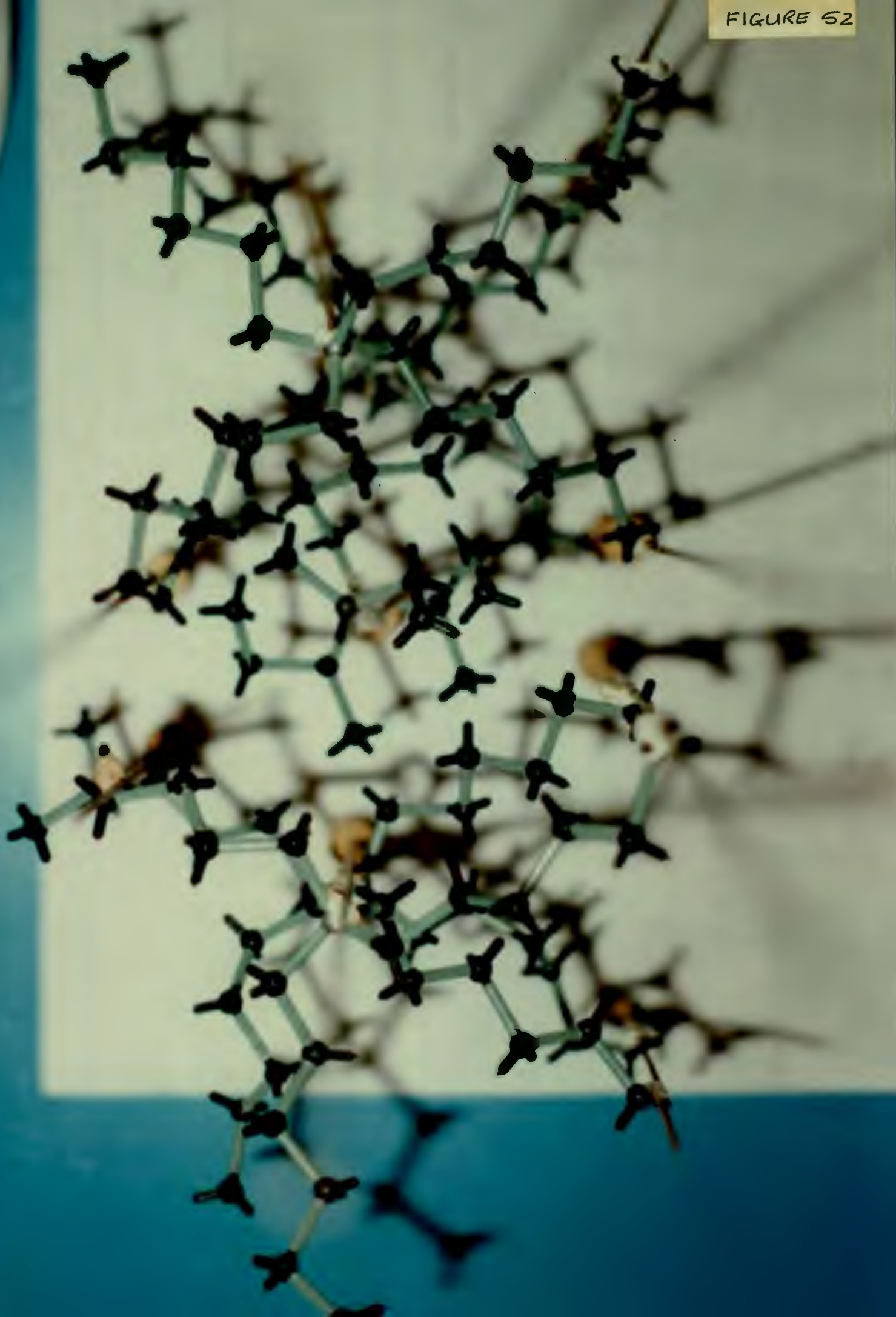


FIGURE 52



credence should be given to this because of the high final R value.

A model was built of the parent compound, in which the cations were placed (to scale) in the unit cell. By placing the cations in their correct positions in neighboring unit cells, it was observed that the cation host lattice surrounds a continuous channel; it is within this channel that the borate anion is most likely to be located (indicated by high electron densities ($1-2 \text{ e } \text{\AA}^{-3}$)) and where the anion is anticipated to be. (A perspective view of the channel is shown in Figure 51 and 52). It was thought that the position of the anion was not found owing to the fact that it was able to move up and down this channel. It was also proposed that, in the liquid clathrate, similar channels would be formed and the trapped guest would also be located in these channels.

6.2.1 Preliminary X-Ray Analysis of Parent Compound: Tetrahexylammonium Tetrphenylborate

The symmetry displayed by the oscillation and Weissenberg photographs indicated a monoclinic space group. The cell parameters estimated from the photographs were as follows:
 $a = 19.1 \text{ \AA}$, $b = 11.8 \text{ \AA}$, $c = 16.8 \text{ \AA}$, $\beta = 98^\circ$ and $z = 4$.

The conditions for non-extinction of reflections evident from the zero and upper layer Weissenberg photographs were:

$$hkl : h + k = 2n$$

$$h0l : l = 2n \quad (h = 2n)$$

$$0k0 : k = 2n$$

These systematic absences are indicative of the space groups Cc or $C2/c$.⁴⁶

6.2.2 Intensity Data Collection

3214 unique reflections collected within the range

$1^\circ < 2\theta < 25^\circ$ constituted the diffractometer data set. Of these, 2533 had $I_{rel} > 2\sigma I_{rel}$ and constituted the "observed" data. The data set was obtained on an Enraf-Nonius CAD4 diffractometer (MoK α radiation, $\lambda = 0.7107 \text{ \AA}$).

Accurate cell parameters, determined by least-squares analysis, are listed in Table 29.

Table 29 Crystal Data

Molecular formula	$C_{48}H_{72}NB$
Molecular weight	673.95 gmol^{-1}
Space group	$C2/c$
a	$20.351(3) \text{ \AA}$
b	$12.210(2) \text{ \AA}$
c	$17.484(9) \text{ \AA}$
β	$99.12(3)^\circ$
V	$4289(2) \text{ \AA}^3$
ρ_c	1.04 gcm^{-1} for $z = 4$
$\mu(\text{MoK}\alpha)$	0.57 cm^{-1}
F(000)	1888
Scan mode	w-2 θ
Scan width (in w)	$(0.95 + 0.35\tan\theta)^\circ$
Aperture width	$(1.12 + 1.05\tan\theta) \text{ mm}$
Scan speed	variable
Crystal dimensions	$(0.38 \times 0.45 \times 0.45) \text{ mm}^3$

6.2.3 Solution and Refinement of the Parent Compound (Tetrahexylammonium Tetrphenylborate) Structure

The space group was chosen to be $C2/c$, and solution of the structure in that space group vindicated this choice. Taking the volume of a non-hydrogen atom as 18 \AA^3 , we calculated that there must be $4289 - (18 \times 50) = 4.7 \approx 4$ molecules per unit cell. Assuming the space group $C2/c$, we

are required to place the ions in special positions. Wyckoff positions a, b, c and d require the ions to be centrosymmetric, and this is impossible by virtue of the tetrahedron nature of the central nitrogen and boron atoms in the cation and anion respectively. Therefore we recognised that the ions would be situated on the diad at Wyckoff position e. This was indeed found by the direct methods solution, which we obtained by using the direct methods package of SHELXS-86⁴⁷.

Subsequent use of the refinement program SHELX76⁴⁸ resulted in the positions of all non-hydrogen atoms of the host being located. After applying least-squares refinements on the established coordinates, and the structure factors calculated, the R value was equal to 11.3%.

Anisotropic temperature factors were employed for all non-hydrogen atoms and included in the following least-squares refinement, reducing R to 8.75 %. Subsequently, the hydrogen atoms were placed in calculated positions and the least-squares refinement repeated to yield a value of 6.45% for R (the number of parameters being equal to 245). Thus the host molecule was successfully refined.

After the final cycle of refinement an analysis of variance was calculated (Table 30) and indicated a satisfactory weighting scheme. The final atomic coordinates with

TABLE 30: ANALYSIS OF VARIANCE

a) By parity groups

Group	ggg	ugg	gug	uug	ggu	ugu	guu	uuu	All
N	761	0	0	607	560	0	0	605	2533
V	233	0	0	194	182	0	0	177	200

b) As a function of sin(theta)

sin(theta)	0.00 -	0.18 -	0.23 -	0.26 -	0.29 -	0.31 -	0.34 -	0.36 -	0.38 -	0.40 -	0.43
N	273	285	233	267	221	352	244	221	224	213	
V	456	234	177	134	135	124	109	87	87	83	

c) As a function of (F/Fmax)

(F/Fmax)	0.00 -	0.15 -	0.17 -	0.18 -	0.20 -	0.22 -	0.25 -	0.27 -	0.32 -	0.39 -	1.00
N	338	302	134	246	259	327	174	279	225	249	
V	104	128	126	153	154	170	188	161	229	423	

d) As a function of Miller index

h	0	1	2	3	4	5	6	7	8	9	10	11	12	13	REST
N	95	165	178	157	169	154	156	156	156	142	146	122	116	100	521
V	284	242	328	225	268	213	199	203	169	189	171	126	142	138	104

k	0	1	2	3	4	5	6	7	8	9	10	11	12	13	REST
N	159	271	261	257	271	229	213	187	179	144	147	88	74	36	17
V	348	232	264	237	205	155	162	150	133	118	98	91	93	108	67

l	0	1	2	3	4	5	6	7	8	9	10	11	12	13	REST
N	116	201	220	190	210	169	189	163	172	140	141	106	112	82	322
V	331	184	333	240	199	217	189	183	183	146	129	119	128	113	94

N = No. of reflections in the group

V = 100[M (F - F) / N] where M = total no. of reflections

corresponding thermal motion parameters are listed in Tables 31 and 32. Lists of observed and calculated structure factors are presented in Appendix VI(b).

6.2.4 Molecular Structure

A perspective view of the host complex is shown in Figures 53-54. The host molecule is positioned on a crystallographic two-fold axis (both the boron and nitrogen atoms being in special positions), the atomic nomenclature is therefore self-explanatory. Intra-molecular bond lengths and angles are listed in tables 33 and 34 respectively. The torsion angles are tabulated in Table 35. The hexyl chains are tetrahedrally arranged around the nitrogen atom. Similarly, the phenyl rings are tetrahedrally arranged around the boron atom.

An illustration of the packing of the host molecules in the unit cell is shown in projection down the x, and y axis (see Figures 55-56).

This host compound was not observed to form liquid clathrates when added to various hydrocarbon guests. It was suggested that the host was in the α -form.

TABLE 31: Fractional atomic coordinates ($\text{\AA} \times 10^4$)
 and Thermal Parameters ($^{\circ}\text{A}^2 \times 10^3$)
 with e.s.d.'s in parentheses for Host (1e).

Atom	x/a	y/b	z/c	Uequiv
N(1)	0(0)	1720(3)	-2500(0)	44(1)
C(31)	498(1)	961(2)	-2802(2)	47(1)
C(32)	1036(2)	1528(3)	-3161(2)	56(1)
C(33)	1503(2)	707(3)	-3440(2)	54(1)
C(34)	2031(2)	1267(3)	-3830(2)	54(1)
C(35)	2503(1)	479(2)	-4133(2)	53(1)
C(36)	2991(2)	1043(3)	-4583(2)	66(1)
C(41)	345(1)	2480(2)	-1870(2)	48(1)
C(42)	740(2)	1927(3)	-1167(2)	58(1)
C(43)	1025(2)	2771(2)	-564(2)	57(1)
C(44)	1476(2)	2267(3)	122(2)	58(1)
C(45)	1779(2)	3095(3)	718(2)	68(2)
C(46)	2251(2)	2609(3)	1388(2)	79(2)
B(1)	0(0)	3343(4)	2500(0)	45(2)
C(11)	446(2)	2503(2)	3106(2)	50(1)
C(12)	213(2)	2085(3)	3759(2)	70(1)
C(13)	578(3)	1293(4)	4239(2)	97(2)
C(14)	1179(3)	905(3)	4100(3)	96(2)
C(15)	1405(2)	1290(3)	3449(3)	87(2)
C(16)	1052(2)	2073(3)	2965(2)	64(1)
C(21)	451(2)	4175(2)	2064(2)	46(1)
C(22)	1064(2)	4589(3)	2436(2)	57(1)
C(23)	1431(2)	5354(3)	2092(2)	68(2)
C(24)	1206(2)	5724(3)	1359(2)	67(2)
C(25)	599(2)	5364(3)	975(2)	67(1)
C(26)	228(2)	4604(3)	1325(2)	56(1)

TABLE 31 continued

Anisotropic atoms have thermal parameters ($^{\circ}\text{A}^2 \times 10^3$) of the form :

$$\text{EXP}(-2\pi^2 (U_{11}x^2 + \dots + 2xU_{12}xhxkx(\alpha^2)x(b^2)+\dots))$$

Atom	U11	U22	U33	U23	U13	U12
N(1)	49(2)	34(2)	52(2)	0(0)	18(2)	0(0)
C(31)	50(2)	37(2)	58(2)	-1(2)	19(2)	5(1)
C(32)	59(2)	46(2)	68(2)	0(2)	29(2)	1(2)
C(33)	56(2)	51(2)	62(2)	1(2)	23(2)	5(2)
C(34)	57(2)	50(2)	57(2)	-4(2)	21(2)	0(2)
C(35)	51(2)	53(2)	57(2)	-2(2)	11(2)	1(2)
C(36)	66(2)	69(2)	69(3)	-6(2)	29(2)	-2(2)
C(41)	51(2)	38(2)	57(2)	-7(2)	17(2)	-3(1)
C(42)	67(2)	45(2)	63(2)	-2(2)	10(2)	2(2)
C(43)	60(2)	48(2)	65(2)	-9(2)	10(2)	8(2)
C(44)	59(2)	54(2)	60(2)	-2(2)	12(2)	9(2)
C(45)	64(2)	62(2)	77(3)	-15(2)	7(2)	12(2)
C(46)	72(3)	97(3)	67(3)	-13(2)	8(2)	11(2)
B(1)	49(3)	46(3)	40(3)	0(0)	9(2)	0(0)
C(11)	58(2)	43(2)	45(2)	-2(2)	-2(2)	-6(2)
C(12)	85(3)	65(2)	56(2)	14(2)	2(2)	-7(2)
C(13)	150(5)	73(3)	57(3)	23(2)	-15(3)	-29(3)
C(14)	124(4)	55(3)	91(4)	-6(3)	-35(3)	-1(3)
C(15)	80(3)	57(3)	108(4)	-23(3)	-30(3)	16(2)
C(16)	67(2)	52(2)	67(2)	-8(2)	-5(2)	7(2)
C(21)	56(2)	41(2)	43(2)	-1(2)	17(2)	7(2)
C(22)	66(2)	54(2)	54(2)	-3(2)	18(2)	-9(2)
C(23)	77(3)	58(2)	75(3)	-11(2)	28(2)	-12(2)
C(24)	93(3)	42(2)	78(3)	-1(2)	50(2)	1(2)
C(25)	94(3)	56(2)	58(2)	15(2)	37(2)	26(2)
C(26)	63(2)	57(2)	50(2)	7(2)	20(2)	14(2)

Table32 Proton atom coordinates (x 10⁴).

Parent atom	H	x/a	y/b	z/c
C(31)	H(311)	245(1)	471(2)	-3205(2)
C(31)	H(312)	722(1)	509(2)	-2359(2)
C(32)	H(321)	822(2)	1974(3)	-3612(2)
C(32)	H(322)	1295(2)	2022(3)	-2765(2)
C(33)	H(331)	1239(2)	197(3)	-3817(2)
C(33)	H(332)	1729(2)	283(3)	-2983(2)
C(34)	H(341)	2299(2)	1765(3)	-3447(2)
C(34)	H(342)	1802(2)	1706(3)	-4277(2)
C(35)	H(351)	2762(1)	84(2)	-3682(2)
C(35)	H(352)	2236(1)	-59(2)	-4483(2)
C(36)	H(361)	3317(2)	512(3)	-4747(2)
C(36)	H(362)	3236(2)	1611(3)	-4237(2)
C(36)	H(363)	2736(2)	1405(3)	-5053(2)
C(41)	H(411)	-5(1)	2941(2)	-1686(2)
C(41)	H(412)	657(1)	2961(2)	-2105(2)
C(42)	H(421)	441(2)	1415(3)	-935(2)
C(42)	H(422)	1113(2)	1502(3)	-1331(2)
C(43)	H(431)	646(2)	3148(2)	-370(2)
C(43)	H(432)	1287(2)	3319(2)	-815(2)
C(44)	H(441)	1207(2)	1733(3)	380(2)
C(44)	H(442)	1843(2)	1871(3)	-76(2)
C(45)	H(451)	1413(2)	3473(3)	932(2)
C(45)	H(452)	2036(2)	3641(3)	460(2)
C(46)	H(461)	2413(2)	3209(3)	1760(2)
C(46)	H(462)	2639(2)	2267(3)	1190(2)
C(46)	H(463)	2017(2)	2042(3)	1655(2)
C(12)	H(121)	-219(2)	2355(3)	3889(2)
C(13)	H(131)	394(3)	1009(4)	4699(2)
C(14)	H(141)	-2164(16)	183(30)	-2554(19)
C(15)	H(151)	1838(2)	1003(3)	3328(3)
C(16)	H(161)	1238(2)	2331(3)	2500(2)
C(22)	H(221)	1244(2)	4323(3)	2969(2)
C(23)	H(231)	1863(2)	5628(3)	2379(2)
C(24)	H(241)	1479(2)	6257(3)	1107(2)
C(25)	H(251)	425(2)	5652(3)	444(2)
C(26)	H(261)	-208(2)	4354(3)	1036(2)

TABLE 33: Bond lengths (Angstrom) with e.s.d.'s in parentheses for Host (1e).

N(1)	- C(31)	1.528(3)
N(1)	- C(41)	1.525(4)
C(31)	- C(32)	1.514(5)
C(32)	- C(33)	1.514(6)
C(33)	- C(34)	1.523(6)
C(34)	- C(35)	1.513(5)
C(35)	- C(36)	1.526(5)
C(41)	- C(42)	1.516(5)
C(42)	- C(43)	1.523(5)
C(43)	- C(44)	1.521(5)
C(44)	- C(45)	1.512(5)
C(45)	- C(46)	1.512(5)
C(1)	- C(11)	1.642(4)
B(1)	- C(21)	1.636(5)
C(11)	- C(12)	1.401(5)
C(11)	- C(16)	1.397(6)
C(12)	- C(13)	1.412(6)
C(13)	- C(14)	1.369(9)
C(14)	- C(15)	1.374(8)
C(15)	- C(16)	1.399(5)
C(21)	- C(22)	1.407(5)
C(21)	- C(26)	1.402(5)
C(22)	- C(23)	1.390(6)
C(23)	- C(24)	1.368(5)
C(24)	- C(25)	1.383(5)
C(25)	- C(26)	1.397(6)

TABLE 34: Bond angles (degrees) with e.s.d.'s
in parentheses for Host (1e).

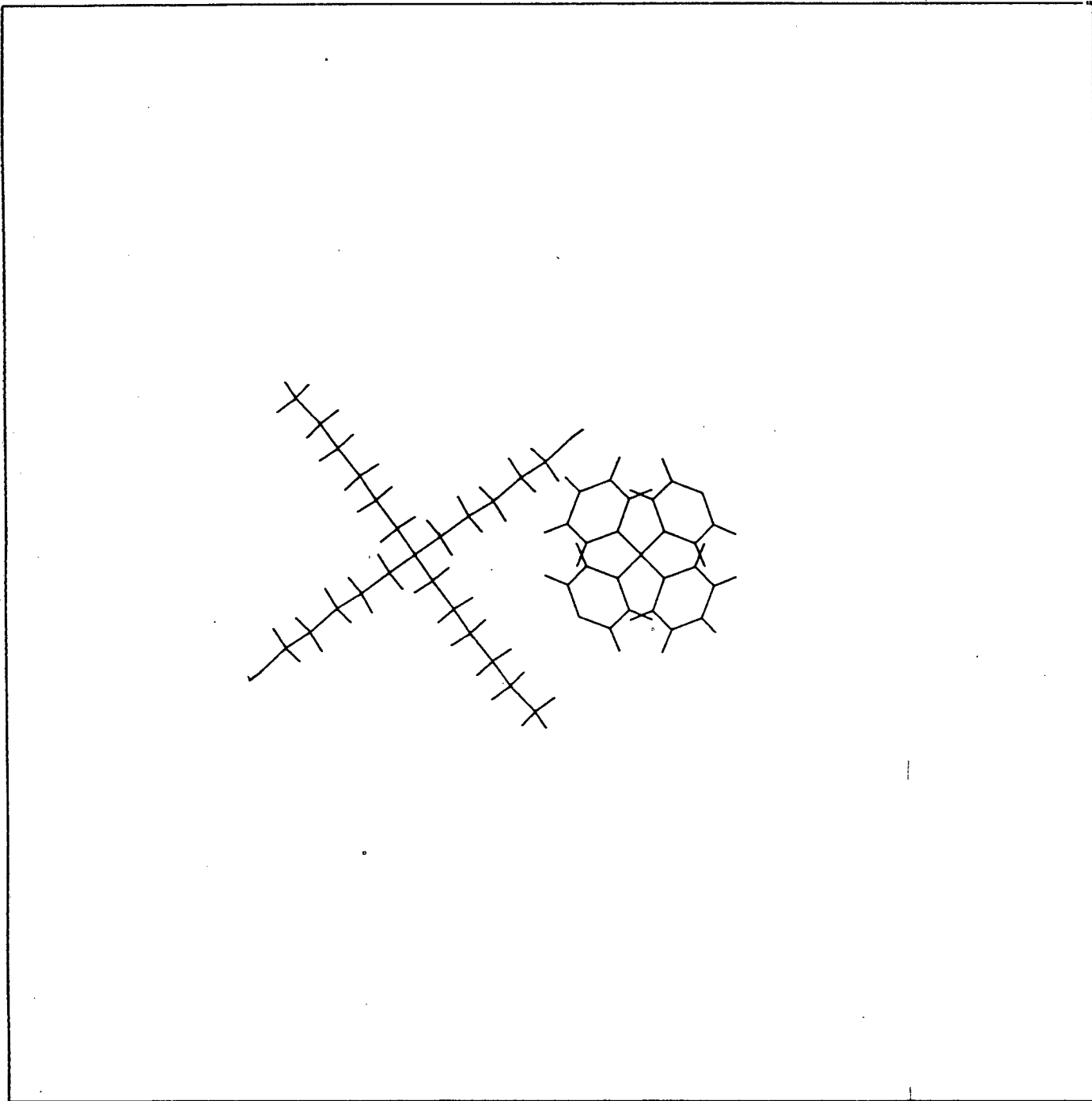
C(31)	- N(1)	- C(41)	111.4(2)
N(1)	- C(31)	- C(32)	115.5(3)
C(31)	- C(32)	- C(33)	111.3(3)
C(32)	- C(33)	- C(34)	111.8(4)
C(33)	- C(34)	- C(35)	113.8(4)
C(34)	- C(35)	- C(36)	113.2(3)
N(1)	- C(41)	- C(42)	115.9(3)
C(41)	- C(42)	- C(43)	110.8(3)
C(42)	- C(43)	- C(44)	112.9(3)
C(43)	- C(44)	- C(45)	113.8(3)
C(44)	- C(45)	- C(46)	114.3(4)
C(11)	- B(1)	- C(21)	113.2(3)
B(1)	- C(11)	- C(16)	122.3(3)
B(1)	- C(11)	- C(12)	121.9(3)
C(12)	- C(11)	- C(16)	115.5(4)
C(11)	- C(12)	- C(13)	121.3(4)
C(12)	- C(13)	- C(14)	122.1(4)
C(13)	- C(14)	- C(15)	117.1(5)
C(14)	- C(15)	- C(16)	121.8(5)
C(11)	- C(16)	- C(15)	122.1(4)
B(1)	- C(21)	- C(26)	122.6(3)
B(1)	- C(21)	- C(22)	122.0(3)
C(22)	- C(21)	- C(26)	115.2(4)
C(21)	- C(22)	- C(23)	122.5(4)
C(22)	- C(23)	- C(24)	120.5(4)
C(23)	- C(24)	- C(25)	119.3(4)
C(24)	- C(25)	- C(26)	120.1(4)
C(21)	- C(26)	- C(25)	122.3(4)

TABLE 35: Torsion angles (degrees) with e.s.d.'s
in parentheses for Host (1e).

(RIGHT-HAND RULE, KLYNE & PRELOG. (1960). EXPERIENTIA, 16, 521)
(E.S.D.'S, FOLLOWING STANFORD & WASER, ACTA
CRYST. (1972). A28, 213)

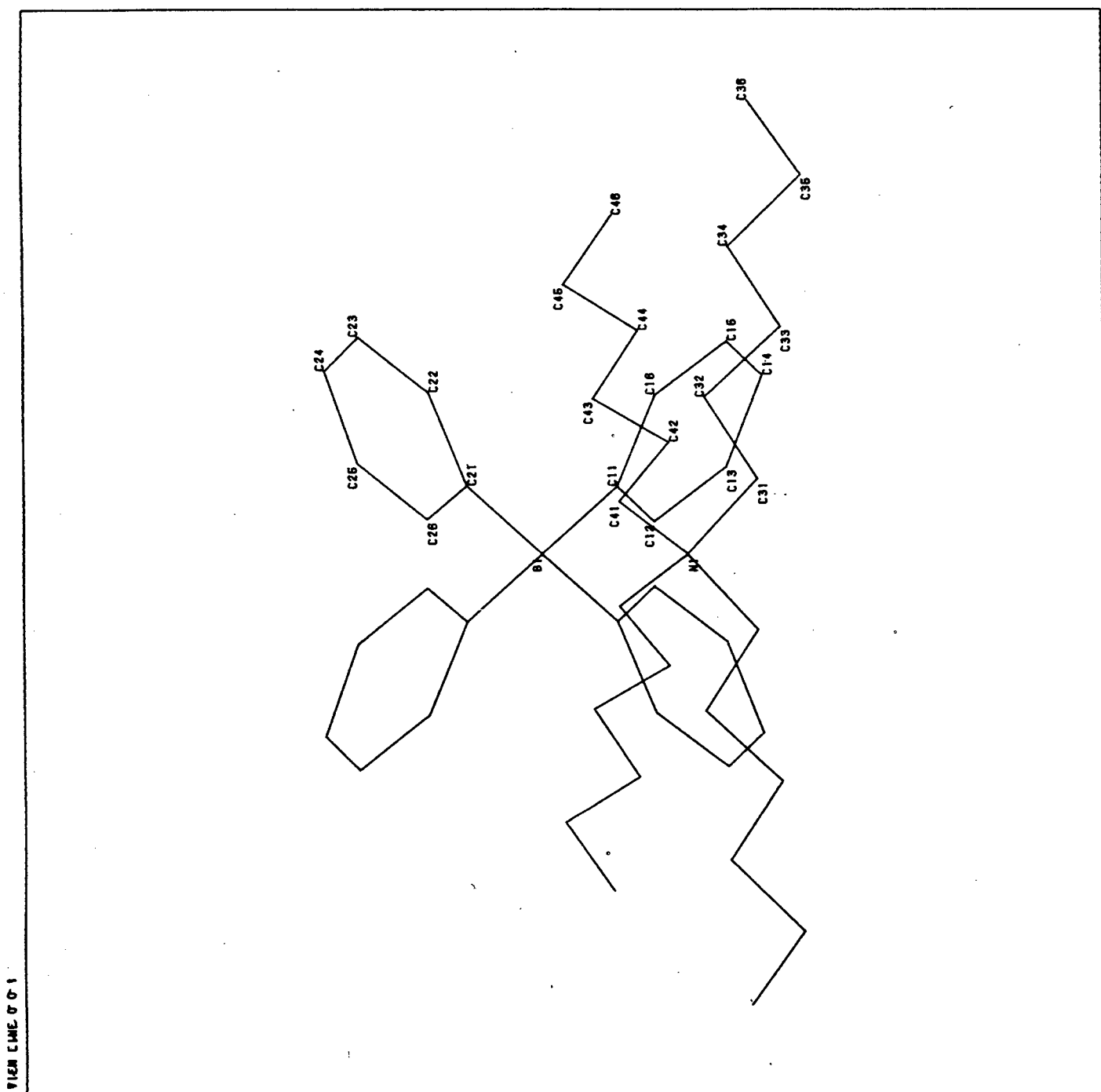
C(31)	- N(1)	- C(41)	- C(42)	-57.9(4)
C(41)	- N(1)	- C(31)	- C(32)	-60.2(4)
N(1)	- C(31)	- C(32)	- C(33)	179.8(3)
C(31)	- C(32)	- C(33)	- C(34)	177.7(3)
C(32)	- C(33)	- C(34)	- C(35)	-179.0(3)
C(33)	- C(34)	- C(35)	- C(36)	175.0(3)
N(1)	- C(41)	- C(42)	- C(43)	-176.7(3)
C(41)	- C(42)	- C(43)	- C(44)	-175.0(3)
C(42)	- C(43)	- C(44)	- C(45)	178.4(4)
C(43)	- C(44)	- C(45)	- C(46)	-177.5(4)
C(11)	- B(1)	- C(21)	- C(22)	-34.3(5)
C(11)	- B(1)	- C(21)	- C(26)	151.5(4)
C(21)	- B(1)	- C(11)	- C(16)	-35.1(5)
C(21)	- B(1)	- C(11)	- C(12)	151.3(4)
B(1)	- C(11)	- C(16)	- C(15)	-174.7(4)
B(1)	- C(11)	- C(12)	- C(13)	174.6(4)
C(12)	- C(11)	- C(16)	- C(15)	-.7(6)
C(16)	- C(11)	- C(12)	- C(13)	.6(6)
C(11)	- C(12)	- C(13)	- C(14)	1.0(8)
C(12)	- C(13)	- C(14)	- C(15)	-2.4(8)
C(13)	- C(14)	- C(15)	- C(16)	2.3(8)
C(14)	- C(15)	- C(16)	- C(11)	-.8(7)
B(1)	- C(21)	- C(26)	- C(25)	176.1(4)
B(1)	- C(21)	- C(22)	- C(23)	-175.6(4)
C(22)	- C(21)	- C(26)	- C(25)	1.5(6)
C(26)	- C(21)	- C(22)	- C(23)	-.9(6)
C(21)	- C(22)	- C(23)	- C(24)	-1.1(7)
C(22)	- C(23)	- C(24)	- C(25)	2.6(7)
C(23)	- C(24)	- C(25)	- C(26)	-2.0(7)
C(24)	- C(25)	- C(26)	- C(21)	-.1(7)

FIGURE 53: A perspective view of Host (1e), viewed down the y-axis.



VIEW LINE. 0 1 0

FIGURE 54: A perspective view of Host (1e), viewed down the z-axis.



VIEW C LIME 0 0 1

FIGURE 55: An illustration of the packing of the Host(1e) molecules in the unit cell, shown in projection down the x-axis.

VIEW LINE 1 0 0

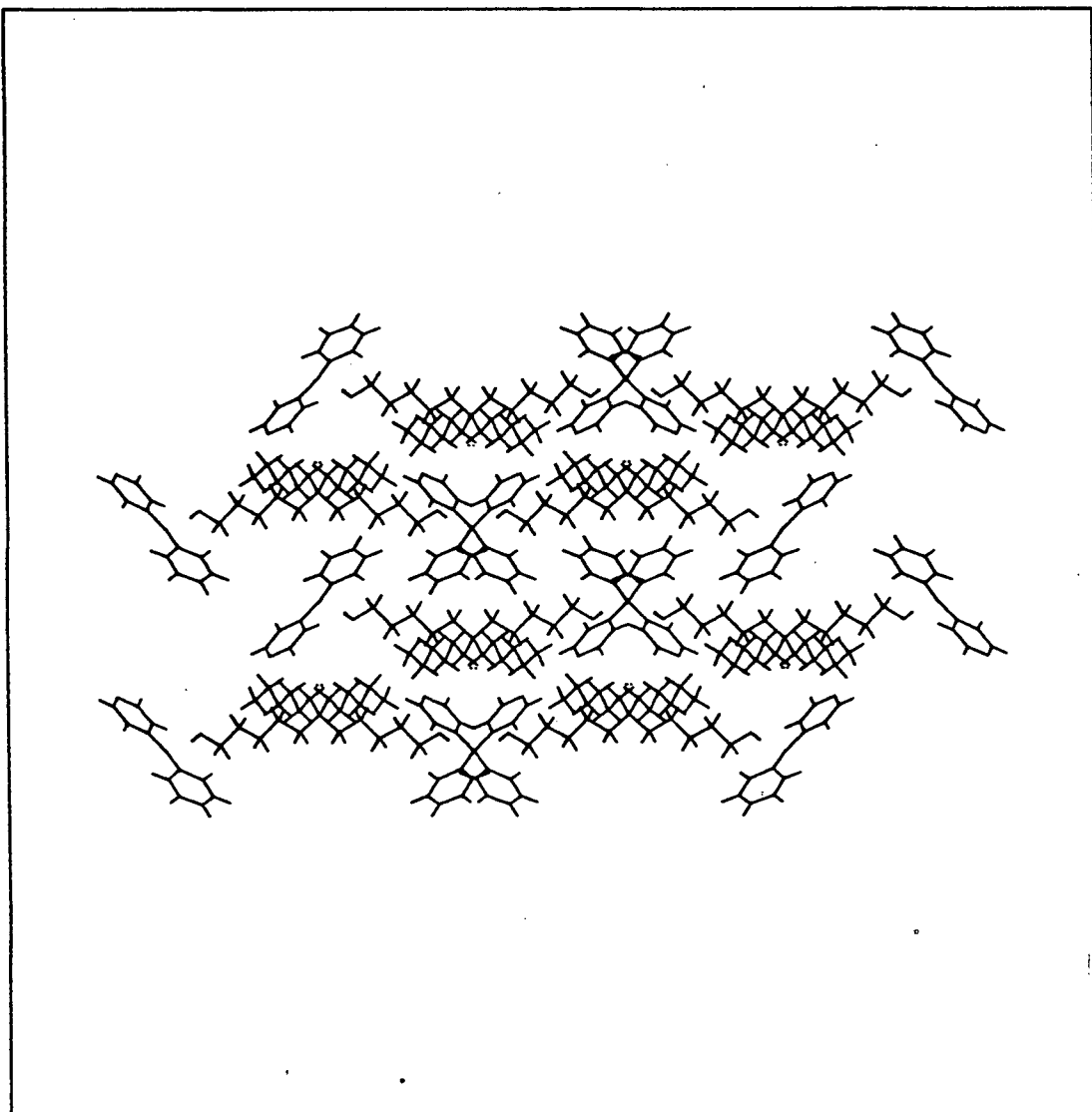
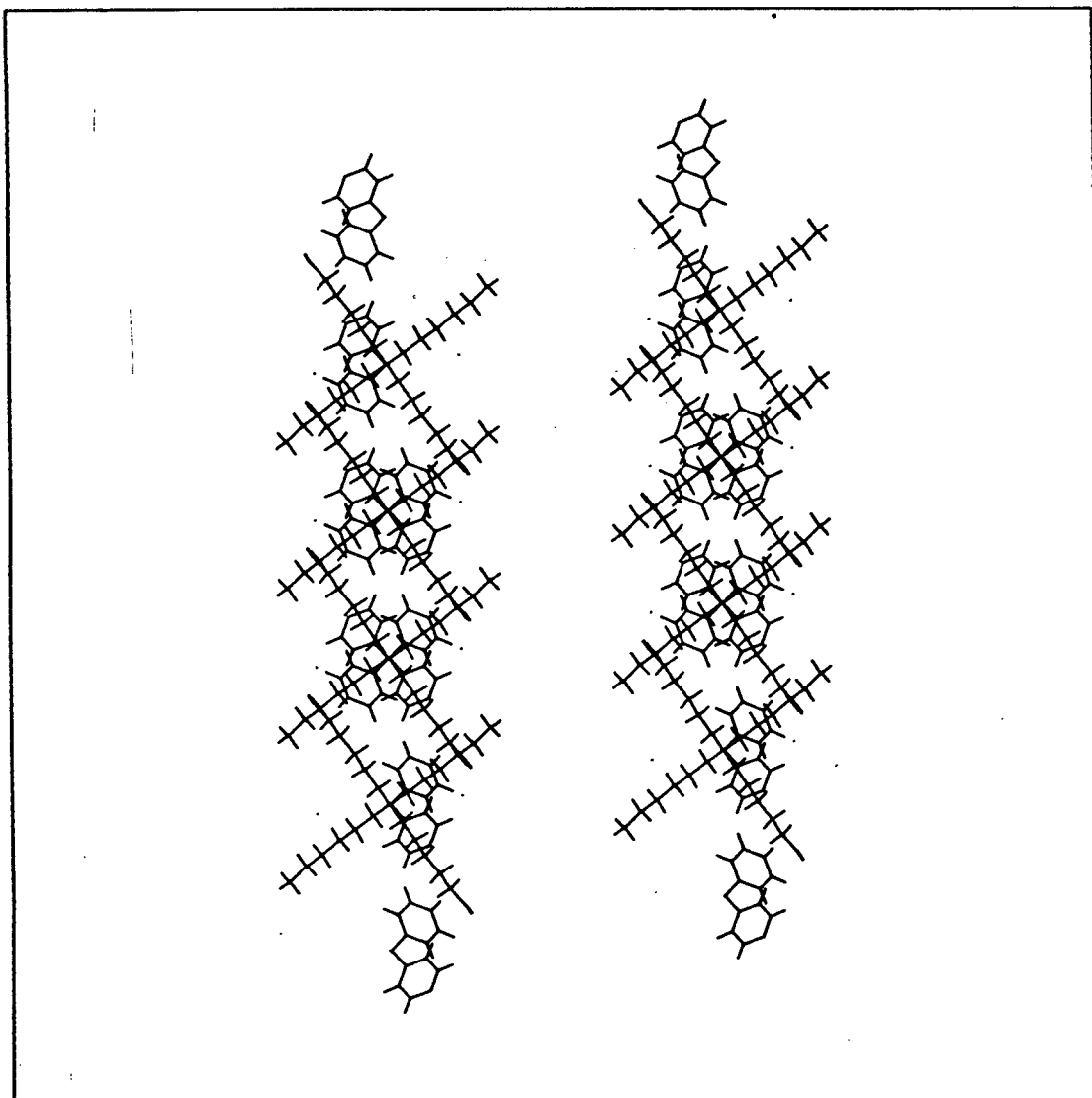


FIGURE 56: An illustration of the packing of the Host (1e) molecules in the unit cell, shown in projection down the y-axis

VIEW LINE 0 1 0



CHAPTER 9: CONCLUSION

From the results of the experimental section, it is evident that the host compounds can be easily prepared in high yields. Of the host compounds 1a,b,c,d and e that were synthesised, only compounds 1a and 1b showed liquid clathrate behavior, on the addition of hydrocarbon guests. It was also observed that the host compound (1a) is the most efficient of these clathrating compounds.

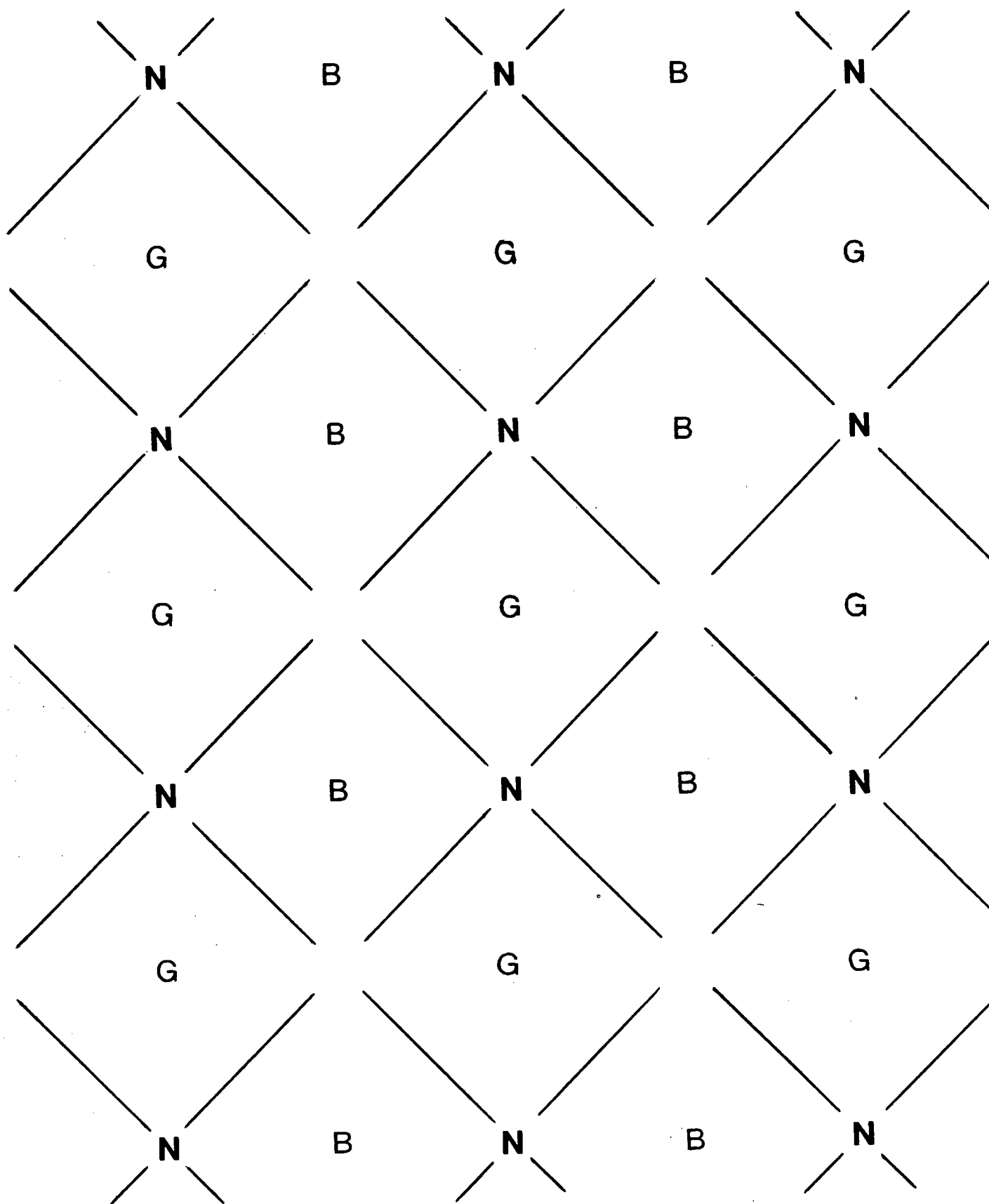
The host material can be retrieved, unchanged, from the liquid clathrate for re-use. This is illustrated in the section on thermal analysis studies on liquid clathrates (see chapter 5). Another method of separating the guest and host follows from the host compounds clathrating the hydrocarbon guests selectively (chapter 4). The selectivity of these host compounds for various hydrocarbons was well established (Table 9,10 and 11).

Difficulties were experienced in trying to determine the enthalpy of clathration between the guest and host molecules. Since the only forces holding the host and guest molecules together are Van der Waals forces, it was expected that the enthalpy would be small in magnitude, making measurement of this value difficult.

The models of the packing of the guest and host molecules, showing the distances between these molecules were obtained from the study of nuclear Overhauser effects (chap 7). The guest molecules are observed to be clathrated in cone shaped cavities, approximately 6 °A in diameter at the outer edge of the cone, between the carbon-chains on the host cations. From the crystallographic studies of Host(1a), these cavities were observed to form channels which are approximately 5 °A x 9.5 °A in cross-section (the packing space between two nitrogen atoms therefore being approximately 11 °A). The structure is shown schematically in figure 57. We observe that for each cation there are two distinct channels. Half of these are filled by the disordered anions, while the other half remain empty. We believe this to be a credible model for an incipient clathrate structure, in that the empty channels can be filled by appropriated guest molecules. The calculated width of the cavity, obtained from nOe results, is therefore consistent with that obtained from crystallographic analysis of host 1a, even though there was no guest present in the crystal.

The guest molecules, benzene, toluene, p-xylene and p-cymene, are all approximately 6.8 °A wide and of an approximate length of 6.8 °A, 7.9 °A, 8.9 °A and 9.6 °A respectively. Taking the size of the guest molecules into

FIGURE 57: Proposed model of the liquid clathrate H.nG.



N: Host cation sites

G: Guest sites

B: Host anion sites

account, it is evident that they must pack length-wise in the cavities between the nitrogen atoms.

The change in the value of n (for H.nG) can also be explained in terms of the size of the guest molecules. Since benzene is the smallest of the aromatic guest molecules, it is expected that more of these molecules will be able to pack into the cavity than other aromatic guest molecules. Hence, the observed decrease in the value of n (going from left to right across the series) for benzene, toluene, p-xylene and p-cymene is expected.

The results of the nOe experiments are consistent with this observation, as indicated by the decrease in the nOe signal between the host and guest protons as one changes the guest from left to right in the series: benzene, toluene, p-xylene, p-cymene. The guest molecules are found to be displaced further from the nitrogen atoms as the size of the guest molecules increases, which is consistent with the more bulky molecules, requiring more packing space, being located further from the apex of the cone shaped cavity. Hence, the more bulky the guest molecules, the smaller the number that can pack into the cavity.

Based on the results of the nOe experiments and the crystallographic studies, a model evolved which is consistent with the properties of the liquid clathrates. Figure 57 provides a two-dimensional representation. It is

believed that the ions of the host interact in a cooperative manner. The cation...anion interaction must be strong, or the ions would separate and a normal solution would result.

The crystallographic study of host 1a revealed that the borate anion was most likely to be located in the channels between the nitrogen atoms (see fig 57). There are four cavities surrounding each nitrogen atom, two of which must contain a borate anion, since the ratio cation : anion is (1 : 1). The guest molecules can, therefore, pack in the remaining two cavities. The fact that no nOe was observed between the guest and anion protons, indicating that the guest molecules are located further from the protons of the anion than the cation, is also consistent with this model.

With reference to Fig. 57, it is easy to see how the observations of Chapter 4 (section 2.2) fit the model. The larger the cation, the more space between layers of anion (1). A larger anion likewise provides more space in the layers. For a given cavity size, the larger the hydrocarbon guest molecules, the smaller the number of guest molecules that can be accommodated (2).

In the course of experiments aimed at a general understanding of liquid clathrate behavior, it was found that a wide range of substances could serve as guests in the medium. Thus, a specific liquid clathrate would incorporate

benzene, n-hexane, p-xylene, and anthracene to varying degrees. These various hydrocarbon guests were considered as simple models of coal and the extraction power of the host compounds determined (chapter 4). The results of this study led to experiments being performed to extract material from coal, using the host compounds as clathrating agents⁵⁰.

APPENDIX I: Parameter settings for obtaining nOe spectra
using the Varian VXR-200.

PARAMETER SETTINGS OF OBTAINING nOe SPECTRA
(USING THE VARIAN VXR-200)

Pulse Sequence: S2PUL
Solvent D2O
File H

AQUISITION

TN 1.5
SW 1803.1
AT 3.74
NP 13504
PW 10
P1 0
D1 10
D2 0
TO -200
NT 128
CT 128
PW90 32
FB 1000
BS 32
SS 0
IL Y
IN Y
DP Y
HS NN
ALOCK N
GAIN 15

DEC. & VT

DN 1.5
DO ARRAY1
DM YYN
DLP 18
HOMO Y

PROCESSING

SE 3.183
LB 0.1
MATH I

DISPLAY

SP -235.6
WP 1803.1
VS 500
SC 0
WC 200
IS 2000
RFL 1640
RFP 1404.4
TH 45
INS 1
AI DC

DO ARRAY (P-CYMENE)

INDEX	VALUE	INDEX	VALUE
1	337.3	6	-581.7
2	538.4	7	-601.2
3	-244.1	8	-619.8
4	-309.2	9	-627.6
5	-417.4	10	-664.8

DO ARRAY (P-XYLENE)

INDEX	VALUE	INDEX	VALUE
1	316.1	4	-417.5
2	530.8	5	-589.3
3	-286.4	6	-659.0

DO ARRAY (TOLUENE)

INDEX	VALUE	INDEX	VALUE
1	316.1	4	-595.9
2	550.7	5	-662.2
3	-428.2	6	

APPENDIX II: Modelling the Borate Anion for the Calculation of its Scattering Factor, using Multan.

a) Diagram of the Borate Anion in a randomly chosen configuration, used for calculating the atom positions .
(Figure 58)

b) Coordinates of the atoms of the Borate Anion. (Table 36).

FIGURE 58: Diagram of the Borate Anion in a randomly chosen configuration.

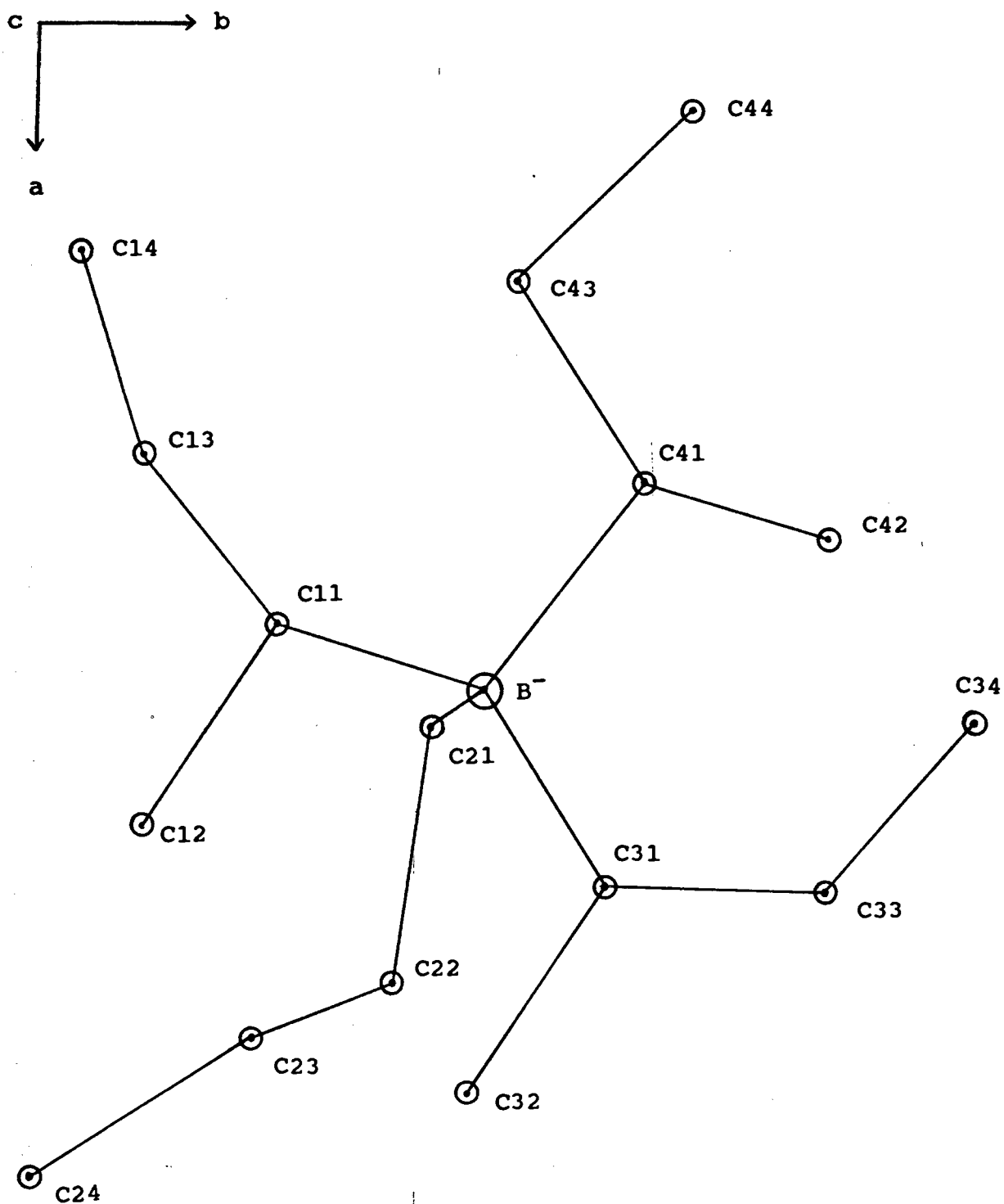


TABLE 36: COORDINATES OF THE ATOMS OF THE BORON ANION (USED IN MULTAN EXP)
 (IN A GENERAL UNIT CELL OF DIMENSIONS 30 Å x 30 Å x 30 Å)

ATOM	a	b	c
----	----	----	----
B	0.45	0.46	0.14
C	0.41	0.34	0.08
C	0.52	0.27	0.07
C	0.32	0.27	0.16
C	0.22	0.24	0.09
C	0.47	0.43	0.27
C	0.6	0.41	0.31
C	0.64	0.33	0.4
C	0.71	0.21	0.39
C	0.55	0.52	0.09
C	0.66	0.45	0.13
C	0.56	0.64	0.16
C	0.46	0.72	0.09
C	0.34	0.54	0.13
C	0.37	0.64	0.05
C	0.23	0.47	0.08
C	0.14	0.56	0.05

APPENDIX III: Determination of the Scattering Factor for the Borate Anion:

- a) Calculated scattering factors, using Multan, for various values of $\sin(\theta)/\lambda$. (Table 37).
- b) Calculated scattering factors for various values of $\sin(\theta)/\lambda$, using a statistical Curve-Fit procedure. (Table 38).
- c) A plot of the scattering factors at various values of $\sin(\theta)/\lambda$, for the Borate Anion (Multan) (Figure 59).
- d) A plot of the scattering factors at various values of $\sin(\theta)/\lambda$, using the Curve-Fit procedure (Figure 60).

TABLE 37: TABULATION OF SCATTERING FACTORS AT VARIOUS VALUES OF SIN(THETA)/LAMBDA (MULTAN)

SINO/ λ	f	SINO/ λ	f	SINO/ λ	f
0.02	100.76	0.36	9.13	0.70	5.96
0.04	58.19	0.38	8.65	0.72	6.00
0.06	23.24	0.40	8.77	0.74	5.96
0.08	19.36	0.42	8.75	0.76	5.86
0.10	19.60	0.44	8.09	0.78	5.85
0.12	20.98	0.46	7.55	0.80	5.93
0.14	16.82	0.48	7.26	0.82	5.88
0.16	18.33	0.50	7.20	0.84	5.76
0.18	21.01	0.52	7.05	0.86	5.81
0.20	16.53	0.54	6.82	0.88	5.85
0.22	13.17	0.56	6.82	0.90	5.85
0.24	12.45	0.58	6.61	0.92	5.73
0.26	12.96	0.60	6.31	0.94	5.77
0.28	12.66	0.62	6.15	0.96	5.84
0.30	11.32	0.64	6.30	0.98	5.80
0.32	10.90	0.66	6.22	1.00	5.77
0.34	10.05	0.68	6.08	1.02	5.80

TABLE 38: TABULATION OF CALCULATED SCATTERING FACTORS (USING CURVE FIT PROCEDURE) AT VARIOUS VALUES OF SIN(THETA)/LAMBDA

SINO/ λ	f (CALC.)	SINO/ λ	f (CALC.)
0.02	100.76	0.28	12.37
0.04	52.75	0.30	11.84
0.06	21.36	0.32	11.34
0.08	18.68	0.34	10.87
0.10	18.15	0.36	10.44
0.12	17.56	0.38	10.03
0.14	16.91	0.40	9.66
0.16	16.22	0.42	9.30
0.18	15.52	0.44	8.98
0.20	14.84	0.46	8.68
0.22	14.17	0.48	8.40
0.24	13.54	0.50	8.15
0.26	12.93	0.52	7.91

APPENDIX IV: Calibration Curve for DTA/TGA samples,
relating the furnace temperature to sample
temperature.
(Figure 61).

CALIBRATION FOR TG/DTA.TEMP.

SEE STANDARD SAMPLES.

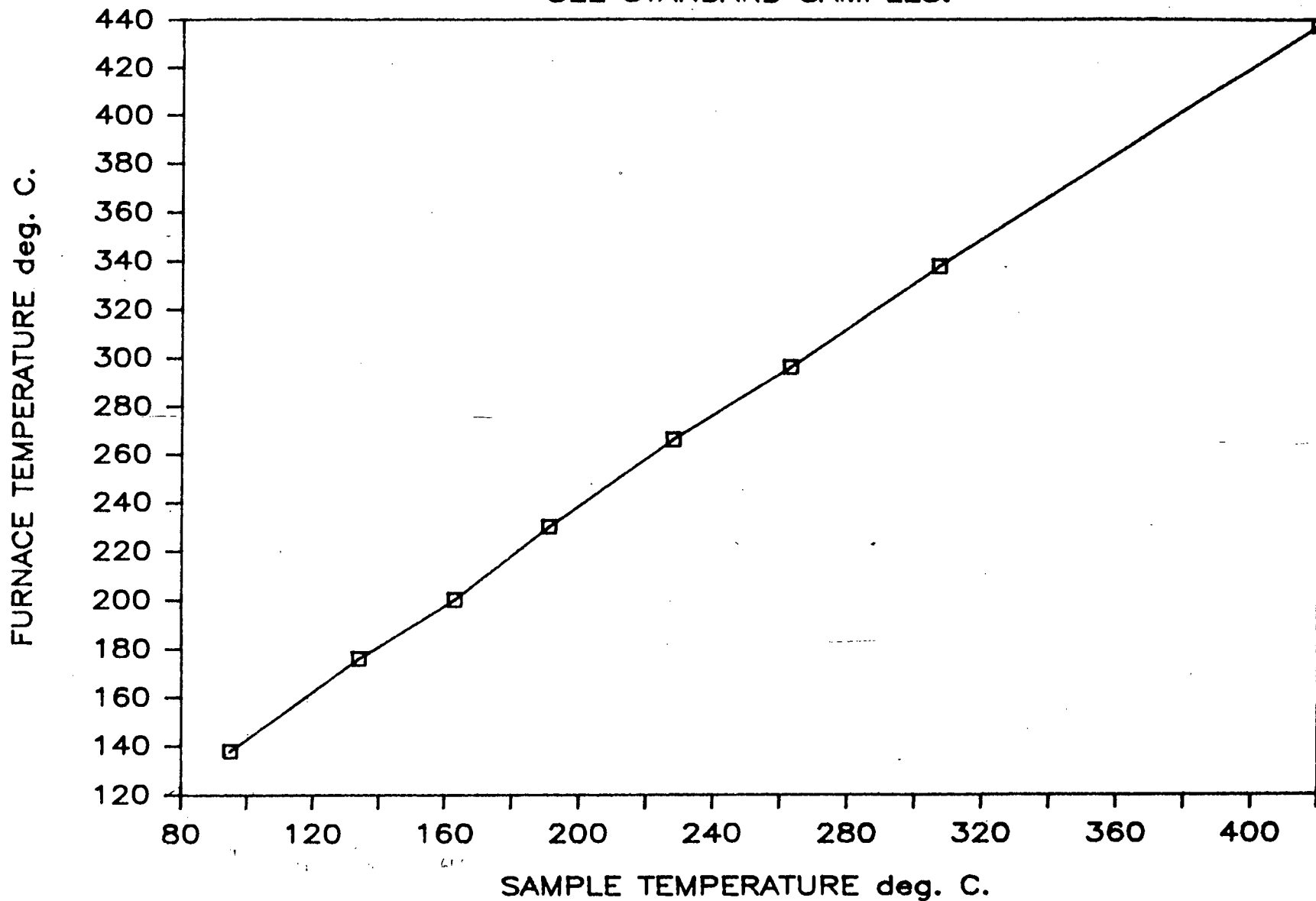


FIGURE 61: Calibration Curve for DTA/TGA samples

APPENDIX V: Observed and Calculated Structure factors for:

a) HOST (1a) [ТНВНГ]

b) HOST (1e) [ТРВН]

OBSERVED AND CALCULATED STRUCTURE FACTORS FOR THBG

PAGE 1

H	K	L	FO	FC	H	K	L	FO	FC	H	K	L	FO	FC	H	K	L	FO	FC	H	K	L	FO	FC
-18	0	0	9	13	-2	2	0	53	62	-5	5	0	9	6	-14	2	1	10	11	10	4	1	6	11
-14	0	0	11	14	0	2	0	8	7	-3	5	0	16	12	-12	2	1	7	10	14	4	1	12	6
-12	0	0	49	44	2	2	0	53	62	-1	5	0	20	19	-8	2	1	8	16	-11	5	1	7	12
-10	0	0	16	17	4	2	0	61	66	1	5	0	19	19	-6	2	1	11	11	-9	5	1	12	11
-8	0	0	58	54	6	2	0	69	63	3	5	0	17	12	-4	2	1	4	12	-3	5	1	21	17
-4	0	0	46	51	8	2	0	37	39	5	5	0	10	6	-2	2	1	11	19	-1	5	1	6	14
-2	0	0	21	20	10	2	0	8	16	7	5	0	9	7	4	2	1	18	7	3	5	1	16	15
2	0	0	24	20	12	2	0	12	11	-6	6	0	12	8	6	2	1	27	43	9	5	1	17	15
4	0	0	52	51	14	2	0	11	10	-4	6	0	10	9	8	2	1	12	14	11	5	1	10	9
8	0	0	64	54	16	2	0	8	12	-2	6	0	14	13	16	2	1	6	6	15	5	1	7	6
10	0	0	19	17	-11	3	0	6	4	0	6	0	36	29	-17	3	1	24	22	-2	6	1	13	9
12	0	0	56	44	-9	3	0	6	4	2	6	0	15	13	-15	3	1	23	20	0	6	1	9	7
14	0	0	12	14	-5	3	0	9	11	4	6	0	9	9	-13	3	1	16	22	2	6	1	10	5
18	0	0	9	13	1	3	0	5	5	6	6	0	11	8	-9	3	1	30	23	3	7	1	9	8
-13	1	0	6	5	3	3	0	8	14	12	6	0	7	6	-7	3	1	8	3	-18	0	2	9	11
-11	1	0	16	15	5	3	0	9	11	-21	1	1	10	11	-5	3	1	32	40	-16	0	2	6	8
-9	1	0	8	9	9	3	0	5	4	-17	1	1	11	11	-3	3	1	65	63	-12	0	2	36	39
-5	1	0	38	36	11	3	0	5	4	-13	1	1	24	23	-1	3	1	21	25	-10	0	2	8	9
-3	1	0	75	82	13	3	0	6	4	-11	1	1	29	37	1	3	1	32	33	-8	0	2	54	61
-1	1	0	27	34	17	3	0	6	3	-9	1	1	34	33	3	3	1	56	61	-6	0	2	43	60
1	1	0	27	34	-14	4	0	7	6	-7	1	1	30	29	5	3	1	24	34	-4	0	2	27	24
3	1	0	78	82	-8	4	0	13	13	-5	1	1	8	15	-7	3	1	24	21	-2	0	2	17	55
5	1	0	42	36	-6	4	0	29	28	-3	1	1	260	255	9	3	1	29	29	0	0	2	216	248
9	1	0	6	9	-4	4	0	38	28	-1	1	1	5	9	13	3	1	23	22	2	0	2	29	40
11	1	0	18	15	-2	4	0	22	19	1	1	1	51	47	15	3	1	21	22	4	0	2	207	169
13	1	0	7	5	0	4	0	14	13	3	1	1	61	70	17	3	1	15	19	6	0	2	184	173
-20	2	0	7	6	2	4	0	22	19	5	1	1	18	23	-16	4	1	10	5	8	0	2	40	42
-16	2	0	7	12	4	4	0	38	28	7	1	1	9	21	-10	4	1	8	8	10	0	2	15	26
-14	2	0	12	10	6	4	0	28	28	9	1	1	75	71	-6	4	1	13	12	12	0	2	42	41
-12	2	0	11	11	8	4	0	14	13	11	1	1	19	21	-4	4	1	13	15	14	0	2	14	18
-10	2	0	8	16	12	4	0	6	5	13	1	1	23	23	-2	4	1	8	14	16	0	2	12	8
-8	2	0	35	39	18	4	0	7	6	17	1	1	10	9	2	4	1	11	14	18	0	2	8	10
-6	2	0	66	63	-11	5	0	6	9	19	1	1	7	9	4	4	1	6	8	-17	1	2	8	4
-4	2	0	59	66	-9	5	0	5	5	21	1	1	9	9	6	4	1	7	8	-15	1	2	6	8

OBSERVED AND CALCULATED STRUCTURE FACTORS FOR THBHG

PAGE 2

H	K	L	FO	FC	H	K	L	FO	FC	H	K	L	FO	FC	H	K	L	FO	FC					
-11	1	2	6	6	-6	4	2	20	20	15	1	3	7	5	12	4	3	14	5	16	0	4	13	12
-7	1	2	5	7	-4	4	2	38	35	17	1	3	13	13	14	4	3	10	6	-19	1	4	8	7
-5	1	2	8	17	0	4	2	20	22	21	1	3	9	7	-13	5	3	10	9	-15	1	4	11	12
-3	1	2	135	119	2	4	2	23	15	-14	2	3	9	6	-9	5	3	10	9	-9	1	4	11	9
-1	1	2	96	103	4	4	2	34	30	-12	2	3	10	12	-7	5	3	6	4	-7	1	4	34	38
1	1	2	8	5	6	4	2	30	25	-6	2	3	23	44	-3	5	3	17	17	-5	1	4	45	47
3	1	2	164	145	-7	5	2	6	8	-4	2	3	11	28	-1	5	3	9	11	-3	1	4	97	89
5	1	2	72	65	-3	5	2	10	5	-2	2	3	16	19	1	5	3	8	11	-1	1	4	80	61
7	1	2	52	49	-1	5	2	10	11	0	2	3	5	9	3	5	3	15	17	1	1	4	6	21
9	1	2	10	18	1	5	2	13	12	2	2	3	11	15	9	5	3	16	16	3	1	4	56	53
11	1	2	7	8	3	5	2	11	10	4	2	3	40	40	11	5	3	15	8	5	1	4	29	32
20	2	2	8	8	5	5	2	15	9	6	2	3	10	15	15	5	3	6	5	7	1	4	24	25
14	2	2	15	11	11	5	2	12	9	8	2	3	9	8	-6	6	3	6	5	9	1	4	20	23
12	2	2	7	9	-4	6	2	10	11	14	2	3	9	7	-2	6	3	12	9	11	1	4	22	21
-8	2	2	38	46	-2	6	2	23	23	-17	3	3	25	21	2	6	3	7	3	13	1	4	14	13
-6	2	2	57	48	0	6	2	31	26	-15	3	3	21	20	4	6	3	7	5	15	1	4	8	7
-4	2	2	66	71	2	6	2	7	8	-13	3	3	15	12	-5	7	3	6	6	-14	2	4	16	14
-2	2	2	44	42	6	6	2	16	12	-11	3	3	13	19	3	7	3	7	8	-8	2	4	36	38
2	2	2	45	34	-21	1	3	8	10	-9	3	3	19	17	9	7	3	9	7	-6	2	4	68	66
4	2	2	83	89	-17	1	3	17	16	-5	3	3	39	48	-18	0	4	13	9	-4	2	4	13	14
6	2	2	56	54	-13	1	3	29	26	-3	3	3	50	43	-16	0	4	20	18	-2	2	4	17	14
8	2	2	18	18	-11	1	3	29	40	-1	3	3	6	8	-12	0	4	20	32	0	2	4	84	88
10	2	2	8	9	-9	1	3	26	24	1	3	3	42	46	-10	0	4	7	12	4	2	4	82	71
12	2	2	12	13	-7	1	3	14	13	3	3	3	35	34	-8	0	4	51	48	6	2	4	40	42
16	2	2	16	15	-5	1	3	30	34	7	3	3	28	26	-6	0	4	36	36	10	2	4	16	11
-1	3	2	5	6	-3	1	3	17	18	9	3	3	17	24	-4	0	4	203	198	12	2	4	13	10
1	3	2	14	7	-1	1	3	73	72	11	3	3	20	12	-2	0	4	14	37	14	2	4	7	3
3	3	2	6	12	1	1	3	131	116	13	3	3	40	27	0	0	4	79	102	16	2	4	13	13
7	3	2	4	4	3	1	3	125	112	15	3	3	27	23	2	0	4	63	60	18	2	4	7	7
13	3	2	6	2	5	1	3	36	40	17	3	3	8	11	4	0	4	133	116	-13	3	4	5	5
15	3	2	13	6	7	1	3	41	39	-4	4	3	7	3	6	0	4	84	77	-9	3	4	7	6
14	4	2	9	9	9	1	3	59	56	0	4	3	9	13	8	0	4	81	81	-3	3	4	12	6
12	4	2	14	7	11	1	3	10	15	2	4	3	21	27	10	0	4	18	20	-1	3	4	6	9
-8	4	2	20	16	13	1	3	22	26	4	4	3	9	12	12	0	4	55	52	1	3	4	12	24

OBSERVED AND CALCULATED STRUCTURE FACTORS FOR THHG

PAGE 3

H	K	L	FO	FC	H	K	L	FO	FC	H	K	L	FO	FC	H	K	L	FO	FC	H	K	L	FO	FC
3	3	4	7	17	-5	1	5	28	22	11	3	5	12	16	4	0	6	35	35	-15	3	6	6	2
9	3	4	6	4	-3	1	5	10	19	13	3	5	35	31	6	0	6	19	17	-13	3	6	6	4
11	3	4	5	4	-1	1	5	90	83	15	3	5	26	20	8	0	6	34	23	-3	3	6	7	8
13	3	4	11	7	1	1	5	129	117	-12	4	5	6	3	10	0	6	34	35	-1	3	6	20	16
15	3	4	11	6	3	1	5	43	38	-4	4	5	7	2	12	0	6	31	32	1	3	6	14	17
-14	4	4	6	10	5	1	5	49	61	2	4	5	14	13	14	0	6	15	15	13	3	6	12	7
-12	4	4	8	6	9	1	5	67	64	10	4	5	14	10	18	0	6	6	8	-8	4	6	22	22
-8	4	4	26	20	13	1	5	10	18	12	4	5	11	6	-13	1	6	13	15	-6	4	6	20	19
-6	4	4	22	22	15	1	5	8	5	-15	5	5	6	5	-9	1	6	10	5	-4	4	6	20	20
-4	4	4	30	22	17	1	5	13	14	-13	5	5	6	9	-7	1	6	4	16	0	4	6	24	24
0	4	4	30	27	19	1	5	8	8	-11	5	5	10	9	-5	1	6	56	59	2	4	6	21	20
2	4	4	17	18	-12	2	5	7	2	-7	5	5	8	3	-3	1	6	54	49	4	4	6	38	31
4	4	4	36	32	-10	2	5	8	11	-3	5	5	6	10	-1	1	6	65	69	8	4	6	6	8
6	4	4	15	14	-8	2	5	8	14	-1	5	5	9	5	1	1	6	9	10	10	4	6	11	9
8	4	4	8	4	-6	2	5	26	27	1	5	5	12	16	3	1	6	42	48	12	4	6	12	7
10	4	4	16	9	-4	2	5	7	17	3	5	5	15	12	5	1	6	14	13	14	4	6	11	9
12	4	4	13	11	-2	2	5	50	54	5	5	5	8	8	7	1	6	33	34	-7	5	6	8	6
14	4	4	11	7	0	2	5	61	61	9	5	5	9	15	9	1	6	12	13	-1	5	6	6	6
-11	5	4	6	7	2	2	5	25	25	11	5	5	12	6	11	1	6	14	14	11	5	6	6	3
-7	5	4	9	8	4	2	5	24	24	-6	6	5	6	7	13	1	6	16	11	-4	6	6	14	12
-1	5	4	8	7	6	2	5	10	13	-4	6	5	6	5	15	1	6	10	6	-2	6	6	24	21
9	5	4	11	7	8	2	5	14	21	-2	6	5	8	5	-14	2	6	17	15	0	6	6	16	15
11	5	4	10	8	-17	3	5	18	19	-5	7	5	7	7	-12	2	6	5	6	10	6	6	7	7
-4	6	4	13	11	-15	3	5	13	15	-18	0	6	14	12	-10	2	6	9	10	-23	1	7	7	5
-2	6	4	27	25	-11	3	5	18	14	-16	0	6	27	21	-8	2	6	32	33	-17	1	7	15	16
0	6	4	21	21	-9	3	5	7	13	-14	0	6	6	4	-6	2	6	46	49	-13	1	7	28	24
2	6	4	7	8	-7	3	5	16	19	-12	0	6	18	16	-4	2	6	11	9	-11	1	7	13	21
6	6	4	12	9	-5	3	5	38	51	-10	0	6	18	18	-2	2	6	29	25	-9	1	7	22	22
-3	7	4	7	5	-3	3	5	19	18	-8	0	6	34	39	0	2	6	58	57	-7	1	7	36	37
-17	1	5	17	15	1	3	5	63	60	-6	0	6	8	22	2	2	6	23	20	-5	1	7	41	40
-13	1	5	34	31	3	3	5	5	20	-4	0	6	232	227	4	2	6	84	79	-3	1	7	45	53
-11	1	5	23	24	5	3	5	15	4	-2	0	6	255	241	8	2	6	15	9	-1	1	7	29	37
-9	1	5	15	12	7	3	5	30	30	0	0	6	123	121	10	2	6	21	22	1	1	7	38	40
-7	1	5	13	25	9	3	5	13	10	2	0	6	23	18	18	2	6	6	6	3	1	7	8	13

OBSERVED AND CALCULATED STRUCTURE FACTORS FOR THHG

PAGE 4

H	K	L	FO	FC	H	K	L	FO	FC	H	K	L	FO	FC	H	K	L	FO	FC					
5	1	7	22	14	4	4	7	6	5	-7	1	8	15	28	4	4	8	23	23	-1	3	9	12	19
7	1	7	33	30	6	4	7	11	9	-5	1	8	14	15	6	4	8	7	8	1	3	9	22	17
9	1	7	44	44	8	4	7	9	3	-3	1	8	16	23	-7	5	8	9	11	3	3	9	11	13
13	1	7	15	17	10	4	7	15	10	-1	1	8	35	36	-4	6	8	13	16	7	3	9	28	29
17	1	7	10	13	-17	5	7	9	7	1	1	8	10	18	-2	6	8	18	18	9	3	9	44	28
-10	2	7	8	2	-13	5	7	11	10	3	1	8	7	17	10	6	8	6	6	11	3	9	19	14
-6	2	7	14	24	-7	5	7	7	8	5	1	8	7	13	-17	1	9	11	13	13	3	9	20	24
-2	2	7	20	24	-1	5	7	6	7	9	1	8	15	13	-13	1	9	22	23	15	3	9	9	7
0	2	7	25	26	1	5	7	10	12	-14	2	8	13	11	-9	1	9	17	15	-6	4	9	9	6
2	2	7	10	6	3	5	7	8	7	-12	2	8	8	6	-7	1	9	14	10	-4	4	9	8	8
4	2	7	27	30	5	5	7	10	7	-10	2	8	11	12	-5	1	9	12	24	-2	4	9	15	17
6	2	7	25	25	7	5	7	7	9	-8	2	8	24	27	-3	1	9	10	14	6	4	9	9	6
10	2	7	8	4	-6	6	7	10	8	-6	2	8	33	34	-1	1	9	26	23	8	4	9	13	2
12	2	7	8	7	-2	6	7	7	2	-4	2	8	19	21	1	1	9	23	22	-13	5	9	12	9
-19	3	7	8	11	1	7	7	7	6	0	2	8	50	48	5	1	9	30	35	-9	5	9	8	5
-17	3	7	14	18	-18	0	8	8	13	2	2	8	45	50	7	1	9	24	25	-5	5	9	5	9
-15	3	7	9	9	-12	0	8	14	15	4	2	8	39	35	9	1	9	22	22	-3	5	9	9	13
-11	3	7	13	8	-10	0	8	38	34	8	2	8	11	12	11	1	9	7	6	1	5	9	6	8
-7	3	7	20	24	-8	0	8	21	18	10	2	8	29	32	13	1	9	14	12	5	5	9	8	8
-5	3	7	30	26	-6	0	8	40	41	12	2	8	25	19	15	1	9	6	7	7	5	9	10	9
-3	3	7	13	20	-4	0	8	80	77	-9	3	8	7	10	-18	2	9	9	7	9	5	9	5	7
-1	3	7	11	12	-2	0	8	-109	107	-3	3	8	8	10	-8	2	9	9	13	11	5	9	6	4
1	3	7	60	60	0	0	8	55	55	-1	3	8	26	22	-6	2	9	21	23	10	6	9	6	3
3	3	7	25	24	2	0	8	14	13	1	3	8	15	12	-4	2	9	8	9	-14	0	10	6	8
7	3	7	27	30	4	0	8	36	37	3	3	8	6	9	2	2	9	8	4	-12	0	10	9	18
9	3	7	13	10	6	0	8	10	11	11	3	8	20	10	4	2	9	6	3	-10	0	10	17	16
11	3	7	13	18	8	0	8	32	42	-20	4	8	7	6	6	2	9	25	27	-8	0	10	54	50
13	3	7	19	28	10	0	8	34	32	-14	4	8	9	7	8	2	9	10	12	-6	0	10	15	22
15	3	7	15	15	14	0	8	6	7	-8	4	8	20	19	12	2	9	16	11	-4	0	10	78	63
-16	4	7	7	5	-19	1	8	8	4	-6	4	8	13	12	-17	3	9	14	17	-2	0	10	45	41
-6	4	7	9	5	-15	1	8	5	7	-4	4	8	12	16	-15	3	9	6	4	0	0	10	11	11
-4	4	7	9	13	-13	1	8	9	8	-2	4	8	11	8	-11	3	9	7	8	2	0	10	27	31
-2	4	7	9	15	-11	1	8	14	16	0	4	8	17	25	-7	3	9	17	16	4	0	10	15	19
2	4	7	7	5	-9	1	8	4	10	2	4	8	15	14	-5	3	9	18	16	6	0	10	5	12

OBSERVED AND CALCULATED STRUCTURE FACTORS FOR THBG

PAGE 5

H	K	L	FO	FC	H	K	L	FO	FC	H	K	L	FO	FC	H	K	L	FO	FC					
8	0	10	26	26	-12	4	10	11	7	-2	2	11	15	17	2	0	12	15	20	-2	4	12	14	11
10	0	10	17	18	-10	4	10	6	5	0	2	11	14	13	6	0	12	16	15	0	4	12	12	14
14	0	10	6	9	-8	4	10	15	15	4	2	11	9	16	8	0	12	21	22	2	4	12	12	11
-15	1	10	8	10	-6	4	10	12	9	8	2	11	7	3	10	0	12	5	8	4	4	12	10	7
-9	1	10	28	31	-4	4	10	7	8	10	2	11	8	6	14	0	12	8	9	12	4	12	8	11
-7	1	10	8	18	-2	4	10	16	15	12	2	11	19	11	-15	1	12	6	8	-9	5	12	6	3
-5	1	10	21	23	0	4	10	14	18	-17	3	11	13	16	-11	1	12	5	6	-2	6	12	10	9
-1	1	10	5	9	2	4	10	13	12	-13	3	11	8	8	-9	1	12	32	27	8	6	12	7	7
1	1	10	18	16	4	4	10	13	17	-7	3	11	12	10	-7	1	12	9	13	-15	1	13	9	5
3	1	10	18	21	6	4	10	15	9	-5	3	11	13	21	-5	1	12	22	27	-7	1	13	19	17
5	1	10	8	7	-7	5	10	7	8	-3	3	11	11	12	-3	1	12	14	18	-5	1	13	9	13
7	1	10	8	9	-5	5	10	8	8	-1	3	11	4	11	1	1	12	11	23	-1	1	13	23	25
11	1	10	5	1	-6	6	10	7	8	1	3	11	5	9	3	1	12	8	11	3	1	13	11	5
15	1	10	10	6	-4	6	10	11	18	3	3	11	10	10	5	1	12	7	5	5	1	13	14	18
-14	2	10	11	11	-2	6	10	13	13	5	3	11	14	14	7	1	12	12	11	7	1	13	9	8
-12	2	10	8	6	-17	1	11	6	10	7	3	11	19	12	-10	2	12	9	8	9	1	13	14	14
-10	2	10	11	14	-15	1	11	11	10	9	3	11	25	25	-8	2	12	20	19	11	1	13	7	1
-8	2	10	16	16	-13	1	11	10	13	11	3	11	15	15	-4	2	12	32	32	15	1	13	7	6
-6	2	10	16	15	-9	1	11	8	6	13	3	11	21	20	-2	2	12	16	18	-12	2	13	17	12
-4	2	10	34	33	-7	1	11	28	30	-12	4	11	9	9	0	2	12	21	19	-10	2	13	12	16
0	2	10	27	26	-5	1	11	30	32	-8	4	11	10	9	2	2	12	15	17	-6	2	13	12	13
2	2	10	32	27	-3	1	11	21	23	-4	4	11	10	6	4	2	12	11	8	-2	2	13	8	14
4	2	10	21	27	-1	1	11	26	37	-2	4	11	12	15	6	2	12	5	17	0	2	13	10	11
6	2	10	7	6	1	1	11	18	13	6	4	11	6	6	10	2	12	13	10	4	2	13	9	5
10	2	10	28	19	5	1	11	27	29	-11	5	11	7	1	-11	3	12	7	7	18	2	13	6	2
12	2	10	13	15	7	1	11	11	13	-9	5	11	7	5	-7	3	12	6	6	-15	3	13	6	2
-17	3	10	7	4	9	1	11	11	17	-7	5	11	8	7	-5	3	12	9	13	-13	3	13	8	7
-5	3	10	5	6	13	1	11	10	10	1	5	11	7	5	-3	3	12	7	12	-11	3	13	14	11
-3	3	10	15	13	15	1	11	11	10	-10	0	12	17	22	7	3	12	13	13	-9	3	13	20	15
-1	3	10	8	13	-18	2	11	10	8	-8	0	12	30	36	9	3	12	12	7	-3	3	13	9	11
5	3	10	8	5	-16	2	11	8	6	-6	0	12	58	53	-14	4	12	6	7	3	3	13	10	14
9	3	10	19	10	-12	2	11	8	11	-4	0	12	56	56	-12	4	12	11	7	9	3	13	9	17
11	3	10	11	4	-8	2	11	8	4	-2	0	12	33	28	-10	4	12	6	5	11	3	13	12	17
-14	4	10	15	9	-6	2	11	20	20	0	0	12	11	12	-8	4	12	23	20	-12	4	13	10	9

OBSERVED AND CALCULATED STRUCTURE FACTORS FOR THXMG

PAGE 6

H	K	L	FO	FC	H	K	L	FO	FC	H	K	L	FO	FC	H	K	L	FO	FC					
-10	4	13	8	6	8	2	14	9	12	-3	3	15	14	13	8	2	16	7	10	-8	0	18	12	17
-4	4	13	9	1	10	2	14	7	13	3	3	15	10	13	1	3	16	7	5	-4	0	18	7	12
-2	4	13	15	13	18	2	14	6	3	5	3	15	8	7	5	3	16	8	7	-11	1	18	8	11
4	4	13	10	9	-7	3	14	14	8	7	3	15	10	8	-8	4	16	6	8	-7	1	18	9	10
-10	0	14	12	9	-5	3	14	21	14	9	3	15	12	16	-4	4	16	8	12	1	1	18	5	12
-8	0	14	7	8	-3	3	14	10	7	11	3	15	8	12	0	4	16	10	12	-8	2	18	13	15
-6	0	14	29	26	7	3	14	12	8	4	4	15	11	9	-6	6	16	6	8	-4	2	18	18	16
-4	0	14	31	35	-8	4	14	12	14	-10	0	16	5	8	-9	1	17	8	8	-9	3	18	6	5
-2	0	14	17	32	-4	4	14	14	14	-8	0	16	6	10	-3	1	17	8	9	3	3	18	7	7
0	0	14	11	12	0	4	14	11	13	-6	0	16	13	17	3	1	17	7	7	-4	4	18	9	9
6	0	14	11	13	-6	6	14	7	9	-4	0	16	13	16	-8	2	17	8	14	-7	1	19	9	14
8	0	14	13	22	-3	1	15	9	10	-2	0	16	7	8	-6	2	17	6	2	-5	1	19	14	17
-13	1	14	6	11	-1	1	15	6	13	6	0	16	11	12	-4	2	17	19	13	-8	2	19	7	9
-9	1	14	10	10	3	1	15	7	6	10	0	16	8	6	-2	2	17	10	10	-6	2	19	6	3
-3	1	14	21	20	5	1	15	8	13	-13	1	16	8	9	0	2	17	9	10	6	2	19	6	4
-1	1	14	7	10	7	1	15	6	5	-1	1	16	9	12	4	2	17	5	6	1	3	19	7	2
1	1	14	10	8	9	1	15	11	10	1	1	16	5	8	6	2	17	7	5	-8	0	20	14	17
3	1	14	7	7	-10	2	15	13	14	7	1	16	5	6	8	2	17	7	6	-12	2	20	6	6
7	1	14	10	13	-8	2	15	15	11	9	1	16	6	3	-5	3	17	11	15	0	2	20	8	8
-8	2	14	15	23	-6	2	15	20	15	-16	2	16	6	5	-3	3	17	13	10	2	2	20	9	8
-6	2	14	7	8	-4	2	15	10	14	-8	2	16	24	24	-1	3	17	16	14	0	2	21	8	6
-4	2	14	24	24	4	2	15	8	10	-6	2	16	6	9	3	3	17	11	12	5	3	21	6	8
-2	2	14	11	13	8	2	15	10	7	-4	2	16	9	16	7	3	17	8	10	-8	0	22	5	11
0	2	14	15	20	-9	3	15	16	15	-2	2	16	9	4	9	3	17	7	14	-4	0	22	8	12
2	2	14	8	8	-7	3	15	19	13	0	2	16	11	16	-10	0	18	8	12	-3	1	22	8	7

OBSERVED AND CALCULATED STRUCTURE FACTORS FOR TPBH

PAGE 1

H	K	L	FO	FC	H	K	L	FO	FC	H	K	L	FO	FC	H	K	L	FO	FC					
2	0	0	141	166	9	3	0	21	-20	16	6	0	15	15	9	11	0	10	10	-12	2	1	7	-8
4	0	0	85	-79	11	3	0	18	19	1	7	0	19	17	11	11	0	5	5	-8	2	1	57	-56
6	0	0	7	-10	13	3	0	8	5	3	7	0	11	-10	15	11	0	4	-3	-6	2	1	7	-9
8	0	0	46	47	15	3	0	5	-4	5	7	0	6	-7	0	12	0	8	-7	-4	2	1	83	87
10	0	0	34	-32	17	3	0	11	10	7	7	0	25	-24	2	12	0	16	17	-2	2	1	54	-58
12	0	0	63	-63	19	3	0	7	-8	9	7	0	18	17	4	12	0	11	12	0	2	1	137	151
14	0	0	26	-24	23	3	0	8	9	11	7	0	3	6	6	12	0	10	10	2	2	1	124	121
16	0	0	5	-5	0	4	0	28	32	13	7	0	22	-23	10	12	0	7	-8	4	2	1	118	119
18	0	0	6	3	2	4	0	44	39	17	7	0	10	11	12	12	0	9	-10	8	2	1	15	-14
20	0	0	33	34	4	4	0	38	42	0	8	0	23	-24	3	13	0	11	-10	10	2	1	27	29
1	1	0	21	-22	6	4	0	19	-21	2	8	0	13	-13	7	13	0	14	12	12	2	1	22	20
3	1	0	28	-27	8	4	0	38	36	4	8	0	21	22	0	14	0	9	-9	14	2	1	5	-5
5	1	0	37	-33	10	4	0	34	-33	8	8	0	26	-28	2	14	0	10	-10	16	2	1	10	-8
7	1	0	3	-4	12	4	0	14	16	10	8	0	11	-10	4	14	0	20	-20	20	2	1	17	18
9	1	0	12	-9	14	4	0	24	-25	12	8	0	35	-36	-21	1	1	12	-11	22	2	1	6	5
13	1	0	23	22	16	4	0	27	-27	16	8	0	18	-19	-19	1	1	7	7	-21	3	1	4	-4
15	1	0	7	6	18	4	0	4	-3	18	8	0	4	-4	-17	1	1	14	-13	-19	3	1	21	23
17	1	0	5	-5	20	4	0	11	-10	1	9	0	36	35	-15	1	1	23	21	-15	3	1	7	8
19	1	0	7	7	1	5	0	4	-3	5	9	0	6	-6	-13	1	1	27	24	-13	3	1	30	30
0	2	0	95	-101	3	5	0	31	31	7	9	0	11	10	-11	1	1	8	-8	-11	3	1	14	-13
2	2	0	60	-63	5	5	0	3	4	9	9	0	6	-6	-9	1	1	17	-18	-9	3	1	17	-14
4	2	0	38	-32	9	5	0	26	28	11	9	0	16	-17	-7	1	1	26	-24	-7	3	1	25	22
6	2	0	3	-5	11	5	0	13	13	13	9	0	7	-4	-5	1	1	70	-70	-5	3	1	47	47
8	2	0	17	14	15	5	0	7	6	15	9	0	10	10	-3	1	1	10	11	-3	3	1	109	-114
10	2	0	48	-44	17	5	0	8	-7	0	10	0	19	-18	-1	1	1	3	3	-1	3	1	205	-217
12	2	0	11	-12	19	5	0	6	-6	2	10	0	6	-5	1	1	1	12	-9	1	3	1	240	261
14	2	0	4	6	0	6	0	91	-88	4	10	0	11	-11	3	1	1	16	14	3	3	1	18	-22
16	2	0	20	20	2	6	0	21	-20	8	10	0	22	-22	5	1	1	15	-15	5	3	1	16	-11
18	2	0	10	-9	4	6	0	6	4	10	10	0	12	11	11	1	1	47	43	7	3	1	34	-36
20	2	0	6	4	6	6	0	9	9	14	10	0	4	5	21	1	1	8	7	9	3	1	6	-5
22	2	0	10	-10	8	6	0	6	6	16	10	0	5	5	-20	2	1	17	18	11	3	1	30	-31
1	3	0	213	-233	10	6	0	49	51	1	11	0	13	13	-18	2	1	15	16	13	3	1	7	-6
3	3	0	24	-23	12	6	0	54	52	3	11	0	14	14	-16	2	1	9	9	17	3	1	7	7
5	3	0	73	74	14	6	0	18	18	5	11	0	19	-19	-14	2	1	14	-15	21	3	1	13	14

OBSERVED AND CALCULATED STRUCTURE FACTORS FOR TPBH

PAGE 2

H	K	L	FO	FC	H	K	L	FO	FC	H	K	L	FO	FC	H	K	L	FO	FC					
-22	4	1	6	-5	11	5	1	43	-44	13	7	1	27	28	11	9	1	13	-13	6	12	1	6	-6
-20	4	1	-14	14	13	5	1	18	-19	15	7	1	18	18	13	9	1	20	-20	-7	13	1	9	8
-16	4	1	34	-36	-20	6	1	10	-10	19	7	1	5	-5	15	9	1	14	-15	-1	13	1	13	-12
-14	4	1	37	-37	-18	6	1	6	-8	-18	8	1	5	6	-16	10	1	4	-3	3	13	1	12	11
-10	4	1	29	-29	-16	6	1	12	12	-16	8	1	12	-12	-14	10	1	10	-10	7	13	1	5	3
-8	4	1	35	-30	-14	6	1	21	-20	-14	8	1	15	-15	-12	10	1	19	-21	9	13	1	6	-5
-6	4	1	7	6	-12	6	1	17	-20	-12	8	1	17	16	-10	10	1	7	8	-4	14	1	8	-7
-4	4	1	20	16	-10	6	1	30	-29	-10	8	1	57	57	-8	10	1	16	16	-2	14	1	14	13
-2	4	1	74	74	-8	6	1	14	13	-8	8	1	42	43	-6	10	1	16	-14	0	14	1	9	8
0	4	1	38	36	-4	6	1	27	26	-6	8	1	13	-13	-4	10	1	7	-10	2	14	1	13	13
2	4	1	8	7	-2	6	1	20	16	-4	8	1	12	14	-2	10	1	27	-26	4	14	1	15	13
4	4	1	41	42	2	6	1	35	-39	-2	8	1	22	19	0	10	1	32	-31	-22	0	2	8	-8
6	4	1	27	-25	4	6	1	7	-3	0	8	1	27	29	2	10	1	16	-17	-20	0	2	6	-7
8	4	1	23	23	6	6	1	5	4	2	8	1	4	2	4	10	1	13	13	-18	0	2	24	-25
10	4	1	24	-20	8	6	1	9	9	4	8	1	32	-35	6	10	1	11	-12	-16	0	2	7	9
12	4	1	42	-42	10	6	1	6	-8	6	8	1	6	-4	8	10	1	18	-18	-14	0	2	17	16
14	4	1	23	-23	12	6	1	54	57	8	8	1	53	53	10	10	1	22	21	-12	0	2	10	8
16	4	1	5	-7	14	6	1	17	17	10	8	1	55	55	14	10	1	10	-10	-10	0	2	24	25
18	4	1	5	-6	16	6	1	8	-7	12	8	1	15	13	-15	11	1	8	8	-8	0	2	54	-54
20	4	1	9	9	20	6	1	7	-5	14	8	1	17	-14	-13	11	1	12	12	-6	0	2	22	23
22	4	1	9	-7	-17	7	1	13	12	16	8	1	15	14	-11	11	1	16	-15	-4	0	2	130	-149
-19	5	1	13	-15	-15	7	1	17	17	-17	9	1	8	-7	-9	11	1	15	-16	-2	0	2	141	-165
-17	5	1	21	-23	-13	7	1	12	12	-15	9	1	4	1	-7	11	1	25	-26	0	0	2	124	-155
-15	5	1	36	37	-11	7	1	5	3	-13	9	1	7	-6	-3	11	1	15	16	2	0	2	192	-235
-13	5	1	19	22	-9	7	1	31	-33	-11	9	1	26	26	-1	11	1	11	-11	4	0	2	137	146
-11	5	1	6	6	-7	7	1	24	24	-9	9	1	18	19	1	11	1	10	-12	6	0	2	24	-21
-9	5	1	59	-59	-5	7	1	21	-22	-7	9	1	12	-11	5	11	1	19	19	8	0	2	56	-55
-7	5	1	56	55	-3	7	1	9	-9	-5	9	1	8	-8	7	11	1	7	-6	12	0	2	43	42
-3	5	1	36	-38	-1	7	1	27	30	-3	9	1	6	-5	9	11	1	17	-19	14	0	2	11	9
-1	5	1	15	-14	1	7	1	5	5	-1	9	1	10	-10	15	11	1	12	12	16	0	2	12	12
1	5	1	23	-23	3	7	1	27	-31	1	9	1	6	5	-8	12	1	18	-17	18	0	2	16	-18
3	5	1	34	-34	7	7	1	21	-23	5	9	1	18	20	-6	12	1	5	4	20	0	2	18	-18
7	5	1	27	25	9	7	1	15	15	7	9	1	9	8	-4	12	1	9	9	22	0	2	16	-17
9	5	1	36	-34	11	7	1	33	-32	9	9	1	10	-11	-2	12	1	9	9	-21	1	2	12	11

OBSERVED AND CALCULATED STRUCTURE FACTORS FOR TPBH

PAGE 3

H	K	L	FO	FC	H	K	L	FO	FC	H	K	L	FO	FC	H	K	L	FO	FC					
-19	1	2	22	-22	-19	3	2	13	13	8	4	2	15	13	6	6	2	18	-16	-2	8	2	27	-28
-13	1	2	10	9	-17	3	2	12	14	10	4	2	12	-12	8	6	2	46	-45	0	8	2	15	14
-11	1	2	30	-28	-15	3	2	14	-14	12	4	2	57	56	10	6	2	52	-51	2	8	2	38	35
-9	1	2	16	-17	-11	3	2	18	-19	14	4	2	7	7	12	6	2	65	-65	8	8	2	50	51
-5	1	2	67	-70	-9	3	2	80	73	16	4	2	5	-7	14	6	2	15	-16	10	8	2	24	25
-3	1	2	178	-189	-7	3	2	9	13	18	4	2	9	-8	16	6	2	6	6	-13	9	2	7	7
-1	1	2	12	8	-5	3	2	34	-34	20	4	2	6	7	18	6	2	4	3	-11	9	2	10	11
1	1	2	19	14	-3	3	2	86	-83	22	4	2	6	4	-21	7	2	6	-3	-9	9	2	27	-28
3	1	2	180	191	-1	3	2	98	102	-17	5	2	18	-19	-19	7	2	14	15	-7	9	2	23	24
5	1	2	40	-40	1	3	2	39	32	-13	5	2	9	6	-17	7	2	5	7	-5	9	2	12	12
7	1	2	62	62	3	3	2	68	-59	-11	5	2	17	-15	-15	7	2	11	-11	-3	9	2	8	8
9	1	2	47	44	5	3	2	42	-42	-7	5	2	57	-55	-11	7	2	45	46	-1	9	2	13	-11
13	1	2	16	-15	7	3	2	10	13	-1	5	2	32	-34	-9	7	2	20	-18	5	9	2	10	10
15	1	2	7	-6	9	3	2	25	21	1	5	2	5	-4	-7	7	2	22	-24	9	9	2	7	8
19	1	2	11	12	11	3	2	52	51	3	5	2	43	-43	-5	7	2	15	13	11	9	2	10	-11
21	1	2	11	-12	13	3	2	23	-23	5	5	2	65	65	-3	7	2	23	22	13	9	2	23	23
-18	2	2	8	-8	15	3	2	11	-11	7	5	2	58	58	-1	7	2	18	18	17	9	2	-5	-5
-16	2	2	14	15	17	3	2	8	-7	9	5	2	35	-37	1	7	2	14	-17	-16	10	2	15	-16
-14	2	2	-12	-12	19	3	2	6	-6	11	5	2	26	-24	3	7	2	12	-9	-14	10	2	8	-8
-10	2	2	45	41	21	3	2	10	10	13	5	2	22	24	5	7	2	15	-15	-12	10	2	-11	-11
-8	2	2	91	92	-20	4	2	10	9	15	5	2	29	26	7	7	2	7	-7	-10	10	2	8	10
-4	2	2	268	319	-18	4	2	25	26	17	5	2	8	-8	9	7	2	19	18	-8	10	2	30	29
-2	2	2	168	188	-16	4	2	15	15	21	5	2	6	7	11	7	2	16	-18	-6	10	2	23	26
0	2	2	32	-40	-14	4	2	12	13	-20	6	2	11	-11	13	7	2	9	-8	-4	10	2	14	-14
2	2	2	88	-86	-12	4	2	6	-7	-18	6	2	4	-4	19	7	2	7	-8	-2	10	2	20	-21
4	2	2	50	-48	-10	4	2	13	-13	-16	6	2	9	-13	-20	8	2	13	14	0	10	2	19	22
6	2	2	67	-65	-8	4	2	31	30	-14	6	2	24	-26	-18	8	2	8	8	2	10	2	22	23
8	2	2	67	-66	-6	4	2	18	-15	-10	6	2	52	-51	-16	8	2	10	8	6	10	2	4	-4
10	2	2	11	-11	-4	4	2	47	-47	-8	6	2	57	-53	-14	8	2	20	19	8	10	2	16	-15
12	2	2	17	-18	-2	4	2	15	20	-4	6	2	30	30	-12	8	2	6	7	10	10	2	17	16
14	2	2	5	-7	0	4	2	33	-37	-2	6	2	32	32	-10	8	2	9	8	16	10	2	8	8
16	2	2	5	4	2	4	2	3	1	0	6	2	20	20	-8	8	2	25	-27	-13	11	2	11	-10
18	2	2	11	11	4	4	2	13	12	2	6	2	24	21	-6	8	2	9	10	-9	11	2	18	17
-21	3	2	4	-3	6	4	2	29	28	4	6	2	13	16	-4	8	2	24	-22	-7	11	2	10	9

OBSERVED AND CALCULATED STRUCTURE FACTORS FOR TPRH

PAGE 4

H	K	L	FO	FC	H	K	L	FO	FC	H	K	L	FO	FC	H	K	L	FO	FC					
-5	11	2	9	-8	-5	1	3	215	-250	-13	3	3	17	-18	-21	5	3	11	10	16	6	3	11	10
-3	11	2	10	10	-3	1	3	121	128	-11	3	3	21	-22	-19	5	3	11	11	18	6	3	-7	-8
-1	11	2	15	-17	-1	1	3	71	72	-9	3	3	18	19	-17	5	3	22	21	-15	7	3	5	5
5	11	2	11	-11	1	1	3	122	-124	-7	3	3	16	-13	-15	5	3	8	-6	-9	7	3	6	-6
7	11	2	22	-21	3	1	3	134	-137	-5	3	3	3	8	-13	5	3	35	-34	-7	7	3	43	-40
11	11	2	6	6	5	1	3	7	6	-3	3	3	10	-12	-11	5	3	23	-25	-5	7	3	37	-38
15	11	2	13	-11	7	1	3	17	-14	-1	3	3	20	24	-9	5	3	13	12	-3	7	3	10	-11
-10	12	2	12	11	9	1	3	3	-7	1	3	3	92	-94	-7	5	3	29	-24	-1	7	3	32	37
-6	12	2	20	-19	11	1	3	3	6	3	3	3	32	32	-5	5	3	115	-118	1	7	3	18	13
-4	12	2	22	-22	13	1	3	7	-7	5	3	3	84	81	-3	5	3	28	29	3	7	3	22	20
-2	12	2	12	-12	17	1	3	5	5	7	3	3	38	40	-1	5	3	45	43	5	7	3	41	-38
0	12	2	19	-19	19	1	3	20	20	9	3	3	18	-19	1	5	3	35	35	7	7	3	26	-25
2	12	2	24	-25	21	1	3	11	-11	11	3	3	9	9	3	5	3	26	-27	11	7	3	17	-17
4	12	2	25	-26	23	1	3	10	-12	13	3	3	24	24	5	5	3	25	-23	13	7	3	7	-7
6	12	2	10	11	-20	2	3	6	-7	15	3	3	13	-13	7	5	3	11	-11	17	7	3	8	8
8	12	2	12	13	-18	2	3	52	-54	19	3	3	6	-5	9	5	3	13	-13	19	7	3	5	5
10	12	2	11	12	-14	2	3	7	5	-20	4	3	9	10	11	5	3	33	34	-18	8	3	5	-5
12	12	2	7	6	-12	2	3	27	28	-18	4	3	24	-23	17	5	3	12	13	-16	8	3	9	-10
-9	13	2	12	-12	-10	2	3	54	49	-14	4	3	14	15	19	5	3	14	14	-12	8	3	11	9
-5	13	2	9	10	-8	2	3	29	-25	-12	4	3	20	20	-20	6	3	6	-5	-10	8	3	27	-25
-3	13	2	21	20	-6	2	3	74	70	-10	4	3	18	-15	-14	6	3	17	17	-8	8	3	6	-10
3	13	2	15	-13	-4	2	3	11	10	-8	4	3	120	113	-12	6	3	30	33	-6	8	3	11	-12
5	13	2	13	12	-2	2	3	83	-81	-6	4	3	132	130	-10	6	3	28	-31	-4	8	3	9	7
-2	14	2	16	16	0	2	3	77	-76	-4	4	3	104	102	-8	6	3	34	34	-2	8	3	17	-14
0	14	2	9	9	2	2	3	278	-303	-2	4	3	44	-40	-4	6	3	16	16	0	8	3	18	20
2	14	2	7	7	4	2	3	65	65	0	4	3	51	-51	-2	6	3	32	-28	2	8	3	18	17
4	14	2	5	5	8	2	3	61	-59	4	4	3	78	73	0	6	3	19	16	4	8	3	11	-10
-23	1	3	6	8	10	2	3	11	-11	6	4	3	9	-5	2	6	3	16	14	6	8	3	14	14
-21	1	3	15	15	12	2	3	17	16	8	4	3	41	39	4	6	3	9	-10	8	8	3	29	31
-17	1	3	12	-12	16	2	3	8	-9	10	4	3	26	23	6	6	3	12	-10	10	8	3	21	-24
-15	1	3	4	-3	22	2	3	18	-19	12	4	3	25	27	8	6	3	15	-16	12	8	3	32	-31
-11	1	3	22	21	-21	3	3	12	-11	14	4	3	16	16	10	6	3	45	-48	14	8	3	18	-17
-9	1	3	49	41	-17	3	3	7	6	18	4	3	11	-12	12	6	3	8	10	18	8	3	12	-13
-7	1	3	83	-73	-15	3	3	4	3	20	4	3	9	10	14	6	3	22	-23	-17	9	3	7	8

OBSERVED AND CALCULATED STRUCTURE FACTORS FOR TPDH

PAGE 5

H	K	L	FO	FC	H	K	L	FO	FC	H	K	L	FO	FC	H	K	L	FO	FC					
-13	9	3	23	-22	-2	12	3	9	-8	-15	1	4	6	-6	-19	3	4	8	-8	8	4	4	10	-9
-11	9	3	5	-5	4	12	3	18	-17	-13	1	4	3	3	-17	3	4	7	-7	10	4	4	6	-8
-9	9	3	12	-13	6	12	3	8	-8	-11	1	4	7	7	-13	3	4	9	11	12	4	4	12	-11
-7	9	3	7	-5	12	12	3	6	-5	-9	1	4	10	12	-11	3	4	19	-17	14	4	4	25	26
-5	9	3	11	12	-9	13	3	12	-13	-7	1	4	22	-26	-9	3	4	4	-1	16	4	4	16	17
3	9	3	8	-7	-7	13	3	6	4	-3	1	4	34	30	-7	3	4	63	-64	20	4	4	9	2
5	9	3	12	12	-5	13	3	8	10	-1	1	4	20	25	-5	3	4	61	58	-21	5	4	13	14
7	9	3	4	-4	-3	13	3	6	6	1	1	4	59	-61	-3	3	4	59	56	-19	5	4	5	4
9	9	3	14	12	-1	13	3	19	-18	3	1	4	174	176	-1	3	4	83	83	-17	5	4	19	-22
11	9	3	22	21	3	13	3	13	13	5	1	4	27	33	1	3	4	36	31	-15	5	4	7	10
-16	10	3	13	13	0	14	3	22	-22	7	1	4	20	17	3	3	4	55	50	-13	5	4	4	1
-10	10	3	14	13	2	14	3	8	-7	9	1	4	35	-32	5	3	4	8	10	-11	5	4	11	-10
-8	10	3	8	11	4	14	3	8	-9	11	1	4	12	-10	7	3	4	57	-56	-9	5	4	30	27
-6	10	3	7	8	-20	0	4	19	19	15	1	4	8	-9	9	3	4	12	-10	-7	5	4	37	-36
-2	10	3	7	7	-18	0	4	37	38	19	1	4	6	-6	11	3	4	7	9	-5	5	4	33	33
0	10	3	7	8	-14	0	4	5	-4	-22	2	4	9	7	13	3	4	10	-10	-3	5	4	10	-8
2	10	3	12	-12	-12	0	4	11	10	-18	2	4	19	18	15	3	4	20	18	-1	5	4	8	10
4	10	3	21	21	-8	0	4	31	29	-16	2	4	7	-5	17	3	4	11	-11	1	5	4	9	-10
6	10	3	16	18	-6	0	4	75	72	-12	2	4	8	-8	19	3	4	10	-10	3	5	4	110	-109
8	10	3	18	17	-4	0	4	85	-88	-8	2	4	154	-151	-22	4	4	7	-6	5	5	4	31	32
12	10	3	8	-10	-2	0	4	73	-73	-6	2	4	69	-70	-20	4	4	5	5	7	5	4	58	58
14	10	3	6	6	-2	0	4	147	-157	-4	2	4	35	36	-18	4	4	21	-22	11	5	4	14	-13
16	10	3	6	-5	0	0	4	121	115	-2	2	4	114	-115	-16	4	4	27	-30	13	5	4	9	-9
-11	11	3	13	12	2	0	4	19	-12	0	2	4	8	-6	-14	4	4	17	-15	17	5	4	6	5
-9	11	3	14	15	4	0	4	4	-2	2	2	4	75	71	-12	4	4	4	-4	-18	6	4	9	8
-1	11	3	7	-7	6	0	4	51	-50	4	2	4	31	35	-10	4	4	14	15	-16	6	4	6	8
3	11	3	6	5	8	0	4	32	32	6	2	4	9	-9	-8	4	4	45	46	-12	6	4	9	9
5	11	3	15	-15	10	0	4	8	-10	8	2	4	48	43	-6	4	4	97	93	-10	6	4	21	18
7	11	3	16	-14	14	0	4	12	13	10	2	4	34	33	-4	4	4	36	-36	-8	6	4	42	43
9	11	3	5	5	18	0	4	27	28	14	2	4	11	-11	-2	4	4	14	12	-6	6	4	18	17
-12	12	3	13	12	20	0	4	21	21	16	2	4	15	-16	0	4	4	14	16	-4	6	4	27	-30
-10	12	3	14	15	22	0	4	5	-5	18	2	4	7	-7	2	4	4	96	-99	-2	6	4	15	15
-8	12	3	9	-9	-21	1	4	23	-23	20	2	4	17	-18	4	4	4	216	-206	0	6	4	10	9
-6	12	3	10	9	-19	1	4	31	31	-21	3	4	13	-14	6	4	4	63	-59	2	6	4	34	-35

OBSERVED AND CALCULATED STRUCTURE FACTORS FOR TPBH

PAGE 6

H	K	L	FO	FC	H	K	L	FO	FC	H	K	L	FO	FC	H	K	L	FO	FC	H	K	L	FO	FC
4	6	4	34	33	6	8	4	12	-11	5	11	4	10	-9	15	1	5	17	-18	-22	4	5	6	-6
6	6	4	22	23	8	8	4	29	-31	7	11	4	9	-10	17	1	5	11	-12	-20	4	5	7	8
8	6	4	55	52	10	8	4	33	-35	9	11	4	14	14	19	1	5	6	6	-18	4	5	10	8
10	6	4	28	27	12	8	4	23	24	-12	12	4	5	6	-18	2	5	13	14	-16	4	5	19	21
12	6	4	16	16	-17	9	4	8	-7	-6	12	4	17	18	-16	2	5	55	57	-14	4	5	9	-10
14	6	4	14	16	-13	9	4	11	11	-4	12	4	34	33	-10	2	5	33	31	-12	4	5	16	-17
16	6	4	-4	5	-11	9	4	6	-7	-2	12	4	7	8	-8	2	5	12	13	-10	4	5	8	11
18	6	4	5	2	-9	9	4	26	-28	0	12	4	17	18	-6	2	5	58	50	-8	4	5	55	-53
-21	7	4	7	-8	-5	9	4	28	-32	2	12	4	23	24	-4	2	5	88	-84	-6	4	5	184	-178
-17	7	4	8	9	-3	9	4	4	-1	4	12	4	23	24	-2	2	5	28	-27	-4	4	5	63	-58
-15	7	4	10	10	1	9	4	21	-22	8	12	4	16	-15	0	2	5	41	38	-2	4	5	18	-19
-13	7	4	7	-7	3	9	4	24	-24	10	12	4	5	-5	2	2	5	5	-3	0	4	5	16	21
-11	7	4	11	-13	7	9	4	8	10	-7	13	4	7	8	4	2	5	117	114	2	4	5	28	-31
-9	7	4	11	-7	9	9	4	4	4	-3	13	4	9	-9	6	2	5	55	50	4	4	5	60	-54
-7	7	4	28	24	11	9	4	20	-19	1	13	4	6	7	8	2	5	13	10	6	4	5	46	-43
-5	7	4	30	-27	15	9	4	12	-11	3	13	4	16	-18	12	2	5	8	-9	8	4	5	35	36
-1	7	4	17	-17	17	9	4	8	8	5	13	4	14	-15	14	2	5	4	1	10	4	5	4	1
1	7	4	11	10	-14	10	4	10	9	7	13	4	12	-10	18	2	5	5	-5	12	4	5	27	-27
3	7	4	58	58	-10	10	4	17	-17	0	14	4	6	-8	22	2	5	8	10	14	4	5	20	-22
5	7	4	33	31	-8	10	4	24	-23	-19	1	5	10	-8	-19	3	5	9	-10	16	4	5	7	-8
7	7	4	25	-26	-6	10	4	35	-35	-17	1	5	19	18	-15	3	5	30	-32	-15	5	5	19	-19
9	7	4	16	-14	-4	10	4	4	-4	-11	1	5	14	-13	-13	3	5	9	10	-13	5	5	9	9
11	7	4	20	18	-2	10	4	8	-8	-9	1	5	62	62	-9	3	5	92	-92	-9	5	5	16	20
13	7	4	10	12	4	10	4	32	31	-7	1	5	60	54	-7	3	5	28	-28	-7	5	5	86	-85
15	7	4	18	-20	6	10	4	24	26	-5	1	5	20	24	-5	3	5	75	73	-5	5	5	59	59
17	7	4	8	-10	8	10	4	11	11	-3	1	5	29	25	-3	3	5	93	90	-3	5	5	63	56
-20	8	4	14	-14	10	10	4	4	-5	-1	1	5	34	-31	1	3	5	98	-93	-1	5	5	27	30
-18	8	4	18	-17	12	10	4	12	-13	1	1	5	4	-2	3	3	5	30	28	1	5	5	10	-11
-14	8	4	7	-6	14	10	4	13	-13	3	1	5	94	94	5	3	5	42	-37	3	5	5	6	5
-10	8	4	7	8	-13	11	4	15	-14	5	1	5	10	9	7	3	5	67	65	5	5	5	13	17
-8	8	4	34	33	-7	11	4	12	12	7	1	5	29	-26	9	3	5	17	-17	7	5	5	22	-21
-2	8	4	21	21	-5	11	4	13	14	9	1	5	14	-13	13	3	5	11	13	9	5	5	6	-6
0	8	4	5	6	-1	11	4	19	-18	11	1	5	18	-17	15	3	5	33	33	11	5	5	17	18
4	8	4	21	-22	1	11	4	15	16	13	1	5	16	16	19	3	5	14	-14	13	5	5	17	-16

OBSERVED AND CALCULATED STRUCTURE FACTORS FOR TPBH

PAGE 7

H	K	L	FO	FC	H	K	L	FO	FC	H	K	L	FO	FC	H	K	L	FO	FC					
-20	6	5	11	-11	-2	8	5	14	-14	-1	11	5	9	10	14	0	6	12	13	4	2	6	36	-36
-16	6	5	12	11	4	8	5	26	-25	1	11	5	17	18	16	0	6	37	-39	6	2	6	39	40
-12	6	5	11	9	6	8	5	21	-20	3	11	5	5	4	18	0	6	23	-23	8	2	6	13	12
-10	6	5	37	38	8	8	5	7	8	5	11	5	9	-10	-23	1	6	10	-9	10	2	6	10	10
-8	6	5	49	49	10	8	5	11	10	7	11	5	16	16	-21	1	6	7	8	12	2	6	22	24
-6	6	5	31	-31	12	8	5	21	20	11	11	5	9	-9	-19	1	6	23	23	14	2	6	19	20
-4	6	5	15	-13	14	8	5	9	8	-12	12	5	10	8	-15	1	6	16	-17	16	2	6	30	31
-2	6	5	4	-7	18	8	5	9	8	-10	12	5	7	7	-13	1	6	17	16	18	2	6	19	20
0	6	5	20	-18	-13	9	5	10	10	-8	12	5	9	-10	-11	1	6	34	32	-19	3	6	10	10
2	6	5	6	7	-11	9	5	19	-18	-4	12	5	10	-11	-9	1	6	11	-10	-13	3	6	16	12
4	6	5	42	40	-9	9	5	23	-26	0	12	5	15	13	-7	1	6	23	22	-11	3	6	6	7
8	6	5	44	-44	-7	9	5	16	17	4	12	5	8	7	-3	1	6	15	-12	-9	3	6	26	-28
12	6	5	6	5	-5	9	5	14	15	6	12	5	14	14	-1	1	6	37	35	-5	3	6	23	20
14	6	5	27	-28	-3	9	5	27	-28	-7	13	5	9	-8	1	1	6	18	15	-3	3	6	13	15
18	6	5	6	8	-1	9	5	15	15	-5	13	5	7	-9	3	1	6	91	-88	-1	3	6	19	-18
-17	7	5	16	-16	3	9	5	18	-17	-3	13	5	9	8	5	1	6	33	-33	1	3	6	36	37
-15	7	5	7	-9	5	9	5	10	-13	5	13	5	7	7	7	1	6	23	23	3	3	6	101	98
-13	7	5	10	-9	9	9	5	11	12	-2	14	5	6	6	9	1	6	5	-8	5	3	6	14	-10
-11	7	5	22	-20	-14	10	5	5	5	-20	0	6	16	-13	11	1	6	8	-8	7	3	6	50	-47
-9	7	5	7	-6	-8	10	5	7	7	-18	0	6	10	-11	15	1	6	5	-7	9	3	6	9	7
-7	7	5	8	5	-6	10	5	9	8	-16	0	6	57	-57	17	1	6	10	-11	11	3	6	17	-16
-5	7	5	78	75	-4	10	5	9	-8	-14	0	6	18	18	-22	2	6	6	6	15	3	6	15	14
-3	7	5	5	-6	0	10	5	23	-21	-12	0	6	72	-69	-20	2	6	19	-20	17	3	6	7	6
-1	7	5	19	-20	2	10	5	29	-31	-10	0	6	69	-73	-18	2	6	20	-22	-22	4	6	7	7
1	7	5	18	17	4	10	5	12	-12	-8	0	6	87	86	-16	2	6	24	-26	-20	4	6	4	4
3	7	5	44	42	6	10	5	12	-12	-6	0	6	21	16	-14	2	6	11	11	-16	4	6	33	36
7	7	5	11	10	8	10	5	10	-10	-4	0	6	7	-7	-12	2	6	12	11	-14	4	6	7	7
11	7	5	14	14	10	10	5	16	-15	-2	0	6	63	-57	-10	2	6	57	56	-12	4	6	27	-26
15	7	5	20	20	12	10	5	9	7	0	0	6	61	-60	-8	2	6	19	-21	-10	4	6	37	-39
17	7	5	6	-6	14	10	5	4	4	2	0	6	14	-11	-6	2	6	94	90	-8	4	6	37	-34
-12	8	5	16	17	-13	11	5	8	-7	4	0	6	39	-39	-4	2	6	4	-3	-6	4	6	16	12
-10	8	5	11	14	-11	11	5	7	-9	6	0	6	81	80	-2	2	6	28	33	-4	4	6	50	-45
-8	8	5	32	32	-7	11	5	17	18	8	0	6	34	-37	0	2	6	84	-84	-2	4	6	11	9
-4	8	5	8	-8	-3	11	5	5	-6	10	0	6	14	-12	2	2	6	26	-24	0	4	6	36	35

OBSERVED AND CALCULATED STRUCTURE FACTORS FOR TPBH

PAGE 8

H	K	L	FO	FC	H	K	L	FO	FC	H	K	L	FO	FC	H	K	L	FO	FC					
2	4	6	67	61	4	6	6	6	-10	-11	9	6	9	-9	-5	13	6	16	-15	-17	3	7	16	17
4	4	6	123	120	6	6	6	34	-33	-9	9	6	5	7	-1	13	6	9	8	-15	3	7	20	-20
6	4	6	33	31	8	6	6	27	25	-7	9	6	20	20	5	13	6	15	14	-13	3	7	52	52
8	4	6	7	-10	10	6	6	9	9	1	9	6	16	-17	-15	1	7	34	-36	-9	3	7	6	-8
10	4	6	6	6	12	6	6	9	-11	5	9	6	7	8	-13	1	7	28	-25	-7	3	7	57	57
12	4	6	11	-11	14	6	6	18	-17	9	9	6	10	-9	-9	1	7	36	35	-5	3	7	5	-8
16	4	6	26	-27	-17	7	6	6	-6	13	9	6	9	7	-7	1	7	24	19	-1	3	7	36	-33
20	4	6	7	-5	-11	7	6	10	-10	-16	10	6	10	8	-5	1	7	11	12	1	3	7	18	19
19	5	6	6	5	-9	7	6	20	19	-14	10	6	5	5	-3	1	7	46	42	3	3	7	16	-18
17	5	6	7	10	-5	7	6	23	-22	-10	10	6	8	10	-1	1	7	27	25	5	3	7	82	-84
15	5	6	10	10	-3	7	6	7	8	-8	10	6	32	35	1	1	7	24	-21	7	3	7	13	17
13	5	6	14	-12	-1	7	6	22	-19	-6	10	6	26	26	3	1	7	30	26	9	3	7	6	5
11	5	6	8	-8	1	7	6	11	11	-4	10	6	40	40	5	1	7	47	-43	11	3	7	6	-4
7	5	6	6	6	3	7	6	9	10	0	10	6	15	-15	7	1	7	51	49	13	3	7	12	-13
5	5	6	21	20	5	7	6	7	-5	2	10	6	18	-18	9	1	7	27	26	15	3	7	7	7
3	5	6	10	-10	7	7	6	6	10	4	10	6	16	-16	11	1	7	21	20	-18	4	7	7	6
1	5	6	29	29	9	7	6	11	12	6	10	6	37	-39	13	1	7	7	8	-16	4	7	6	-6
3	5	6	49	46	11	7	6	5	5	8	10	6	13	-14	15	1	7	18	-19	-14	4	7	17	14
5	5	6	32	-30	13	7	6	7	-6	12	10	6	16	16	17	1	7	6	8	-12	4	7	6	7
7	5	6	60	-58	15	7	6	10	11	-13	11	6	15	-15	-16	2	7	49	-49	-10	4	7	24	20
9	5	6	39	-35	17	7	6	11	11	-9	11	6	12	-14	-14	2	7	42	-41	-8	4	7	31	-30
11	5	6	5	-7	-18	8	6	9	8	-7	11	6	7	-8	-12	2	7	8	-9	-6	4	7	40	-35
13	5	6	6	5	-10	8	6	5	-2	-5	11	6	18	16	-10	2	7	19	-14	-4	4	7	14	14
15	5	6	21	-20	-8	8	6	4	3	-1	11	6	14	-14	-8	2	7	32	-31	-2	4	7	30	-28
14	6	6	18	-18	-6	8	6	45	-46	1	11	6	22	-23	-4	2	7	38	36	0	4	7	49	45
12	6	6	5	-7	-4	8	6	6	6	3	11	6	8	9	-2	2	7	42	42	2	4	7	62	64
10	6	6	15	15	-2	8	6	6	-7	5	11	6	18	18	0	2	7	21	-21	4	4	7	50	-52
8	6	6	33	30	0	8	6	32	32	-10	12	6	14	-12	2	2	7	74	-69	6	4	7	10	-11
6	6	6	20	-21	2	8	6	11	13	-8	12	6	16	-18	4	2	7	85	-83	8	4	7	11	-8
4	6	6	58	-57	4	8	6	19	19	-6	12	6	6	-6	6	2	7	17	-12	10	4	7	11	-13
2	6	6	39	-39	6	8	6	43	45	0	12	6	17	16	10	2	7	8	7	12	4	7	7	7
0	6	6	20	22	8	8	6	9	11	4	12	6	6	-3	12	2	7	22	-22	14	4	7	32	34
2	6	6	43	-43	12	8	6	4	4	6	12	6	19	-20	16	2	7	19	20	16	4	7	14	14
4	6	6	54	-51	14	8	6	13	-14	-7	13	6	12	-13	20	2	7	6	-7	18	4	7	6	6

OBSERVED AND CALCULATED STRUCTURE FACTORS FOR TPBH

PAGE 9

H	K	L	FO	FC	H	K	L	FO	FC	H	K	L	FO	FC	H	K	L	FO	FC					
20	4	7	5	3	5	7	7	18	16	15	9	7	5	-6	-14	0	8	98	99	15	1	8	10	8
-19	5	7	11	-11	7	7	7	7	8	-16	10	7	12	11	-12	0	8	20	19	-22	2	8	8	-8
-15	5	7	7	7	9	7	7	8	-9	-14	10	7	18	19	-10	0	8	56	57	-18	2	8	14	16
-13	5	7	8	-6	13	7	7	16	-16	-12	10	7	8	6	-8	0	8	30	28	-16	2	8	6	-9
-9	5	7	54	48	15	7	7	9	-8	-10	10	7	10	-11	-6	0	8	27	-25	-14	2	8	44	-43
-7	5	7	29	29	17	7	7	12	-12	-8	10	7	10	-14	-4	0	8	39	34	-10	2	8	29	25
-5	5	7	34	32	-18	8	7	14	14	-6	10	7	8	-8	-2	0	8	8	-7	-6	2	8	51	-49
-3	5	7	46	-46	-14	8	7	6	4	-4	10	7	21	21	0	0	8	7	9	-4	2	8	64	-61
-1	5	7	56	53	-12	8	7	8	8	-2	10	7	12	12	4	0	8	25	22	-2	2	8	7	5
1	5	7	13	-13	-10	8	7	14	-18	0	10	7	12	-12	6	0	8	67	68	0	2	8	37	38
3	5	7	24	21	-8	8	7	34	-33	2	10	7	24	26	8	0	8	61	60	2	2	8	77	70
5	5	7	20	20	-6	8	7	18	-20	4	10	7	22	23	10	0	8	8	10	4	2	8	14	-12
7	5	7	15	14	-4	8	7	43	-44	6	10	7	15	14	12	0	8	11	12	8	2	8	19	-16
11	5	7	8	9	-2	8	7	42	-43	8	10	7	4	5	14	0	8	23	24	10	2	8	13	14
15	5	7	7	-7	0	8	7	19	-18	10	10	7	7	8	16	0	8	5	4	12	2	8	32	-33
17	5	7	17	-17	2	8	7	35	36	12	10	7	6	7	18	0	8	11	-9	14	2	8	41	-42
-14	6	7	5	7	4	8	7	7	4	-9	11	7	4	3	20	0	8	13	-14	16	2	8	12	-12
-10	6	7	34	-31	6	8	7	23	-22	-7	11	7	6	7	-23	1	8	12	12	-21	3	8	7	8
-8	6	7	54	-56	8	8	7	6	-6	-3	11	7	25	26	-21	1	8	11	12	-19	3	8	7	7
-6	6	7	6	-4	14	8	7	7	-6	1	11	7	12	-11	-17	1	8	20	-21	-13	3	8	23	-23
-2	6	7	20	22	16	8	7	11	-9	3	11	7	8	-7	-15	1	8	39	38	-11	3	8	27	-23
0	6	7	35	-35	-15	9	7	11	-12	9	11	7	8	-7	-13	1	8	14	-13	-7	3	8	20	20
2	6	7	20	-17	-11	9	7	5	5	-12	12	7	8	-7	-11	1	8	20	-18	-5	3	8	61	-58
4	6	7	51	49	-9	9	7	34	33	-10	12	7	8	-9	-9	1	8	53	-47	-3	3	8	7	7
6	6	7	58	58	-7	9	7	12	14	-6	12	7	12	12	-7	1	8	5	3	-1	3	8	52	-48
8	6	7	5	6	-5	9	7	11	-11	-2	12	7	12	-13	-5	1	8	16	19	1	3	8	43	-39
12	6	7	18	-19	-3	9	7	14	15	2	12	7	6	-6	-3	1	8	44	39	5	3	8	16	-15
14	6	7	12	13	-1	9	7	29	28	-5	13	7	6	-6	-1	1	8	7	8	7	3	8	14	-13
-17	7	7	4	2	1	9	7	6	-4	1	13	7	7	-7	1	1	8	54	-53	9	3	8	9	-10
-13	7	7	4	-7	3	9	7	5	4	3	13	7	11	-11	3	1	8	64	-63	11	3	8	5	-7
-9	7	7	29	29	5	9	7	16	-19	-22	0	8	12	-15	5	1	8	49	48	13	3	8	18	18
-5	7	7	16	16	7	9	7	25	-23	-20	0	8	10	-8	7	1	8	16	-16	15	3	8	6	-9
-3	7	7	16	-17	9	9	7	6	-5	-18	0	8	11	9	9	1	8	5	-7	19	3	8	6	8
3	7	7	19	-19	11	9	7	15	16	-16	0	8	21	22	13	1	8	14	15	-18	4	8	5	-7

OBSERVED AND CALCULATED STRUCTURE FACTORS FOR TPBH

PAGE 10

H	K	L	FO	FC	H	K	L	FO	FC	H	K	L	FO	FC	H	K	L	FO	FC	H	K	L	FO	FC
-12	4	8	9	10	-2	6	8	34	31	-3	9	8	15	-18	-13	1	9	16	-16	-7	3	9	12	11
10	4	8	15	13	0	6	8	18	19	-1	9	8	29	30	-11	1	9	19	-20	-1	3	9	12	12
-8	4	8	7	6	2	6	8	61	59	1	9	8	14	15	-9	1	9	20	-19	1	3	9	6	4
-6	4	8	24	24	4	6	8	12	10	5	9	8	4	-5	-7	1	9	12	-9	3	3	9	16	-16
-4	4	8	33	-34	6	6	8	30	-28	7	9	8	15	16	-5	1	9	34	-35	5	3	9	10	11
-2	4	8	7	-4	8	6	8	6	-5	9	9	8	9	12	-3	1	9	8	8	7	3	9	6	6
2	4	8	14	-16	12	6	8	10	-12	13	9	8	12	-13	-1	1	9	6	6	11	3	9	32	-34
4	4	8	7	7	14	6	8	5	2	-10	10	8	18	-20	1	1	9	10	10	13	3	9	12	-11
6	4	8	32	-29	-17	7	8	6	7	-8	10	8	14	-15	5	1	9	14	-15	15	3	9	5	-4
10	4	8	12	-11	-9	7	8	17	17	-6	10	8	27	-27	7	1	9	20	-19	-22	4	9	6	-6
12	4	8	12	14	-7	7	8	6	-5	-4	10	8	9	8	9	1	9	27	-26	-18	4	9	6	-5
14	4	8	8	11	-5	7	8	31	30	-2	10	8	17	16	11	1	9	35	35	-16	4	9	8	-8
-17	5	8	4	4	-3	7	8	25	-26	0	10	8	7	8	15	1	9	7	-9	-14	4	9	9	11
-13	5	8	11	13	-1	7	8	48	-49	2	10	8	9	9	17	1	9	7	7	-12	4	9	18	-20
-11	5	8	8	5	1	7	8	7	-6	6	10	8	12	12	19	1	9	8	8	-10	4	9	9	11
-9	5	8	10	-8	3	7	8	6	5	10	10	8	15	-15	-20	2	9	5	6	-8	4	9	5	-5
-7	5	8	18	15	5	7	8	21	-21	-13	11	8	6	4	-18	2	9	10	10	-6	4	9	11	9
-5	5	8	18	-17	9	7	8	11	13	-11	11	8	5	6	-14	2	9	58	57	-4	4	9	52	-51
-3	5	8	27	23	13	7	8	7	-8	-7	11	8	10	-8	-12	2	9	8	-8	-2	4	9	26	-25
-1	5	8	40	42	15	7	8	10	11	-1	11	8	19	18	-10	2	9	9	9	0	4	9	12	14
1	5	8	17	18	-16	8	8	10	-9	1	11	8	5	6	-6	2	9	47	-42	2	4	9	18	18
3	5	8	14	-15	-10	8	8	5	-6	3	11	8	21	22	-4	2	9	7	7	4	4	9	14	-15
5	5	8	6	-7	-6	8	8	20	22	9	11	8	7	-8	-2	2	9	43	41	6	4	9	36	35
7	5	8	19	19	-2	8	8	66	-66	-10	12	8	5	5	0	2	9	22	24	8	4	9	18	-15
9	5	8	7	-6	0	8	8	27	-27	-8	12	8	12	10	2	2	9	8	-8	10	4	9	4	-6
11	5	8	16	15	2	8	8	35	-33	-6	12	8	10	-11	4	2	9	6	6	14	4	9	7	-6
13	5	8	11	11	4	8	8	15	-18	-4	12	8	19	-20	6	2	9	36	34	16	4	9	15	-15
-18	6	8	10	-8	10	8	8	9	9	0	12	8	14	-15	8	2	9	7	-6	-19	5	9	5	5
-16	6	8	11	-11	14	8	8	4	3	2	12	8	20	-19	10	2	9	39	38	-17	5	9	8	10
-14	6	8	15	-15	16	8	8	8	8	6	12	8	12	11	12	2	9	14	15	-15	5	9	10	9
-10	6	8	13	-13	-15	9	8	5	-6	8	12	8	12	10	-17	3	9	12	-13	-13	5	9	16	-15
-8	6	8	19	-19	-11	9	8	14	13	3	13	8	7	9	-13	3	9	29	31	-7	5	9	20	22
-6	6	8	43	42	-9	9	8	15	16	-17	1	9	20	22	-11	3	9	6	-5	-5	5	9	36	-37
-4	6	8	72	72	-5	9	8	7	-5	-15	1	9	21	22	-9	3	9	6	8	-3	5	9	39	-41

H	K	L	FO	FC	H	K	L	FO	FC	H	K	L	FO	FC	H	K	L	FO	FC					
-1	5	9	20	-21	-6	8	9	47	48	2	12	9	12	12	-20	2	10	10	11	-6	4	10	15	14
1	5	9	12	-10	-4	8	9	24	26	6	12	9	9	-10	-18	2	10	22	23	-2	4	10	14	14
3	5	9	16	13	-2	8	9	45	43	-18	0	10	24	-23	-16	2	10	21	21	0	4	10	22	21
5	5	9	14	-12	0	8	9	18	21	-16	0	10	6	-8	-14	2	10	12	14	4	4	10	7	8
7	5	9	11	-11	2	8	9	17	17	-14	0	10	37	-39	-12	2	10	36	38	6	4	10	34	33
-14	6	9	6	-11	8	8	9	7	-9	-12	0	10	33	-34	-10	2	10	9	-9	10	4	10	29	-31
-12	6	9	17	-19	10	8	9	11	-13	-10	0	10	20	-21	-6	2	10	21	-22	16	4	10	6	6
-10	6	9	8	-8	14	8	9	15	13	-8	0	10	13	-12	-4	2	10	38	38	-19	5	10	5	5
-8	6	9	4	6	-13	9	9	14	16	-6	0	10	18	-16	-2	2	10	4	3	-17	5	10	4	-6
-4	6	9	35	-38	-11	9	9	11	12	-4	0	10	34	28	0	2	10	11	-9	-15	5	10	24	-24
-2	6	9	51	54	-7	9	9	14	-15	-2	0	10	84	83	2	2	10	32	-30	-13	5	10	9	9
0	6	9	9	9	-5	9	9	8	7	0	0	10	27	24	4	2	10	10	10	-11	5	10	10	-10
4	6	9	17	-16	-3	9	9	20	19	2	0	10	7	-6	8	2	10	6	5	-9	5	10	7	6
6	6	9	15	-14	-1	9	9	37	-37	4	0	10	24	-25	16	2	10	6	7	-7	5	10	6	8
8	6	9	13	17	1	9	9	28	-27	6	0	10	44	-41	-21	3	10	7	-7	-5	5	10	51	-53
10	6	9	20	23	3	9	9	6	7	8	0	10	42	-43	-17	3	10	6	-4	-3	5	10	17	-18
14	6	9	7	8	5	9	9	16	14	10	0	10	61	-67	-13	3	10	6	7	1	5	10	27	28
16	6	9	11	-10	9	9	9	14	-14	14	0	10	5	-5	-11	3	10	5	6	3	5	10	14	13
-17	7	9	7	-7	-14	10	9	14	-15	16	0	10	7	7	-9	3	10	4	-3	5	5	10	8	8
-13	7	9	16	14	-12	10	9	26	-26	18	0	10	9	9	-5	3	10	15	14	7	5	10	8	8
-11	7	9	16	19	-6	10	9	24	-23	-21	1	10	11	-11	-3	3	10	30	31	9	5	10	7	-6
-9	7	9	6	-6	-4	10	9	6	7	-15	1	10	12	-12	-1	3	10	48	-46	11	5	10	13	12
-7	7	9	10	-10	-2	10	9	7	6	-13	1	10	59	-60	1	3	10	3	4	15	5	10	8	-6
-5	7	9	35	38	0	10	9	13	12	-11	1	10	28	28	3	3	10	6	5	-16	6	10	14	15
-1	7	9	27	-28	4	10	9	9	-10	-9	1	10	13	11	5	3	10	6	3	-14	6	10	14	15
1	7	9	19	-19	6	10	9	6	-6	-7	1	10	11	13	7	3	10	34	34	-10	6	10	8	7
3	7	9	25	-25	8	10	9	18	-19	-3	1	10	29	-26	9	3	10	11	10	-6	6	10	31	-30
7	7	9	4	6	-11	11	9	12	14	-1	1	10	8	-7	11	3	10	8	-9	-4	6	10	59	-61
9	7	9	8	8	-7	11	9	11	-11	1	1	10	10	10	15	3	10	5	-4	-2	6	10	72	-71
13	7	9	7	7	-3	11	9	9	-8	7	1	10	31	-29	-18	4	10	16	-16	0	6	10	19	-19
-14	8	9	7	-7	-1	11	9	17	-18	9	1	10	48	48	-16	4	10	7	6	2	6	10	8	-6
-12	8	9	13	-13	9	11	9	10	10	11	1	10	21	22	-14	4	10	27	29	6	6	10	5	4
-10	8	9	8	-7	-2	12	9	7	-8	17	1	10	6	7	-12	4	10	9	10	10	6	10	16	17
-8	8	9	10	13	0	12	9	14	13	-22	2	10	10	7	-10	4	10	12	-11	12	6	10	8	8

OBSERVED AND-CALCULATED STRUCTURE FACTORS FOR TPDH

PAGE 12

H	K	L	FO	FC	H	K	L	FO	FC	H	K	L	FO	FC	H	K	L	FO	FC					
16	6	10	14	-14	-3	11	10	4	-4	-19	3	11	8	8	9	5	11	15	14	-10	10	11	22	23
-11	7	10	5	2	1	11	10	8	-7	-17	3	11	9	-5	15	5	11	8	-6	-4	10	11	9	10
-9	7	10	14	-12	5	11	10	5	-4	-13	3	11	33	-33	-12	6	11	16	20	-2	10	11	6	7
-7	7	10	7	-8	-6	12	10	5	4	-11	3	11	15	14	-10	6	11	14	14	2	10	11	20	-21
-5	7	10	36	38	-2	12	10	10	10	-7	3	11	5	-4	-8	6	11	6	-3	4	10	11	5	-1
-3	7	10	17	16	2	12	10	8	7	-5	3	11	28	-29	-4	6	11	29	30	6	10	11	13	12
1	7	10	22	-21	4	12	10	12	-10	-3	3	11	17	-18	-2	6	11	24	24	-11	11	11	6	-6
3	7	10	8	7	-21	1	11	11	-13	-1	3	11	30	29	0	6	11	51	-52	-9	11	11	17	-19
7	7	10	7	-9	-19	1	11	15	-15	1	3	11	17	18	2	6	11	14	-14	-3	11	11	12	-11
9	7	10	17	-16	-17	1	11	16	15	5	3	11	12	-14	6	6	11	10	-14	-1	11	11	11	10
-12	8	10	9	-11	-15	1	11	17	19	9	3	11	28	29	10	6	11	4	-4	-4	12	11	7	7
-10	8	10	8	-9	-13	1	11	11	-13	13	3	11	10	10	-9	7	11	17	-17	-20	0	12	16	15
-8	8	10	15	16	-11	1	11	8	9	-18	4	11	7	5	-7	7	11	9	-10	-18	0	12	5	7
-6	8	10	47	47	-7	1	11	7	6	-14	4	11	7	-7	-5	7	11	28	-29	-16	0	12	21	20
-4	8	10	5	6	-5	1	11	18	-17	-8	4	11	4	3	-3	7	11	17	-17	-12	0	12	48	46
-2	8	10	31	31	-3	1	11	27	-24	-6	4	11	43	44	1	7	11	22	23	-10	0	12	27	-30
0	8	10	10	10	-1	1	11	18	-16	-4	4	11	55	55	-14	8	11	4	-5	-6	0	12	20	-21
2	8	10	5	-4	3	1	11	5	-5	-2	4	11	17	17	-12	8	11	6	6	-4	0	12	22	-21
6	8	10	5	-5	5	1	11	24	23	0	4	11	9	8	-6	8	11	15	17	-2	0	12	32	-28
8	8	10	9	-9	7	1	11	47	-46	2	4	11	20	20	-4	8	11	9	-9	0	0	12	23	-22
-11	9	10	4	-4	9	1	11	22	-24	4	4	11	13	13	-2	8	11	13	-13	2	0	12	6	-5
-1	9	10	31	31	13	1	11	8	6	6	4	11	14	12	0	8	11	12	-13	6	0	12	32	33
3	9	10	13	-12	15	1	11	4	5	8	4	11	5	-4	12	8	11	4	-3	8	0	12	34	34
5	9	10	5	-7	-18	2	11	5	-6	10	4	11	14	15	-15	9	11	9	9	12	0	12	23	24
9	9	10	5	-4	-12	2	11	49	-48	14	4	11	8	-9	-11	9	11	15	-15	-17	1	12	7	-8
-8	10	10	4	-4	-10	2	11	5	-6	-19	5	11	8	-7	-7	9	11	6	7	-13	1	12	19	18
-6	10	10	16	-15	-8	2	11	12	-11	-11	5	11	13	14	-5	9	11	15	-14	-11	1	12	8	9
-4	10	10	9	-9	-4	2	11	24	25	-9	5	11	13	12	-3	9	11	15	-16	-7	1	12	10	8
2	10	10	12	12	-2	2	11	9	-10	-5	5	11	46	-47	1	9	11	30	28	-3	1	12	12	-13
4	10	10	8	-8	2	2	11	21	19	-3	5	11	16	16	5	9	11	12	13	-1	1	12	32	31
6	10	10	11	11	6	2	11	38	-38	-1	5	11	31	-32	7	9	11	12	11	1	1	12	13	12
8	10	10	14	15	8	2	11	44	-43	1	5	11	13	-11	9	9	11	6	8	5	1	12	11	12
10	10	10	10	12	10	2	11	12	-12	3	5	11	7	-9	11	9	11	8	-6	7	1	12	17	19
-7	11	10	7	-8	12	2	11	12	-13	5	5	11	17	16	-12	10	11	10	12	9	1	12	7	-6

OBSERVED AND CALCULATED STRUCTURE FACTORS FOR TPBH

PAGE 13

H	K	L	FO	FC	H	K	L	FO	FC	H	K	L	FO	FC	H	K	L	FO	FC	H	K	L	FO	FC	.
11	1	12	21	-22	0	4	12	10	-9	-12	8	12	7	-4	13	1	13	7	-6	-7	5	13	13	-12	
13	1	12	6	-5	2	4	12	7	-7	-10	8	12	18	-17	-20	2	13	5	4	-5	5	13	26	26	
17	1	12	6	-7	4	4	12	12	14	-8	8	12	9	-12	-12	2	13	30	32	-3	5	13	39	38	
-18	2	12	7	7	6	4	12	18	18	-6	8	12	26	-26	-10	2	13	36	37	-1	5	13	7	-9	
-16	2	12	6	-6	8	4	12	13	-11	-4	8	12	24	-24	-8	2	13	26	27	5	5	13	16	17	
-14	2	12	18	-20	10	4	12	11	11	-2	8	12	34	35	-4	2	13	13	-13	7	5	13	10	-12	
-8	2	12	7	8	-17	5	12	6	-7	6	8	12	11	11	-2	2	13	20	-21	9	5	13	6	-5	
-4	2	12	14	12	-13	5	12	10	11	-13	9	12	10	-11	2	2	13	20	18	13	5	13	10	11	
-2	2	12	10	-9	-11	5	12	14	-14	-11	9	12	11	-12	8	2	13	27	29	-14	6	13	12	-12	
0	2	12	6	9	-9	5	12	15	15	-5	9	12	12	-12	10	2	13	7	7	-10	6	13	17	18	
2	2	12	4	2	-7	5	12	21	23	-3	9	12	17	-14	-15	3	13	6	4	-8	6	13	26	27	
4	2	12	15	-16	-1	5	12	28	-29	-1	9	12	7	-7	-13	3	13	6	7	0	6	13	15	15	
6	2	12	69	-71	1	5	12	30	-29	7	9	12	8	-10	-11	3	13	27	26	4	6	13	19	-17	
10	2	12	9	9	5	5	12	14	14	-12	10	12	5	4	-9	3	13	49	-51	6	6	13	8	-10	
12	2	12	8	7	7	5	12	7	-9	-10	10	12	15	14	-7	3	13	13	-14	-15	7	13	5	-4	
-21	3	12	10	-8	9	5	12	11	-10	-8	10	12	9	10	-1	3	13	11	-12	-13	7	13	6	7	
-19	3	12	6	-6	-14	6	12	15	-15	-6	10	12	15	15	1	3	13	10	12	-11	7	13	8	6	
-17	3	12	4	-4	-12	6	12	12	-13	-2	10	12	11	-12	3	3	13	21	24	-3	7	13	32	29	
-13	3	12	11	10	-10	6	12	31	32	0	10	12	19	-19	5	3	13	8	7	-1	7	13	11	11	
-9	3	12	4	5	-8	6	12	7	8	8	10	12	5	-8	9	3	13	5	5	1	7	13	17	16	
-5	3	12	17	17	-6	6	12	15	16	-1	11	12	10	-9	11	3	13	8	-7	9	7	13	7	-7	
-3	3	12	6	4	-4	6	12	38	36	-15	1	13	8	-9	-10	4	13	21	-21	-10	8	13	12	-13	
1	3	12	16	17	-2	6	12	33	35	-11	1	13	24	26	-8	4	13	17	16	0	8	13	16	13	
5	3	12	4	2	0	6	12	23	22	-9	1	13	9	-10	-6	4	13	8	9	8	8	13	7	6	
7	3	12	13	14	6	6	12	7	-9	-7	1	13	8	-8	-4	4	13	24	-24	-13	9	13	15	-14	
13	3	12	6	-6	8	6	12	13	-12	-5	1	13	11	10	-2	4	13	54	-55	-11	9	13	8	-8	
-20	4	12	15	14	10	6	12	10	-10	-3	1	13	7	6	0	4	13	21	-21	-7	9	13	8	-9	
-16	4	12	9	7	-11	7	12	16	16	-1	1	13	16	17	2	4	13	25	-27	-3	9	13	11	13	
-14	4	12	6	-7	-9	7	12	9	-8	1	1	13	7	-7	4	4	13	18	-19	-1	9	13	7	7	
-12	4	12	28	-31	-3	7	12	26	26	3	1	13	25	25	6	4	13	10	-12	3	9	13	4	-2	
-10	4	12	20	-19	-1	7	12	10	11	5	1	13	26	28	12	4	13	8	7	5	9	13	6	-5	
-8	4	12	23	-25	1	7	12	10	-12	7	1	13	13	-13	-19	5	13	6	3	-8	10	13	6	-5	
-6	4	12	26	-26	3	7	12	8	-9	9	1	13	8	11	-11	5	13	17	-17	-4	10	13	13	-13	
-2	4	12	27	-30	5	7	12	7	-9	11	1	13	11	-13	-9	5	13	16	-18	2	10	13	6	-6	

H	K	L	FO	FC	H	K	L	FO	FC	H	K	L	FO	FC	H	K	L	FO	FC					
6	10	13	8	-7	4	2	14	31	32	11	5	14	6	-5	-10	2	15	30	-30	-1	5	15	16	15
-20	0	14	9	-8	6	2	14	15	14	-16	6	14	7	-8	-8	2	15	7	-7	1	5	15	8	7
-18	0	14	11	-13	8	2	14	11	13	-14	6	14	11	-11	-6	2	15	28	-28	3	5	15	5	-5
-16	0	14	6	-6	12	2	14	5	5	-8	6	14	22	-24	0	2	15	19	-21	5	5	15	17	-17
-12	0	14	14	-14	-17	3	14	10	9	-4	6	14	8	8	4	2	15	17	17	7	5	15	6	-7
-10	0	14	50	-51	-15	3	14	5	-5	-2	6	14	12	-13	6	2	15	17	18	9	5	15	6	-6
-8	0	14	12	15	-11	3	14	22	22	0	6	14	13	-15	10	2	15	17	-16	-14	6	15	12	-11
-6	0	14	8	7	-9	3	14	11	10	6	6	14	8	7	-11	3	15	8	-6	-10	6	15	9	8
-2	0	14	5	6	-7	3	14	16	-13	12	6	14	6	-4	-7	3	15	29	31	-6	6	15	12	-10
0	0	14	6	8	-5	3	14	12	-13	-9	7	14	19	-20	-5	3	15	14	14	-2	6	15	15	-14
2	0	14	32	-29	-3	3	14	19	-17	-1	7	14	14	-14	-3	3	15	7	-7	0	6	15	9	7
4	0	14	27	-30	-1	3	14	7	6	1	7	14	18	20	-1	3	15	7	8	4	6	15	15	15
8	0	14	8	-8	7	3	14	7	-6	3	7	14	14	15	1	3	15	6	7	-11	7	15	10	-11
10	0	14	16	-15	11	3	14	8	9	-14	8	14	8	9	3	3	15	21	-22	-7	7	15	13	14
-17	1	14	6	7	-18	4	14	13	-14	-12	8	14	18	18	5	3	15	14	-16	-3	7	15	7	-8
-13	1	14	12	12	-16	4	14	9	-8	-10	8	14	9	8	7	3	15	8	-7	1	7	15	9	10
-11	1	14	7	-8	-14	4	14	10	8	-8	8	14	13	12	-9	3	15	5	-5	5	7	15	8	-7
-9	1	14	23	24	-12	4	14	14	15	-4	8	14	8	8	-14	4	15	7	9	9	7	15	7	6
-7	1	14	9	-9	-10	4	14	29	33	0	8	14	7	-7	-12	4	15	16	18	-12	8	15	6	8
3	1	14	5	4	-8	4	14	16	16	2	8	14	7	8	-10	4	15	9	-9	-8	8	15	9	-9
5	1	14	13	-14	-6	4	14	13	15	4	8	14	8	-7	-6	4	15	27	-27	-6	8	15	4	-7
7	1	14	13	-12	-4	4	14	14	13	6	8	14	11	-10	-4	4	15	4	3	-2	8	15	15	-15
9	1	14	17	-18	2	4	14	54	-53	1	9	14	13	12	-2	4	15	20	20	0	8	15	15	-15
11	1	14	9	6	4	4	14	16	-17	-2	10	14	16	15	0	4	15	13	14	2	8	15	16	-17
13	1	14	5	-5	8	4	14	7	6	0	10	14	14	14	2	4	15	8	-9	-7	9	15	6	-6
-14	2	14	8	-7	10	4	14	10	11	2	10	14	11	9	4	4	15	12	14	-5	9	15	5	-5
-12	2	14	20	-20	12	4	14	5	4	-15	1	15	9	8	6	4	15	10	10	3	9	15	5	5
-10	2	14	30	-32	-17	5	14	13	14	-11	1	15	11	-11	8	4	15	6	5	-18	0	16	5	4
-8	2	14	6	-7	-15	5	14	11	9	-7	1	15	15	16	10	4	15	12	-10	-14	0	16	12	-14
-6	2	14	5	6	-7	5	14	4	4	-5	1	15	10	10	-15	5	15	10	10	-12	0	16	8	-5
-4	2	14	7	-5	-5	5	14	9	-8	1	1	15	23	-24	-9	5	15	11	11	-10	0	16	46	46
-2	2	14	3	3	1	5	14	17	-18	3	1	15	24	24	-7	5	15	13	13	-8	0	16	31	31
0	2	14	12	11	7	5	14	5	5	5	1	15	15	14	-5	5	15	14	14	-6	0	16	14	13
2	2	14	44	47	9	5	14	6	7	-14	2	15	11	-12	-3	5	15	4	-3	-2	0	16	32	34

OBSERVED AND CALCULATED STRUCTURE FACTORS FOR TPRH

PAGE 15

H	K	L	FO	FC	H	K	L	FO	FC	H	K	L	FO	FC	H	K	L	FO	FC	H	K	L	FO	FC
0	0	16	23	25	7	3	16	6	6	-7	1	17	8	-10	-14	0	18	15	16	4	4	18	-10	-9
2	0	16	16	16	11	3	16	7	-6	-5	1	17	9	-9	-12	0	18	22	23	-7	5	18	7	-7
4	0	16	20	21	-12	4	16	14	-15	-3	1	17	11	10	-8	0	18	42	-42	-5	5	18	8	-9
8	0	16	10	-9	-10	4	16	7	-10	-1	1	17	10	-9	-6	0	18	18	-18	5	5	18	6	6
10	0	16	13	14	-2	4	16	21	23	1	1	17	20	-21	-4	0	18	34	-34	-8	6	18	4	6
15	1	16	9	10	0	4	16	16	17	3	1	17	12	-12	-2	0	18	7	-9	-2	6	18	5	-1
13	1	16	11	10	10	4	16	11	-11	7	1	17	13	13	0	0	18	18	-20	2	6	18	7	-7
11	1	16	15	-16	-11	5	16	8	-8	9	1	17	9	8	2	0	18	11	-10	-7	1	19	20	-19
9	1	16	9	-9	-9	5	16	12	-11	-8	2	17	21	22	-4	0	18	6	8	-3	1	19	7	7
7	1	16	29	-29	-7	5	16	14	14	-6	2	17	4	4	6	0	18	17	17	3	1	19	8	-8
1	1	16	13	-13	-3	5	16	11	13	-4	2	17	14	15	-13	1	18	18	-18	5	1	19	10	-9
3	1	16	11	13	-1	5	16	20	20	4	2	17	7	-7	-11	1	18	12	-11	-8	2	19	14	-15
5	1	16	6	6	1	5	16	7	7	6	2	17	5	6	-5	1	18	6	5	-4	2	19	5	-4
11	1	16	8	8	5	5	16	10	-11	-15	3	17	7	7	1	1	18	9	10	4	2	19	9	-9
14	2	16	8	-6	-14	6	16	10	11	-9	3	17	21	21	-14	2	18	9	9	-7	3	19	5	-3
10	2	16	28	29	-12	6	16	8	7	-3	3	17	20	-20	-12	2	18	13	14	-5	3	19	13	14
8	2	16	15	15	-2	6	16	7	-8	1	3	17	7	-9	-10	2	18	6	5	-3	3	19	6	-6
4	2	16	4	-4	0	6	16	8	9	3	3	17	5	-6	-8	2	18	11	-10	-2	4	19	7	8
2	2	16	19	-19	-11	7	16	5	6	7	3	17	7	4	-6	2	18	17	17	2	4	19	9	9
0	2	16	38	-39	-9	7	16	7	8	-8	4	17	5	5	-4	2	18	17	16	-7	5	19	6	-6
2	2	16	10	-10	-5	7	16	10	-10	6	4	17	9	-10	-2	2	18	4	-4	-8	0	20	20	22
4	2	16	12	-14	-3	7	16	6	-6	-7	5	17	12	-14	2	2	18	7	8	-6	0	20	13	14
10	2	16	8	8	-1	7	16	6	6	-3	5	17	8	9	-13	3	18	12	-13	-4	0	20	10	-12
15	3	16	6	-6	1	7	16	5	6	1	5	17	23	-24	-7	3	18	18	17	-7	1	20	12	13
13	3	16	9	8	3	7	16	12	-12	-8	6	17	15	-16	5	3	18	10	-11	-1	1	20	8	-9
9	3	16	24	-25	-10	8	16	13	-12	0	6	17	12	12	7	3	18	8	-8	1	1	20	9	-8
7	3	16	6	-6	-8	8	16	9	-8	4	6	17	10	10	-10	4	18	5	5	-8	2	20	15	-16
5	3	16	4	3	-6	8	16	6	-7	6	6	17	8	-7	-8	4	18	11	12	-4	2	20	8	-8
3	3	16	5	-5	-2	8	16	8	-8	1	7	17	12	-12	-4	4	18	8	-8	-5	3	20	7	6
1	3	16	16	-16	-1	9	16	6	-4	-4	8	17	4	-7	0	4	18	10	-9	-3	3	20	13	13
3	3	16	5	-5	-9	1	17	11	12	0	8	17	19	19										

REFERENCES

1. J.L. Atwood, J.E.D. Davies and D.D. MacNicol (ed.):
Inclusion Compounds, 1, (7; 375-405), 1984.
2. H.M. Powell, J. Chem. Soc., 61, 1948.
3. J.E.D. Davies Et.Al, Journal of inclusion Phenomena,
1, 1, (4-20), 1983.
4. E. Weber, Topics in Current Chem., 140, (3-13), 1987.
5. J.E.D. Davies, J. Mol. Struct., 75, 1, 1981.
6. M.H. Gorin and L. Rosenstein, U.S. Patent 2 774 752
(Dec. 18 1956).
7. Y. Go and O. Kratky, Z Physik. Chem., B26, 439, 1934.
8. D.W. Breck and J.V. Smith, Sci. American, 200, 85, 1959.
9. C.J. Pedersen, J. Am. Chem. Soc., 89, 2495,7017, 1967.
10. B. Dietrich, J.M. Lehn and J.P. Sauvage, Terahedron
Lett., 2885, 2889, 1969.
11. F. Vögtle (ed.): Host-Guest Complex Chem., I and II,
Springer, Berlin, 1981.
12. M. Hagan (ed.): Clathrate Inclusion Compounds, New
York, Reinhold Publ. Corp., 1962.
13. E.H. Wiebenga, Ned. Tijdschr. Natuurk., 19, 289, 1953.
14. D.J. Chleck and C.A. Ziegler, Nucleonics, 17, 9, 130,
1959.
15. R.J. Cross, J.J. McKendrick and D.D. MacNicol, Nature,
245, 146, 1973.
16. C.K. Johnson, Fr.P. 1 530 511, 1968, (Chem. Abs., 71,
13, 717, 1969.

17. J.E. Kropp, M.G. Allen and G.W.B. Warren, Ger. Offen. 2 012 103, (Chem. Abs., 74, 43, 074, 1971.
18. J.E.D. Davies, J. Chem. Educ., 54, 563, 1977.
19. L. Mandelcorn (ed.): Non-Stoichiometric Compounds, New York, London, Academic Press, 1964.
20. V.M. Bhatnagar (ed.): Clathrate Compounds, New Delhi, S. Chand & Co., 1968.
21. G. Gawalek (ed.): EinschluBverbindungen, Additionsverbindungen, Clathrate, Berlin, V.E.B. Deutscher Verlag der Wissenschaft, 1969.
22. G.F. El-Fayoumy, M.A. Wahab and M. I. Roushdy, Inclusion Compounds, 3, 372.
23. R.C. Weast, M.J. Astle and W.H. Beyer (ed.): CRS Handbook of Chemistry and Physics, 66th Ed., (1985-1986)
24. M. Moore, Structure Activity Relationships in Werner Clathrates, 216-223, 1987.
25. B.D. Davies, R. Dulbecco, H.N. Eisen and H.S. Ginsberg, Microbiology, 3rd. Ed., 299.
26. E.A. Davies, Quantitative Problems in Biochemistry, 6th Ed., 88-90, 1980.
27. C.R. Cantor and P.R. Schimmel, Biophysical Chem., Part III, 850-859.
28. K.J. Zemke, BSc. (Hons) Project, 10-14, 1983.
29. P. Main: MULTAN 78, University of York.
30. G.H. Stout and L.H. Jensen, X-ray Structure Determination, Macmillan, London, 1968.

31. A.C.T. North, D.C. Phillips and F. Scott Mathews, *Acta Cryst.*, A24, 351, 1968.
32. M.J. Buerger, *Crystal-Structure Analysis*, J. Wiley and Sons, Inc., New York, 1967.
33. L Pauling, *The Nature of the Chemical Bond*, Cornell Univ. Press, Ithaca, New York, 1960.
34. D.T. Cromer and J.B. Mann, *Acta Cryst.*, A24, 321, 1968.
35. R.F. Stewart, E.R. Davidson and W.T. Simpson, *J. Phys. Chem.*, 42, 3175, 1965.
36. W.D.S. Motherwell, Cambridge, unpublished.
37. M.F. Lappert, *Chem. Res.*, 55, 1035, 1956.
38. T. Thompson & T.S. Stephens, *J. Chkem. Soc.*, 556, 1933.
39. H.I. Schlesinger and H.C. Brown, *ibid.*, 65, 3429, 1940.
40. D.T. Hurd, *J. Org. Chem.*, 13, 711, 1948.
41. R. Damico, *J. Org. Chem.*, 29, 1972, 1964.
42. G.F. El-Fayoumy, M.A. Wahab and M.I. Roushdy, *Inclusion Compounds*, 3, 372.
43. A. Bax, *J. International Soc. of Magn. Reson.*, 7(4), 167, 1985.
44. S.B. Ferguson and F. Diederich, *Angew. Chem. Int. Ed. Engl.*, 25, 12, 1127, 1986.
45. A.E. Derome, *Modern NMR Techniques for Chemistry Research*, 6, 97-139, 1987.
46. J.S. Kasper and K. Ionsdale (ed.): *International Tables for x-ray Crystallography*, 1, Kynock Press, Birmingham, 1969.

47. G.M. Sheldrick, SHELXS-86 Direct Methods Program, Preliminary version, Private Communication, 1983.
48. G.M. Sheldrick, SHELX-76 Program in "Computing in Crystallography", H. Schenk, P. Olthof-Hazenkamp, J. van Koningsveld and G.C. Bassi (ed.), Delft University Press, 1978.
49. J.G. Jones, S. Schwarzbaum and L. Lessinger, Acta Cryst. B38, 1207, 1982.
50. M. Hofmeyr, MSc.Thesis, unpublished.